The effect of an aspalathin-rich rooibos extract on inflammatory crosstalk between adipocytes and muscle cells

By

Nnini Jennifer Obonye

Thesis presented in fulfillment of the requirements for the degree of Masters in Science (Medical Physiology) in the Faculty of Medicine and Health Sciences at Stellenbosch University

Supervisor: Prof C.J.F. Muller

Co-supervisors: Prof S.E. Mazibuko-Mbeje and Prof H. Strijdom

December 2021

Declaration

By submitting this thesis electronically, I declare that the entirety of the work contained therein is my own, original work, that I am the sole author thereof (save to the extend explicitly otherwise stated), that reproduction and publication thereof by Stellenbosch University will not infringe any third party rights and that I have not previously in its entirety or in part submitted it for obtaining any qualification.

Nnini Jennifer Obonye December 2021

Abstract

The skeletal muscle not only plays a role in maintaining posture and generating force (contraction), but also is a dynamic metabolically active tissue that plays a central role in the regulation of glucose metabolism. Western diets and a sedentary lifestyle reduce the contribution of skeletal muscle to the regulation of blood glucose. In addition, inflammation resulting from chronic elevated levels of pro-inflammatory cytokines is implicated in the development of insulin resistance, metabolic disease and loss of skeletal muscle mass.

The gut plays a central role in the maintenance of metabolic health and disease. Metabolic disease is associated with gut dysbiosis and "leaky" gut syndrome releasing lipopolysaccharide (LPS) into the circulation driving a chronic proinflammatory cytokine response.

To date there have been numerous studies demonstrating that *Aspalathus linearis* (rooibos) plant polyphenols protect against the development of metabolic diseases. The aim of this study was three-fold. Firstly, study the effects of LPS on skeletal muscle growth and metabolism *in vitro* using murine C2C12 myoblasts. Secondly, to study the effect(s) of 3T3-L1 adipocyte derived adipokines on LPS-induced pro-inflammatory cytokine secretion by myoblasts, and thirdly, to investigate the effect of an aspalathin-rich green rooibos extract (Afriplex GRT™) on the LPS-induced immune responses.

To establish the skeletal muscle model of inflammation, C2C12 myoblasts were exposed to LPS (0.1 µg/mL and 1 µg/mL) for 24 hours and treated with Afriplex GRT™ (GRT) (1 µg/mL and 10 µg/mL) for 24 hours. Cell viability, inflammation (IL-6 secretion), glucose uptake, and expression of relevant genes and proteins were assessed. Furthermore, C2C12 myoblasts were differentiated in the presence of LPS to assess the effects of inflammation on myogenesis. A co-culture system using C2C12 myoblasts and 3T3-L1 pre-adipocytes and mature adipocytes were used to study the secretion of IL-6 and adiponectin.

LPS was a potent inducer of pro-inflammatory IL-6 cytokine response, specifically in myoblasts as opposed to myotubules, suggesting that IL-6 is differentially regulated in myotubules. Myoblasts exposed to LPS during differentiation results in decreased myotube width and number suggesting that metabolic endotoxemia affects muscle mass and potentially affecting skeletal muscle energy metabolism. The myogenic regulatory factors, myogenin, MyoD and myostatin were downregulated by LPS during myoblast differentiation. In co-culture, LPS significantly increased IL-6 secretion in both myoblasts and 3T3-L1 pre-adipocytes, whereas IL-6 secretion

was modulated by the differentiated 3T3-L1 adipocytes in co-culture. A dramatic increase in adiponectin levels secreted by the differentiated 3T3-L1 adipocytes compared to the pre-adipocytes could have accounted for the lower IL-6 secretion in the co-culture. GRT was unable to ameliorate the effects of LPS-induced inflammation.

Opsomming

Die skeletspier speel nie slegs 'n rol met liggaamshouding en die lewering van krag (sametrekking) nie, maar is ook 'n dinamiese metabolies-aktiewe weefsel wat 'n sentrale rol in die regulering van glukose-metabolisme speel. Westerse diëte en 'n onaktiewe lewenstyl verminder skeletspiere se vermoë om bloedglukose vlakke te help reguleer. Ook is inflammasie, as gevolg van chroniese verhoogde vlakke van pro-inflammatoriese sitokiene, betrokke by die ontwikkeling van insulienweerstandigheid, metaboliese siektes en verlies aan skeletspiermassa. Die dermkanaal speel 'n sentrale rol in die instandhouding van metaboliese gesondheid en siektes. Die 'lekkende' dermsindroom, wat met metaboliese siekte geassosieer word, veroorsaak dat lipopolisakkaried (LPS) vrygestel word in die sirkulasie wat dan 'n kroniese pro-inflammatoriese sitokienrespons dryf. Tans is daar talle studies wat toon dat *Aspalathus linearis* (rooibos) en sy polifenool aspalatien teen die ontwikkeling van metaboliese siektes beskerm. Die doel van hierdie studie was drievoudig. Eerstens om die effek van LPS op skeletspiergroei en metabolisme te bestudeer deur muis C2C12 mioblaste te gebruik. Tweedens, om die effek(te) wat 3T3-L1 adiposiete op LPS-geïnduseerde pro-inflammatoriese sitokienafskeiding het deur mioblaste te bestudeer, en derdens om te bepaal of 'n aspalatienryke groen rooibosekstrak (Afriplex GRT ™) die LPS-geïnduseerde immuunresponse kan beïnvloed.

Om die inflammatoriese skeletspiermodel te vestig, is C2C12 mioblaste 24 uur lank aan LPS (0,1 µg/mL en 1 µg/mL) blootgestel en ook behandel met Afriplex GRT™ (GRT) (1 µg/mL en 10 µg/ml) vir 24 uur. Sellewensvatbaarheid, inflammasie (IL-6-afskeiding), glukose-opname en uitdrukking van relevante gene en proteïene is bepaal. Verder is C2C12 mioblaste gedifferensieer in die teenwoordigheid van LPS om die effekte van inflammasie op miogenese te bepaal. 'n Ko-kultuurmodel van C2C12 mioblaste en 3T3-L1 pre-adiposiete en adiposiete is gebruik om die afskeiding van IL-6 en adiponektien te bestudeer.

LPS was 'n kragtige induseerder van pro-inflammatoriese IL-6 sitokienrespons, spesifiek in mioblaste in teenstelling met miotubules, wat daarop dui dat IL-6 differensiaal in miotubules gereguleer is. As mioblaste tydens differensiasie aan LPS blootgestel word, is daar 'n afname in miotubule-breedte en -getal wat daarop dui dat LPS die spiermassa beïnvloed en moontlik die energiemetabolisme van die skeletspier beïnvloed. Die regulatoriese miogene, miogenien, MioD en miostatien, word deur LPS gedurende die mioblastdifferensiasie afgereguleer. In ‘n ko-kultuur model het LPS die IL-6-afskeiding in beide mioblaste en 3T3-L1-preadiposiete beduidend verhoog, terwyl IL-6-afskeiding deur die gedifferensieerde 3T3-L1-adiposiete in ko-kultuur

gemoduleer is. 'n Dramatiese toename in adiponektienvlakke wat deur die gedifferensieerde 3T3-L1-adiposiete afgeskei word, in vergelyking met die pre-adiposiete, het waarskynlik IL-6-afskeiding in die mede-kultuur gemoduleer. GRT kon nie die effekte van LPS-geïnduseerde inflammasie verbeter nie.

Acknowledgements

First and foremost, I give my utmost gratitude to my Heavenly Father for the opportunity I had to study my MSc and the lessons learnt during this time of my study/research. I am grateful for the knowledge that I have acquired and the skills that have been enhanced during this tremendous growth process.

Thank you to the people who were constantly around, showing me the way and motivating me to be the best I can possibly be. I am grateful for the knowledge that I have obtained with the help of my fellow colleagues Mrs Ruzayda Van Aarde and Dr Oelfah Patel. I am extremely grateful to my supervisors, Prof C.J.F Muller and Prof S.E. Mazibuko-Mbeje for their invaluable advice, constructive criticism, continuous support, and patience during my MSc study. Your immense knowledge and experience have encouraged me during my academic research. To Dr N. Chellan, I am grateful for imparting the wealth of knowledge and support during my studies.

I am further grateful for the support of my parents, Josiah Mohapi and Elizabeth Mohapi. To my amazing husband, Letlhogonolo T. Obonye, I am eternally grateful for your love, constant support and motivation in this journey of completing my studies. Without your tremendous understanding and encouragement in the past few years, it would be impossible for me to complete my studies.

I would like to acknowledge the South African Medical Research Council, Biomedical Research and Innovation Platform (BRIP) for the support and growth as a young researcher as well as the vast knowledge that I have obtained. Lastly, I would like to thank Prof H. Strijdom and Stellenbosch University, Medical Physiology Division, for the academic support.

Outputs of the Study

Obonye, N.J., Mbeje-Mazibuko, S.E., & Muller, C.J.F. Effect of an aspalathin-rich green rooibos tea (GRT) on skeletal muscle metabolism. **Poster presentation**, South African Medical Research Council, Biomedical Research and Innovation Platform Annual Research Symposium, Cape Town, South Africa, October 2019.

Obonye, N.J., Mbeje-Mazibuko, S.E., Strijdom, H., & Muller, C.J.F. Effect of LPS-induced inflammation on skeletal muscle differentiation and function. **Oral presentation**, South African Medical Research Council, Biomedical Research and Innovation Platform Annual Research Symposium, Cape Town, South Africa, October 2020.

Table of Contents

List of Abbreviations

β-cells:	Beta cells
2DG:	2-deoxyglucose
2DG6P:	2-deoxyglucose-6-phosphate
4EBP:	eIF4E-binding protein
AA:	Antimycin A
ACC:	Acetyl-CoA carboxylase
ADP:	Adenosine diphosphate
ADM:	Adipocyte differentiation medium
Akt:	Protein kinase B
AMM:	Adipocyte maintenance medium
AMPK:	5' adenosine monophosphate-activated protein kinase
ANOVA:	Analysis of variance
AS160:	Akt substrate of 160 kDa
ATCC:	American Type Culture Collection
ATP:	Adenosine triphosphate
BSA:	Bovine serum albumin
cDNA:	Complementary DNA
CO_2:	Carbon dioxide
CPT1:	Carnitine palmitoyltransferase 1
DPBS:	Dulbecco’s phosphate buffered saline
DMEM:	Dulbecco’s modified eagles medium
DMSO:	Dimethyl sulfoxide

DNA:	Deoxyribonucleic acid
dNTP:	Deoxynucleoside triphosphate
DTAB:	Dodecyltrimethylammonium bromide
ECAR:	Extracellular acidification rate
eIF4-E:	Eukaryotic initiation factor 4 subunit E
eIF3-F:	Eukaryotic initiation factor 3 subunit F
ELISA:	Enzyme-linked immunosorbent assay
ETC:	Electron transport chain
ERK 1/2:	Extracellular regulated kinase 1/2
$FADH_2$:	Flavin adenine dinucleotide
FBS:	Foetal bovine serum
FCCP:	Trifluoromethoxy carbonyl cyanide phenylhydrazone
FFA:	Free fatty acid
FGF21:	Fibroblast growth factor 21
FOXO:	Forkhead box transcription factors
GLUT4:	Glucose transporter 4
GRE:	Green rooibos extract
GRT:	Afriplex GRT^{TM} (aspalathin-rich green rooibos extract)
GSK-3β:	Glycogen synthase kinase-3 beta
H^+:	Hydrogen ion
H_2O_2:	Hydrogen peroxide
H&E:	Haematoxylin and eosin
HCl:	Hydrochloric acid
HDL:	High-density lipoprotein

HS:	Horse serum
HSP:	Heat shock protein
HUVEC:	Human umbilical vein endothelial cells
IBMX:	1-methyl-3-isobutyl xanthine
IDF:	International Diabetes Federation
IGF-1:	Insulin-like growth factor 1
IL-1:	Interleukin 1
IL-6:	Interleukin 6
IL-10:	Interleukin 10
IL-15:	Interleukin 15
IR:	Insulin resistance
IRS-1:	Insulin receptor substrate 1
KRBH:	Krebs-Ringer bicarbonate HEPES buffer
LDL:	Low-density lipoprotein
LPS:	Lipopolysaccharide
MAFbx:	Muscle atrophy F-box/ Atrogin-1
MRF:	Muscle regulatory factor
mRNA:	messenger ribonucleic acid
mTOR:	Mechanistic target of rapamycin
mTORC1:	Mechanistic target of rapamycin complex 1
mTORC2:	Mechanistic target of rapamycin complex 2
Myf5:	Myogenic factor 5
MyoD:	Myoblast determination protein 1
MuRF1:	Muscle RING-finger protein-1

MTT:	3-(4, 5-dimethylthiazol-2-yl)-2, 5-diphenyltetrazolium bromide
NADPH:	Nicotinamide adenine dinucleotide phosphate
NF-κB:	Nuclear factor kappa-light-chain-enhancer of activated B cells
NOX-4:	NAD(P)H oxidase 4
NTC:	No template control
OCR:	Oxygen consumption rate
O.D:	Optical density
PAGE:	Polyacrylamide gel electrophoresis
Pax 3:	Paired box 3
Pax 7:	Paired box 7
PBS:	Phosphate buffered saline
PDK-1:	Phosphoinositide-dependent kinase 1
PCR:	Polymerase chain reaction
Pi:	Organic phosphate
PI3K:	Phosphoinositide 3-kinase
PIP3:	Phosphatidylinositide-3,4,5-triphosphate
PMSF:	Phenylmethylsulfonyl fluoride
PTP1B:	Protein tyrosine phosphatase 1 B
qRT-PCR:	Quantitative reverse transcription polymerase chain reaction
RCF:	Relative centrifugal force
RNA:	Ribonucleic acid
RNase:	Ribonuclease
RPM:	Revolutions per minute
RPTOR:	Regulatory-associated protein of mTOR

ROS:	Reactive oxygen species
Rot:	Rotenone
RT:	Reverse transcriptase
S6K1:	mTOR Substrate S6 Kinase 1
SD:	Standard deviation
SDS:	Sodium dodecyl sulphate
SDS-PAGE:	Sodium dodecyl sulphate polyacrylamide gel electrophoresis
T2DM:	Type 2 diabetes mellitus
TBS:	Tris-buffered saline
TBS-T:	1 x Tris-buffered saline with 0.1% Tween 20
TCA:	Tricarboxylic acid cycle/ Krebs cycle
TEMED:	Tetramethylethylenediamine
TGF-β1:	Transforming growth factor-β1
TLR2:	Toll-like receptor 2
TLR4:	Toll-like receptor 4
TNF-α:	Tumour necrosis factor alpha
WHO:	World Health Organisation

List of Figures

List of Tables

1 INTRODUCTION

1.1 Background

Skeletal muscle plasticity allows the muscle tissue to be metabolically and structurally flexible, thus being able to adapt to the environmental conditions. It is well-known that exercise can increase skeletal muscle mass (Konopka & Harber, 2014) and improve skeletal muscle insulin sensitivity (Sjøberg *et al*., 2017) and is prescribed as a non-pharmacological intervention for the treatment of metabolic disease. Increasing skeletal muscle mass is associated with increased insulin sensitivity (Cleasby *et al*., 2014; Haines *et al*., 2020; Han *et al*., 2018) where as a decline in muscle mass, often related to aging, results in decreased insulin sensitivity (Shou *et al*., 2020). Insulin resistance is a major predisposing factor to the development and progression of type 2 diabetes mellitus (T2DM) (Boden *et al*., 2005; Chatterjee & Scobie, 2002; Shimabukuro *et al*., 1998) and has also been associated with muscle protein degradation (Wang *et al*., 2006). Lack of exercise and over nutrition are sedentary lifestyle factors that increase the development of insulin resistance (Zimmet, 2017). Chronic low-grade inflammation has been associated with insulin resistance, obesity and T2DM, resulting in increased levels of circulating pro-inflammatory cytokines that have negative effects on skeletal muscle metabolism and structure.

Polyphenols are biomolecules naturally found in plant foods (e.g., herbs, vegetables, spices, tea, etc.), and have been attributed to the prevention and amelioration of metabolic syndrome (Chiva-Blanch & Badimon, 2017). Rooibos is a South African herbal tea produced from *Aspalathus linearis*, a shrub-like bush indigenous to the Cederberg region of the Western Cape Province (Joubert & de Beer, 2012). Rooibos is known for its antioxidant activity and has been associated with various health-promoting properties (Joubert *et al*., 2008; Marnewick *et al*., 2011). In particular, unfermented rooibos extract as well as aspalathin, the major bioactive flavonoid in rooibos, have been shown to ameliorate insulin resistance and glucose uptake skeletal muscle cells *in vitro* (Mazibuko *et al*., 2013; Muller *et al*., 2012).

T2DM is a growing epidemic world-wide and is a major concern in healthcare. Approximately 462 million individuals were affected by T2DM in 2017 and accounting for 1 million deaths and projected to rise over the next decade (Khan *et al*., 2019). Over the years, there has been an increasing interest in herbal/natural remedies (plant polyphenols) and consumption of these polyphenol rich foods has been shown to modulate diet-induced low-grade inflammation (Serrano *et al*., 2020; Zhao *et al*., 2019) a causal factor for the development of T2DM. Research has been geared towards the development of plant polyphenol extracts with the aim of alleviating/combating the symptoms and complications that come with metabolic diseases. Thus, in this study the use

of a pharmaceutical grade green rooibos extract (Afriplex GRT™) has been investigated for its ability to improve or prevent the development of metabolic disease.

1.2 Hypothesis

Aspalathin-rich green rooibos extract (Afriplex GRT™) ameliorates LPS-induced inflammation and muscle wasting in C2C12 myoblasts and modulates inflammatory adipocyte-myocyte crosstalk.

1.3 Aims and Objectives

1.3.1 Aim

The aim of this study is to understand LPS-induced inflammation as a mechanism of skeletal muscle insulin resistance and atrophy as well as the adipocyte-myocyte paracrine crosstalk and to elucidate the modulatory action of an aspalathin-rich green rooibos extract (Afriplex GRT™) on LPS-induced inflammation in C2C12 myoblasts including adipocyte-derived pro-inflammatory cytokines using cell co-culture.

1.3.2 Objectives

In order to address the specific aim of this study, C2C12 skeletal muscle cells will be cultured alone (monoculture) or co-cultured with 3T3-L1 adipocytes in high (33 mM) glucose, and LPS will be used to induce skeletal muscle IR *in vitro*.

- Examine the effects of high glucose and LPS on 3T3-L1 adipocyte pro-inflammatory cytokine secretion.
- Establish the effects of the culture profile on glucose at a functional level including gene and protein expression in the C2C12 muscle and 3T3-L1 adipocytes in co-culture.
- Examine the effects of LPS on myogenesis.

- Examine the effects of rooibos phenolic compounds as a modulating treatment and/or preventative measure on the pathophysiology identified above.

2 LITERATURE REVIEW

2.1 Skeletal muscle structure, physiology and function

The skeletal muscle is the most abundant tissue that represents about half of total body weight and contributes to multiple bodily functions (Costamagna *et al*., 2015; Gransee *et al*., 2012). This dynamic tissue has the unique ability to alter its structural and functional properties in response to growth and aging as well as to stimuli such as muscle injury, mechanical loading and over nutrition (Costamagna *et al*., 2015; Gransee *et al*., 2012). The skeletal muscle tissue is well-structured and organized, as well as highly vascularised and innervated. This is directly related to its functions including contraction and energy metabolism (Mukund & Subramaniam, 2019). Mechanically, the function of the skeletal muscle is to convert chemical energy into mechanical energy to generate force and power, produce movement (locomotion), and maintain posture. Apart from mechanical functions, the skeletal muscle also plays an essential role in the maintenance and regulation of whole-body energy metabolism, thermal homeostasis and storage of energy substrates such as carbohydrates in the form of glycogen (Frontera & Ochala, 2015; Mirzoev, 2020).

2.1.1 Skeletal muscle structure: myofiber to whole muscle

The skeletal muscle tissue is made up of bundles of muscle fibers that are covered with connective tissue. Muscle fibers (myofibers or myocytes) are mature multinucleated cells that form the basic cellular unit of skeletal muscle tissue (Exeter & Connell, 2010; Frontera & Ochala, 2015; Gransee *et al*., 2012; Mukund & Subramaniam, 2019). Each muscle fiber is encapsulated by a sheath of connective tissue known as the endomysium and these bundles of muscle fibers are then encapsulated by another sheath of connective tissue, the perimysium, forming structures known as fascicles. Together, bundles of fascicles form the muscle tissue which is also encapsulated by another sheath of connective tissue, termed the epimysium (Exeter & Connell, 2010; Frontera & Ochala, 2015; Mukund & Subramaniam, 2019). Muscle fibers consist of highly organised structures called myofibrils and each myofibril is composed of a series of subunits called sarcomeres. Sarcomeres are the basic functional units of the myofibril and are made up of thick and thin filaments (thick filaments are mainly composed of myosin, whereas actin, troponin and tropomyosin are the main components of thin filaments) which are anchored to Z-discs (Exeter & Connell, 2010; Gransee *et al*., 2012; Mukund & Subramaniam, 2019). The Z-disc

defines the boundary of the sarcomere and is the attachment site for thin filaments between adjacent sarcomeres. The precise and orderly arrangement of the thick and thin filaments give the skeletal muscle its striated appearance (Frontera & Ochala, 2015; Gransee *et al*., 2012; Lowe & Anderson, 2015).

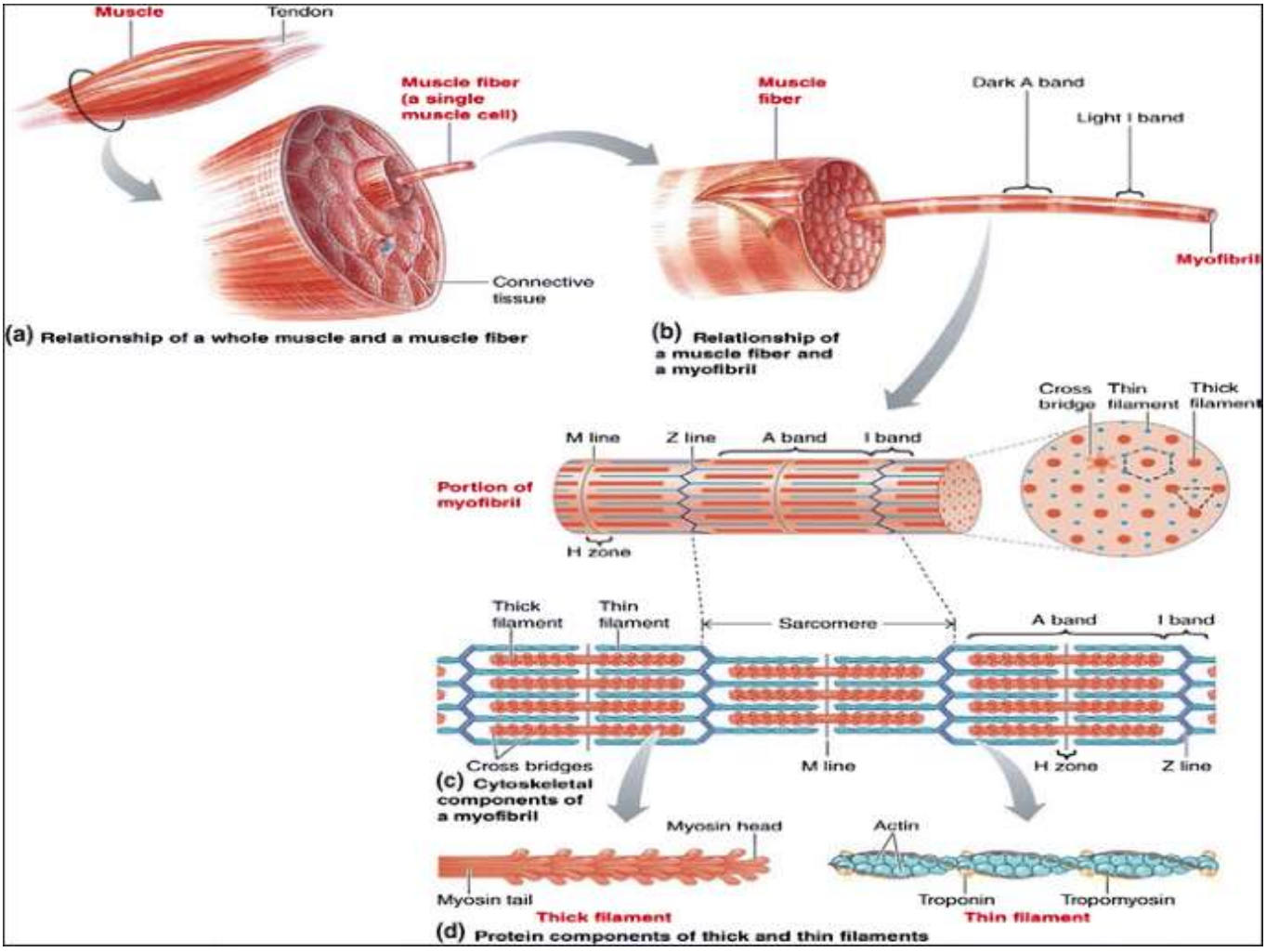

Figure 2.1: Structure of skeletal muscle. Figure obtained from (Frontera & Ochala, 2015).

2.1.2 Skeletal muscle: role in energy metabolism

The skeletal muscle tissue is responsible for approximately 70 - 80% of peripheral insulin-stimulated glucose uptake and clearance from the circulation and, therefore, has a significant

contribution to whole-body glucose homeostasis (DeFronzo & Tripathy, 2009; Kumar & Dey, 2003; Wu & Ballantyne, 2017). In conjunction with carbon-13 nuclear magnetic resonance spectroscopy Cline and colleagues (1998) showed that non-oxidative glucose phosphorylation is the principal pathway for glucose disposal by skeletal muscle (Cline *et al*., 1998; DeFronzo & Tripathy, 2009; Roden *et al*., 1996). The glucose taken up by the skeletal muscle is stored as glycogen and used as an energy substrate for exercise (Jensen *et al*., 2011). Insulin stimulates skeletal muscle glucose uptake by increasing glucose transporter protein concentration at the plasma membrane, particularly glucose transporter 4 (GLUT4) (Jensen *et al*., 2011).

The skeletal muscle is a metabolically flexible tissue, being able to use both glucose and free fatty acids as energy sources for adenosine triphosphate (ATP) production in the fed or fasting state (Goodpaster & Sparks, 2017). In the skeletal muscle, ATP provides the energy to power the contraction in working muscle, thus this energy rich molecule is critical to skeletal muscle function as well as meeting increased energy demands during periods of intense exercise or normal daily activities (Baker *et al*., 2010; Mukund & Subramaniam, 2019). Upon entry into the skeletal muscle, glucose is phosphorylated by hexokinase forming glucose-6-phosphate and is either destined towards glycogen synthesis or glycolysis (Richter & Hargreaves, 2013). The skeletal muscle is an energy consuming tissue and therefore, generation of ATP through glycolysis plays a critical role in skeletal muscle contractile function (Mukund & Subramaniam, 2019). The glycolysis pathway produces 2 ATP molecules as well as 2 pyruvate molecules that are either shunted towards the tricarboxylic acid (TCA) cycle by the oxidation of pyruvate to acetyl-Coenzyme A (acetyl-CoA) by pyruvate dehydrogenase or converted to lactate by lactate dehydrogenase (Lodish *et al*., 2000). The complete oxidation of glucose begins with the entry of pyruvate into the TCA cycle which results in the subsequent production of electron carrier molecules, nicotinamide adenine dinucleotide (NADPH) and flavin adenine dinucleotide ($FADH_2$), which are oxidized in the electron transport chain (ETC) yielding 32 ATP molecules through oxidative phosphorylation in the mitochondria (Brody, 1999; Lodish *et al*., 2000).

In the fasting state, plasma insulin levels decrease with a concomitant decrease in phosphorylated protein kinase B (PKB/Akt) and Akt substrate of 160 kDa (AS160) activity (Soeters *et al*., 2012; Wijngaarden *et al*., 2014). This results in the shift in substrate metabolism, from glucose oxidation to fatty acid oxidation. The increase in AMP-activated protein kinase (AMPK) activity inhibits muscle specific acetyl-CoA carboxylase 2 (ACC 2) isoform by phosphorylating the Serine 221 residue (Serine 212 in mice) (Lange *et al*., 2006; O'Neill *et al*., 2014; Wijngaarden *et al*., 2014). However, studies have shown that although AMPK is not increased in human skeletal muscle,

ACC 2 phosphorylation is decreased in the fasted state (Vendelbo *et al*., 2012; Wijngaarden *et al*., 2014). The inhibition of ACC 2 and activation of malonyl-CoA decarboxylase by AMPK results in the decrease in malonyl-CoA levels, allowing the interaction of free fatty acids with carnitine palmitoyltransferase 1 (CPT1) and thereby enhancing fatty acid oxidation (Beta oxidation) (Foster, 2012). Like the glycolysis pathway, beta oxidation yields acetyl-CoA and electron carrier molecules that enter the TCA cycle and ETC, respectively to produce ATP after each round of oxidation, which is dependent on the length of the fatty acid chain (de Carvalho & Caramujo, 2018). Thus, mitochondria are an essential element in skeletal muscle energy metabolism, especially during increased energy demand and have been implicated in skeletal muscle dysfunction and metabolic disease.

2.1.2.1 Mitochondrial bioenergetics: critical for ATP production

The mitochondria are responsible for the majority ATP production (via oxidative phosphorylation) in times of increased skeletal muscle energy demand. Flavin adenine dinucleotide ($FADH_2$) and nicotinamide adenine dinucleotide (NADH) are high energy electron carriers used to transport electrons generated in glycolysis and TCA cycle to the ETC. The ETC is composed of a series of protein complexes (complex I to IV) embedded in the inner mitochondrial membrane and function to transport/pump hydrogen ions (H^+) across the inner mitochondrial membrane (from mitochondrial matrix into the intermembrane space) creating the proton gradient necessary to drive ATP synthesis (oxidative phosphorylation) (Ahmad *et al*., 2021; Martínez *et al*., 2020). At the inner mitochondrial membrane, the high energy electron carriers become oxidized, NADH to NAD^+ and $FADH_2$ to FAD at complex I and complex II respectively. The donated electrons are then transported across the ETC protein complexes resulting in the pumping of H^+ across the membrane at complexes I, III and IV. The proton gradient is then generated by the accumulation of H^+ in the intermembrane space and a reduction of H^+ concentration in the mitochondrial matrix (Ahmad *et al*., 2021; Martínez *et al*., 2020). The ATP synthase (complex V) can be divided into 2 regions, F_0 region (proton pump subunit) and F_1 region (catalytic subunit). As H^+ from the intermembrane space pass through the F_0 region of ATP synthase, this results in the rotation of the subunits in the F_0 and F_1 region. This rotation catalyses the reaction of adenosine diphosphate (ADP) and organic phosphate (Pi) producing ATP in the beta subunit of the F_1 region (Neupane *et al*., 2019). The ATP synthase is critical to energy production, where mutations, defects or

functional impairments of ATP synthase can result in cardiomyopathy and various neuromuscular disorders and even death (Houštek *et al*., 1999; Kucharczyk *et al*., 2009).

2.1.3 Insulin signalling and regulation

In insulin sensitive tissues, particularly the skeletal muscle, insulin signalling is initiated by the binding of insulin to the insulin receptor. The insulin receptor is a heterotetrametric protein consisting of two α subunits (extracellular) and two β subunits (membrane-spanning). The binding of insulin results in the conformational change of the insulin receptor leading to the phosphorylation of the tyrosine molecules on the receptor (Petersen & Shulman, 2018). Phosphorylation of the insulin receptor results in the internalization of the insulin receptor and recruitment of insulin receptor substrate-1 (IRS-1) (DeFronzo & Tripathy, 2009; Petersen & Shulman, 2018). IRS-1 becomes phosphorylated and activates the p85 regulatory subunit of phosphatidylinositol-3-kinase (PI3-kinase) as well as the p110 catalytic subunit. Activated PI3-kinase catalyses the formation of phosphatidylinositol-3,4,5-triphosphate (PIP3). The increase in PIP3 levels results in the binding of phosphoinositide-dependent kinase-1 (PDK-1) followed by the phosphorylation of protein kinase B (Akt). Activated Akt in turn phosphorylates AS160 and several proteins downstream initiating the translocation of GLUT4 from intracellular storage vesicles to the plasma membrane, facilitating glucose transport into the muscle cells (DeFronzo & Tripathy, 2009; Petersen & Shulman, 2018; Schmitz-Peiffer, 2000).

An increase in the activity of protein tyrosine phosphatase 1B (PTP1B) negatively regulates insulin signalling by dephosphorylating the insulin receptor upon internalisation therefore, terminating insulin signalling. To circumvent the activity of PTP1B, the insulin receptor activates NAD(P)H oxidase 4 (NOX-4) activity. The activation of NOX-4 results in the inhibition of PTP1B via NOX-4-derived H_2O_2 thereby providing a continued amplification of insulin signalling (Petersen & Shulman, 2018; Polonsky & Burant, 2016). Skeletal muscle insulin sensitivity is crucial for energy metabolism, decreased insulin sensitivity and impairment in insulin signalling potentially leads to the development of metabolic diseases and associated complications (DeFronzo, 2004; Jové *et al*., 2006; Perry *et al*., 2016; Stumvoll *et al*., 2005).

2.1.4 Regulation of skeletal muscle mass

Skeletal muscle mass is maintained by an intricate balance between the rate of protein synthesis and degradation. Factors such as inflammation, exercise, growth factors, steroids, muscle disuse/immobility and disease are able to cause a shift between this balance causing changes in composition, appearance and performance of the muscle fiber (Dirks *et al*., 2016; Distefano & Goodpaster, 2018; Hong *et al*., 2019; Meex, Blaak, & Loon, 2019; Mukund & Subramaniam, 2019; Sandri *et al*., 2004; Stitt *et al*., 2004; Teng & Huang, 2019). Of most importance, loss of muscle mass (sarcopenia) is a general feature of ageing as well as a characteristic feature of various pathologies including sepsis, cancer, obesity and diabetes (Lipina & Hundal, 2017; Rosenberg, 1997; Sishi *et al*., 2011; Tisdale, 2008; Trierweiler *et al*., 2018). Skeletal muscle atrophy occurs when the balance is shifted towards degradation, leading to a loss of myofibrillar proteins. Skeletal muscle size can increase either through hypertrophy (the increase in size of existing muscle fibers) or by hyperplasia (an increase in the number of muscle fibers) (Exeter & Connell, 2010). Hypertrophy occurs as a response to normal growth and exercise whereas hyperplasia occurs in response to significant muscle injury (Exeter & Connell, 2010). Loss of muscle mass can impact muscle function, reduce muscle strength and contribute to the development of impaired glucose and lipid homeostasis (Trierweiler *et al*., 2018).

2.1.5 Protein synthesis and degradation

The PI3K/Akt/mTOR pathway is the major pathway that regulates protein synthesis (Bodine *et al*., 2001; Mirzoev, 2020; Rommel *et al*., 2001). Akt1, Akt2 and Akt3 are members of the AKT serine-threonine kinase family. In skeletal muscle, Akt1 and Akt2 are highly expressed compared to Akt3 which is predominantly expressed in the brain. Insulin-like growth factor-1 (IGF-1) activates Akt1, whereas Akt2 is activated by insulin, however insulin is able to activate Akt1 (Kim *et al*., 1999). Studies showed that Akt1 knockout mice displayed growth retardation and muscle atrophy, whereas Akt2 knockout mice became diabetic and Akt3 knockout mice had impaired brain development (Sandri, 2008; Yang *et al*., 2004) demonstrating that Akt is involved in muscle growth and glucose metabolism.

The mechanistic target of rapamycin (mTOR), also referred to as mammalian target of rapamycin is a serine/threonine protein kinase that forms the catalytic subunit of two distinct protein complexes, mTOR Complex 1 (mTORC1) and 2 (mTORC2). Upon phosphorylation of mTOR (Ser2448) by Akt, mTOR forms a complex with the regulatory associated protein of mTOR, complex 1 (RPTOR) to form mTORC1. The mechanistic target of rapamycin complex 1 promotes protein synthesis by directly phosphorylating p70S6 Kinase 1 (S6K1) and eIF4E-binding protein (4EBP), an inhibitor of protein synthesis. The phosphorylation of 4EBP results in its dissociation from eukaryotic initiation factor 4E (eIF4E) which subsequently results in the recruitment of eukaryotic initiation factor 4G (eIF4G) allowing mRNA translation to occur (Gransee *et al*., 2012; Mao & Zhang, 2018; Mukund & Subramaniam, 2019; Saxton & Sabatini, 2017). Another downstream target of Akt is the glycogen synthase pathway. Akt promotes protein synthesis by phosphorylating and inhibiting glycogen synthase kinase-3 beta (GSK-3β). The inhibition of GSK-3β results in the release of eukaryotic initiation factor 2B (eIF2B) and therefore increasing protein synthesis (Mirzoev, 2020; Mukund & Subramaniam, 2019; Rommel *et al*., 2001).

Protein degradation is suppressed when Akt phosphorylates Forkhead box O (FOXO), inhibiting its translocation to the nucleus (Bodine *et al*., 2001; Gransee *et al*., 2012; Mukund & Subramaniam, 2019). The inhibition of Akt results in the failure to suppress FOXO, leading to its subsequent translocation to the nucleus and up-regulating the muscle specific E3 ubiquitin ligases (Frontera & Ochala, 2015; Gransee *et al*., 2012; Hulmi *et al*., 2012; Lipina & Hundal, 2017; Mukund & Subramaniam, 2019). Atrogin-1 (also known as MAFbx) and muscle ring-finger protein-1 (MuRF1) are well known E3 ubiquitin ligases involved in muscle protein degradation and are both implicated in diabetic and obese-induced muscle atrophy, as well as shown to be up-regulated in animal models of muscle wasting as well as studies pertaining to muscle atrophy in obese and diabetic patients as well as animal models of sepsis (Dehoux *et al*., 2004; Lagirand-Cantaloube *et al*., 2008; Ono *et al*., 2020; Pellegrinelli *et al*., 2015; Perry *et al*., 2016; Sishi *et al*., 2011). Atrogin-1 targets MyoD, an essential muscle regulatory factor involved in the process of myogenesis, as well as eukaryotic initiation factor 3 subunit F (eIF3-f) for degradation whereas, MuRF-1 targets myofibrillar proteins including myosin and actin (Clarke *et al*., 2007; Cohen *et al*., 2009; Lagirand-Cantaloube *et al*., 2008; Polge *et al*., 2011; Scicchitano *et al*., 2018; Sishi *et al*., 2011).

Myostatin is abundantly expressed in the muscle tissue and has been positively associated with insulin resistance and obesity (Allen *et al*., 2011; Amor *et al*., 2019). Myostatin is up-regulated in obese and T2DM individuals (Amor *et al*., 2019) and its inhibition reduced TNF-α expression and protected muscle and liver tissue against obesity-induced insulin resistance (Wilkes *et al*., 2009). Myostatin is also thought to be a negative regulator of myogenesis, and exerts its effects through Smad2/3 signalling and inhibiting protein synthesis (Burks & Cohn, 2011; Han *et al*., 2013). Upon phosphorylation, Smad2/3 form a complex with Smad4. The Smad2/3/4 complex then stimulates FOXO-dependent transcription, suppressing Akt/mTOR mediated signalling pathway and up-regulating protein degradation pathways (Burks & Cohn, 2011; Han *et al*., 2013).

2.1.6 Muscle regeneration

Different stimuli, including muscle injury, exercise (muscle overloading), and denervation activate the muscle regeneration process by activating muscle satellite cells which transform into myoblasts. The myoblasts proliferate into myocytes and subsequently fusing with existing muscle fibres or fuse with each other to form multinucleated myotubes and mature to form new muscle fibres (Costamagna *et al*., 2015; Teng & Huang, 2019). Muscle satellite cells are progenitor cells derived from cells that express paired box (Pax) 3/7 during embryogenesis (Buckingham & Relaix, 2015; Gros *et al*., 2005; Tajbakhsh *et al*., 1997; Yablonka-Reuveni, 2011) and are located between the basal lamina and plasma membrane of muscle fibers (Buckingham & Relaix, 2015; Fujimaki *et al*., 2016; Mukund & Subramaniam, 2019; Yin, Price, & Rudnicki, 2013). These progenitor cells are key to skeletal muscle plasticity. Under physiological conditions, muscle satellite cells remain dormant, and are characterised by the expression of Pax7. Pax7 is located upstream of both MyoD and Myf5, regulating the expression of both genes. The expression of Pax7 is also essential for muscle satellite cell expansion and survival (Buckingham, 2007).

Pax7-deficient primary myoblasts and mice exhibited cell-cycle arrest and dysregulation of myogenic regulatory factors, as well as reduced muscle regeneration (von Maltzahn *et al*., 2013), supporting the notion that Pax7 is critical in the maintenance and expansion of the skeletal muscle satellite cell pool as well entry into the myogenic programme. In response to stimulation such as muscle injury, the muscle satellite cells become activated. Upon activation, muscle satellite cells express MyoD, allowing the cells to enter the myogenic programme, committed to the myoblastic proliferation phase. The activated cells proliferate and differentiate into myoblasts, which then

differentiate into mature muscle fibers fusing with existing fibers or creating new muscle fibers. However, some of the stimulated satellite cells do not differentiate into myoblasts, they proliferate and return to a quiescent state to maintain the muscle stem cell pool (Bjornson *et al*., 2012; Mukund & Subramaniam, 2019; Teng & Huang, 2019; Yin *et al*., 2013).

Muscle repair is dependent upon the coordinated activation of inflammatory response and myogenesis. In response to injury, the complement system is activated, stimulating the recruitment of immune cells to the site of injury (Frenette *et al*., 2000). Mast cells and neutrophils are the first inflammatory cells that infiltrate the injured muscle. Skeletal muscle resident mast cells are activated, leading to their subsequent degranulation and release of inflammatory mediators (TNF-α, interferon gamma and IL-1β), stimulating the recruitment of neutrophils to the site of injury (Arnold *et al*., 2007; Bortolotto *et al*., 2004; Howard *et al*., 2020).

Neutrophils function to remove myofiber debris and stimulate the recruitment of other immune cell populations including monocytes and macrophages by secreting IL-1, IL-8 and IL-6. The recruitment of monocytes and macrophages is critical to muscle regeneration-related myogenesis (Howard *et al*., 2020). Lu *et al* (2011) demonstrated Ccr2-/- mice had reduced muscle inflammation and impaired muscle regeneration after barium chloride-induced muscle injury, suggesting that the inhibition of monocyte/macrophage accumulation/recruitment impairs the skeletal muscle regenerative response (Lu *et al*., 2011). Initially, the infiltrating macrophages are polarized towards an M1 pro-inflammatory ($Ly6C^{+}$) phenotype, releasing pro-inflammatory cytokines (TNF-α, IL-1, IL-6) and stimulating myoblast proliferation (Zhang *et al*., 2013). The clearance of muscle debris by neutrophils and clearance of apoptotic neutrophils by M1 macrophages, as well as the release of IL-4 by myoblasts induce the switch from M1 to M2 state (Arnold *et al*., 2007; Chazaud *et al*., 2003; Horsley *et al*., 2003). The M2 macrophage ($Ly\text{-}6C^{-}$) phenotype is anti-inflammatory, releasing anti-inflammatory mediators, including transforming growth factor-β1 (TGF-β1), IGF-1 and IL-10 and the secretion of these anti-inflammatory mediators promote myoblast differentiation, thus supporting myogenesis (Arnold *et al*., 2007; Chazaud *et al*., 2003; Sonnet *et al*., 2006). The tightly orchestrated balance between the duration of pro-/anti-inflammatory factors is essential in the muscle regeneration programme and maintenance of muscle health. An imbalance can lead to deleterious effects such as reduced myofiber growth and regeneration, uncontrolled wound healing and fibrosis, as well as muscle atrophy (Costamagna *et al*., 2015; Segawa *et al*., 2008).

2.2 Effect of metabolic disease on skeletal muscle

2.2.1 Insulin resistance

Insulin Resistance (IR), a characteristic feature of the metabolic syndrome and regarded as the hallmark of type 2 diabetes mellitus (T2DM) has been commonly associated with obesity, hypertension and cardiovascular disease. Insulin resistance is defined as a metabolic disorder where insulin sensitive tissues (skeletal muscle, liver, and adipose tissue) become unresponsive to the action of insulin, thus resulting in the inability of the body to maintain plasma glucose levels at euglycaemic levels (glucose homeostasis). Therefore, to compensate for insulin resistance pancreatic beta cells hyper secrete insulin resulting in hyperinsulinaemia, that further perpetuates insulin unresponsiveness. A decrease in insulin sensitivity results in decreased glucose uptake in skeletal muscle, unhindered lipolysis in adipose tissue and increased gluconeogenesis in the liver resulting in the failure to maintain systemic energy homeostasis (DeFronzo & Tripathy, 2009; Mlinar *et al*., 2007; Schmitz-Peiffer, 2000; Ye, 2013). The ineffective clearance of glucose by skeletal muscle is considered to be a major contributor to glucose intolerance and hyperglycaemia, ultimately leading to the development of T2DM. Thus, the understanding of the aetiology of this metabolic syndrome is of significant importance.

2.2.2 Insulin resistance in skeletal muscle

In a lipid infusion study using healthy subjects, Roden and his colleagues (Roden *et al*., 1996) established that insulin resistance caused the elevation of plasma FFAs and resulted in the reduction of muscle glycogen synthesis and glucose oxidation rates through the inhibition of the glucose transport or phosphorylation activity. Similar data was observed in type 2 diabetic patients (Rothman *et al*., 1992). The use of *in vitro* methodologies (tissue culture) showed that palmitate, a saturated fatty acid, inhibited insulin-stimulated glucose uptake in mouse skeletal muscle cells. This was observed in the reduction in glycogen synthesis and the down-regulation of GLUT4 mRNA expression in palmitate-treated cells compared to the untreated control cells (Jové *et al*., 2005; Mazibuko *et al*., 2013). Palmitate also induced the accumulation of diacylglycerol (DAG) and ceramides in C2C12 myotubes and these effects were not seen in 3T3-L1 adipocytes (Chavez & Summers, 2003).

To further establish how elevated plasma FFAs cause insulin resistance, Dresner and colleagues were able to show that elevated plasma FFAs caused a significant reduction in intracellular glucose concentration compared to the control study, therefore demonstrating that glucose transport is the rate-limiting step responsible for the reduced insulin-stimulated glucose disposal. This was based on the idea that intracellular glucose is an intermediate between glucose transport and hexokinase II and thus its concentration reflects the relative activities of glucose transport and hexokinase II (Dresner *et al*., 1999).

A number of studies have also implicated IRS-1–associated PI3-kinase as mediator in skeletal muscle insulin resistance (Cusi *et al*., 2000; Kruszynska *et al*., 2002; Yu *et al*., 2002). Elevations in plasma FFA concentration abolished the IRS-1-associated PI3-kinase activity thus causing a reduction in insulin-stimulated glucose activity in skeletal muscle (Dresner *et al*., 1999). Other mechanisms independent of insulin-signalling have been proposed as contributing factors to the development of insulin resistance. Plasma FFAs are also TLR4 agonists, suggesting that the inflammatory pathway is also involved in the development of insulin resistance in skeletal muscle (Radin *et al*., 2008; Shi *et al*., 2006).

2.2.3 Type 2 diabetes mellitus

Type 2 diabetes mellitus (T2DM), a life-style disease characterised by raised plasma blood glucose levels, accounts for 90% of all diabetes cases and is a major source of morbidity, mortality and health costs globally (International Diabetes Federation, 2019). Most patients with T2DM are obese, with obesity itself causing some degree of insulin resistance (“Diagnosis and Classification of Diabetes Mellitus,” 2010). Since hyperglycaemia develops gradually over the years, T2DM frequently goes undiagnosed thus the onset of the disease is usually impossible to determine. The International Diabetes Federation estimates that in 2019, 463 million adults worldwide had diabetes. This number is estimated to increase to 578 million cases by 2030, with 700 million cases by the year 2045, thus estimating a 51% increase in diabetes cases worldwide (International Diabetes Federation, 2019).

The pathogenesis of T2DM involves defects in both insulin secretion and action. Although the exact mechanisms are not yet fully understood, hypotheses have been suggested over the years that pancreatic β-cell dysfunction is a more common feature. Chronic insulin resistance results in hyperglycaemia, hyperinsulinaemia and increased plasma FFA concentrations, and the

progressive failure of β-cells to produce sufficient levels of insulin that determines the onset and progression of T2DM (DeFronzo, 1992; DeFronzo, 2004; Leahy, 2005; Poitout & Robertson, 2008).

Studies by Spranger *et al*, (2003) and Pradhan *et al*, (2001) show that subclinical activation of the immune system is involved in the pathogenesis of T2DM, where case subjects (termed as individuals free of T2DM at baseline and developed diabetes in the 2-3 year follow up) showed to have increased levels of circulating cytokines (IL-6, IL-1β and TNF-α). Spranger *et al*, (2003) suggested that IL-6 and IL-1β are determining risk factors for T2DM development. Therefore, β-cell dysfunction/death is a critical factor in the onset and pathogenesis of overt T2DM (Pradhan *et al*., 2001; Spranger *et al*., 2003).

2.2.4 Muscle atrophy in type 2 diabetes mellitus and inflammation

Diseases characterised by chronic inflammation, sepsis and sarcopenia have been associated with muscle dysfunction (Dirks *et al*., 2016; Ono *et al*., 2020; Perry *et al*., 2016; Sishi *et al*., 2011; Sumi *et al*., 2020). Myogenesis is an essential process required for muscle repair, maintenance of skeletal muscle mass and function. Multiple studies have shown that conditions of inflammation, insulin resistance, and obesity disrupt muscle function by up-regulating the protein degradation pathways, including the muscle specific ubiquitin E3 ligases, MuRF-1 and Atrogen-1, targeting the myofibrillar proteins and resulting in a negative balance in muscle homeostasis (Ato *et al*., 2019; Luo *et al*., 2019; Ono *et al*., 2020). Muscle wasting is a gradual process that progresses with age and is more substantial in T2DM patients (Perry *et al*., 2016).

Type 2 diabetes mellitus associated muscle atrophy is thought to be a contributing factor to the progression of other diabetic complications based on the key role skeletal muscle plays in glucose homeostasis and locomotion (Hernandez-Ochoa *et al*., 2017) exacerbating the progression of T2DM over time thus decreasing the capacity to perform activities of daily living and increasing mortality (Hernandez-Ochoa *et al*., 2017; D' Souza *et al*., 2013). As previously mentioned, the skeletal muscle accounts for 70 – 80% of insulin stimulated glucose uptake from circulation and represents up to 40% of body weight. Therefore loss of muscle mass leads to decreased capacity and strength as well as persistent hyperglycaemia, ultimately leading to increased mortality in patients with T2DM (Perry *et al*., 2018).

The myogenic potential of muscle satellite cells is altered in a diabetic environment. Muscle satellite cells derived from T2DM patients were found to retain their diabetic phenotype *(Gaster et al*., 2002; Green *et al*., 2011). Basal glucose uptake as well as insulin-stimulated glycogen synthase activity was reduced in muscle satellite cells isolated for T2DM patients (Gaster *et al*., 2002) as well as reduced proliferative capacity (Petersen *et al*., 2007). Green *et al,* (2011) showed that the inflammatory and insulin resistant phenotype was conserved in muscle satellite cells isolated from obese impaired glucose tolerant and obese T2DM subjects. Nuclear factor-kappa β-p65 DNA binding activity was elevated and insulin-stimulated glucose uptake was suppressed in muscle satellite cells from these individuals (Green *et al*., 2011). Moreover, 3 week-old mice fed a high-fat diet for 3 weeks had reduced muscle mass as well as reduced muscle regeneration capacity (Woo *et al*., 2011). In another study, muscle satellite cell activation and proliferation was impeded in high-fat diet mice after cardiotoxin induced muscle injury (Fu *et al*., 2016). Therefore, the targeted degradation of muscle protein, regulatory and transcription factors as well as altered muscle regeneration in T2DM patients are factors that potentially exacerbate disease progression and co-morbidity development.

Studies have shown the involvement of pro-inflammatory cytokines and endotoxin-derived inflammation in muscle wasting. IL-6 infusion induced muscle wasting and muscle specific degradation genes were up-regulated in a model of sepsis (Haddad *et al*., 2005), whereas Ono *et al*, (2020) showed that LPS-induced inflammation induced the expression of MuRF-1 and Atrogen-1 and a down regulation in muscle regulatory factors (MyoD and myogenin) resulting in a decrease in muscle fiber size (Ono *et al*., 2020). In another study, muscle wasting associated with an increase in ubiquitin and proteasome expression was observed in healthy animals exposed to pro-inflammatory cytokines (Costamagna *et al*., 2015; Tisdale, 2008). The activation of nuclear factor-κB (NF-κB) is thought to be the mediating factor of increased pro-inflammatory cytokines (Ono *et al*., 2020; Ono & Sakamoto, 2017). The activity of NF-κB has been implicated in inflammation-mediated diseases and has been associated with the positive regulation of genes involved in atrophy (Baker *et al*., 2011; Costamagna *et al*., 2015; Holland *et al*., 2011; Tisdale, 2008). Structural proteins, such as myosin and actin, which are essential components in the process of muscle contraction are the major proteins that are degraded in muscle atrophy (Hasselgren *et al*., 2005; Ono *et al*., 2020). Endotoxin has also been shown to suppress insulin signalling via the upregulation of pathways involved in inflammation (Liang *et al*., 2013).

2.3 Obesity-induced inflammation

Adipose tissue plays an essential role in energy homeostasis. Adipocytes function by storing free fatty acids in the form of triglycerides and releasing them as non-esterified fatty acids into the circulation (Tsatsoulis *et al*., 2013). Adipocytes also function as an endocrine and paracrine organ, secreting cytokines such as TNF-α, IL-6, and adipokines including leptin and adiponectin which influence food intake, systemic insulin sensitivity as well as nutrient homeostasis (Makki *et al*., 2013; Sell *et al*., 2006).

Obesity is characterised by the excessive accumulation of fat resulting in increased adipose mass. The increase in adipose mass is thought to be as a result of adipocyte hypertrophy and has been associated with adipocyte dysfunction characterised by increased secretion of free fatty acids, altered production of adipokines and increased secretion of inflammatory factors (Jack *et al*., 2019). Chronic elevated levels of plasma FFAs and pro-inflammatory cytokines, particularly TNF-α and IL-6, induce insulin resistance in peripheral tissues such skeletal muscle and liver and exacerbates β-cell dysfunction (Ruan & Lodish, 2003). Adipose tissue inflammation is also attributed to the infiltration of classically activated macrophages (M2 phase). The accumulation of these macrophages contributes to the secretion of inflammatory factors seen by the formation of crown-like structures as a result of macrophage aggregation around dead adipocytes (Cinti *et al*., 2005; Sam & Mazzone, 2014; Sun *et al*., 2011). Another source of inflammation has been attributed to gut derived endotoxins (Cani *et al*., 2007; Guerville *et al*., 2017). Elevated circulating levels of plasma endotoxin has been associated with metabolic syndrome and contributing to the chronic elevated levels of pro-inflammatory cytokines (Chen *et al*., 2015; Lassenius *et al*., 2011; Liang *et al*., 2013, 2018). Therefore, this supports the notion of a chronic low-grade inflammation observed in obese and T2DM patients, contributing to the development of insulin resistance and pathogenesis of T2DM.

2.3.1 Lipid overload: Fatty acid modulation of skeletal muscle mass and function

Free fatty acids (FFAs) have been identified as mediators of skeletal muscle dysfunction. FFA induce insulin resistance in humans by inhibiting glucose transport and reducing the rate of muscle glycogen synthesis and glucose oxidation by approximately 50% (Roden *et al*., 1996). Palmitate is the most abundant circulating saturated fatty acid and has been shown to suppress

insulin signalling and decrease myotube diameter (Bryner *et al*., 2012; Chavez & Summers, 2003, 2010; Lipina & Hundal, 2017; Mazibuko *et al*., 2013). Saturated FFAs induce skeletal muscle inflammation through interaction with toll-like receptors 2 and 4 (TLR2, TLR4) (Holland *et al*., 2008, 2011; Senn, 2006) and TLR4 deletion improves peripheral insulin sensitivity in animals fed high-fat diets (Cani *et al*., 2008; Kim *et al*., 2007; Poggi *et al*., 2007). In *in vivo* and *in vitro* studies Radin and colleagues were able to show that inhibition or deletion of TLR4 confers protection against lipid-induced insulin resistance as well as palmitate-induced activation of NF-κB (Radin *et al*., 2008). Increased TLR4 expression and signalling is also observed in obese and T2DM subjects (Reyna *et al*., 2008), suggesting that lipid overload modulates muscle function by up-regulating pro-inflammatory genes via NF-κB activation (Green *et al*., 2011; Jové *et al*., 2005; Jové *et al*., 2006).

2.4 Role of gut-derived endotoxin in metabolic syndrome

It is well known that high-fat Western diets and physical inactivity are the major factors responsible for the growing obesity and diabetes epidemic. In particular, the Western diet was shown to alter the intestinal barrier, resulting in the passage of bacterial endotoxin lipopolysaccharides (LPS) into the systemic circulation (Guerville *et al*., 2017; Rohr *et al*., 2019). Lipopolysaccharides are large, heat stable molecules and are the major constituents on the outer membrane of gram-negative bacteria (Caroff & Karibian, 2003; Erridge *et al*., 2002). Low, yet significant amounts of LPS are found in the plasma of obese individuals, described as metabolic endotoxemia, referring to a state of chronically elevated plasma LPS concentration induced by fatty acid rich western diets (Boutagy *et al*., 2016; Clemente-Postigo *et al*., 2019). Thus suggesting that metabolic endotoxemia is a mediating source of increased inflammatory environment seen in obese rodents (Cani *et al*., 2007).

LPS enters the circulation by crossing the gastrointestinal barrier via leaky intestinal tight junctions or by infiltrating lipoproteins involved in the transport of dietary lipids from the gut chylomicrons (Levels *et al*., 2005). Once in circulation, LPS is bound by LPS-binding protein (LBP), an acute phase protein synthesized in the liver in response to LPS, and interacts with tissues such as the liver, adipose tissue, and skeletal muscle as well as triggering the innate immune response. TLR4 is a target ligand for LPS and is ubiquitously expressed in adipose tissue and skeletal muscle. The activation of TLR4 results in the downstream signalling cascade that activates the NF-κB

protein complex. Nuclear factor kappa B then translocates to the nucleus where it induces the expression of pro-inflammatory genes (TNF-α, IL-6) (Baker *et al*., 2011; Ono & Sakamoto, 2017). As previously mentioned, increased pro-inflammatory cytokines exert their mechanisms on peripheral tissue, concomitantly exacerbating pro-inflammatory cytokine concentrations.

2.5 Adipocyte-myocyte crosstalk interaction between skeletal muscle and adipose tissue

It is well known that increased levels of plasma FFAs contribute to insulin resistance in peripheral tissues such as skeletal muscle and liver (Bays *et al*., 2004; Boden *et al*., 2005). The adipose tissue is acknowledged as an endocrine organ secreting various adipokines that have paracrine action on whole body metabolism. It is also well established that the adipose tissue of obese individuals has an altered secretory profile, largely due to expanded and inflamed adipocytes. It has been reported that adipose tissue inflammation is geared towards a pro-inflammatory state, thus secreting elevated levels of pro-inflammatory adipocytokines. These adipocytes have been hypothesised to be involved in the development of insulin resistance (Clemente-Postigo *et al*., 2019; Kershaw & Flier, 2004; Makki *et al*., 2013; Mohamed-Ali *et al*., 1998; Sun *et al*., 2011). Adiponectin is predominantly expressed and secreted by differentiated adipocytes (Körner *et al*., 2005) and its expression has been shown to be decreased in *ob/ob* mice and obese humans (Hu *et al*, 1996). The insulin sensitising effects of adiponectin were demonstrated by Yamauchi *et al* in an insulin resistant lipoatrophic mouse model, which displays both adiponectin and leptin deficiencies. Administration of adiponectin to this mouse model ameliorated insulin resistance by decreasing triglyceride content in liver and muscle (Yamauchi *et al*., 2001), suggesting the association between adiponectin and the development of insulin resistance.

Much like the adipose tissue, the skeletal muscle is also recognised as an endocrine organ, secreting myokines, including myostatin, IL-6, myonectin, fibroblast growth factor-21 (FGF21) and irisin as well as IL-15 (Li *et al*., 2017). Proliferating myoblasts secrete myokines that suppress neurogenesis and adipogenesis, while secreting myokines that specifically promote myotube formation, vascularisation, and neurogenesis during differentiation, suggesting that muscle cells secrete a variety of myokines at different stages of growth (Ojima *et al*., 2014; Podbregar *et al*., 2013). Interleukin-6 is a well-documented myokine and it has been shown that proliferating myoblasts secrete IL-6, which is thought to play a role in myogenesis, including muscle

regeneration (Austin, Bower, Kurek, & Vakakis, 1992; Serrano *et al*., 2008). Skeletal muscle significantly secrete IL-6 during exercise that is related to the intensity and duration of the exercise suggesting that IL-6 may have anti-inflammatory/paracrine effects that mediate hepatic glucose output necessary to maintain blood glucose homeostasis during exercise (Helge *et al*., 2003; Bente Klarlund Pedersen *et al*., 2001). However, as mentioned previously, chronic elevated plasma IL-6 levels derived from inflamed, hypertrophied and dysfunctional adipocytes has the opposite effect, inducing insulin resistance in skeletal muscle tissue (Ruan & Lodish, 2003).

On the other hand, myonectin promotes fatty acid uptake by adipocytes and hepatocytes by upregulating the expression of genes that are involved in lipid uptake, resulting in the reduction of circulating FFAs. Myonectin expression stimulated by exercise is found to be decreased in obesity (Li *et al*., 2017; Seldin *et al*., 2012; Wu & Ballantyne, 2017). Irisin is thought to improve glucose homeostasis and induce browning of white adipose tissue via the upregulation of PGC1-α, however, irisin expression is reduced in obese subjects (Boström *et al*., 2012; Lee *et al*., 2014; Li *et al*., 2017; Vaughan *et al*., 2014; Wu & Ballantyne, 2017). Therefore, a sedentary lifestyle results in the lack of contraction-induced myokines and eventually results in chronic low-grade inflammation, therefore significantly affecting skeletal muscle function and structure.

2.5.1 Co-culture system: Adipocyte-myocyte crosstalk

Co-culture is a developed method using two different cell types cultured in a common medium. This type of cell culture allows interaction between the two cell types, where one cell type may have an influence on cell function and interaction on another cell type (Muthuraman, 2014). This allows for the paracrine communication between two different cell types, mimicking the molecular interaction between different cell types and tissues *in vivo*. A common method of co-culture is using trans-well plates where one cell type is grown on a permeable membrane (trans-well insert) that is suspended in a shared common medium with the second cell type (figure 1). This arrangement allows for the study on the effects of secreted products (e.g. cytokines) on adjacent cell types (Pandurangan & Hwang, 2014).

Using co-culture, Chu *et al,* (2016) showed that differentiated C2C12 myotubes significantly decreased mRNA levels of Cyclin D and Cyclin E, increased FAS mRNA levels, and increased the activity of caspase 3 in 3T3-L1 adipocytes, resulting in the inhibition of cell proliferation and induction of cell apoptosis in 3T3-L1 adipocytes, demonstrating that co-culture is an appropriate

method to study critical regulatory mechanisms between cells types (Chu *et al*., 2016). Moreover, Pandurangan *et al,* (2012) demonstrated that calpain, caspase, and HSP mRNA expressions were significantly changed in the C2C12 and 3T3-L1 co-culture as compared to their respective single monolayer controls (Pandurangan *et al*., 2012). The co-culture of adipocytes and skeletal muscle cells has allowed researchers to study and analyse the adipocyte-myocyte paracrine crosstalk (Dietze-Schroeder *et al*., 2005; Dietze *et al*., 2002; Kudoh *et al*.2018; Sarr *et al*., 2017; Seyoum, Fite, & Abou-Samra, 2011; Vu *et al*., 2007). Adipocyte-skeletal muscle co-culture results in insulin resistance in muscle cells as shown by a decreased IRS-1 and Akt phosphorylation (Dietze *et al*., 2002; Sarr *et al*., 2017) and suppressed insulin-stimulated glucose uptake in muscle cells (Kudoh *et al*., 2018). Muscle cells in co-culture also showed a decreased insulin-induced Akt (Ser473) phosphorylation and was proportional to adipocyte density (Kudoh *et al*., 2018).

These co-culture models have demonstrated that there is direct crosstalk between skeletal muscle and adipose tissue. Adipose tissue not only acts as the main site for energy storage, but also acts as an endocrine organ regulating satiety and energy homeostasis, and more specifically related to this study, energy homeostasis regulation via skeletal muscle and adipose tissue communication with each other through the release of adipokines and myokines (Sell *et al*., 2006; Wu & Ballantyne, 2017). In obesity-induced inflammation, the adipocytes themselves are insulin resistant and dysfunctional, exacerbating metabolic disorders including insulin resistance in skeletal muscle (Sell *et al*., 2006).

2.6 Rooibos (*Aspalathus linearis*)

Aspalathus linearis, commonly known as rooibos, is a South African herbal fynbos plant species enjoyed as a hot or cold beverage and loved for its taste and aroma. The rooibos shrub is indigenous to the Cederberg region of the Western Cape Province of South Africa (Joubert & de Beer, 2012). Rooibos health-promoting benefits include its anti-diabetic and anti-obesity properties, improved appetite, cure for insomnia, stimulation of milk production in breast-feeding women, and reduced nervous tension, has further contributed to its popularity (Canda, *et al.*, 2014; Joubert & de Beer, 2012; Kamakura *et al*., 2015; Muller *et al*., 2012; Sanderson, *et al*., 2014).

Over the past few years there has been much scientific interest in the role of rooibos phenolic compounds in ameliorating metabolic syndrome. Mazibuko *et al,* (2013 and 2015) demonstrated

an ameliorative effect of an aspalathin-enriched green rooibos extract (GRE) and aspalathin (the major flavonoid in rooibos) on insulin resistance in C2C12 skeletal muscle cells and 3T3-L1 adipocytes, respectively. GRE improved insulin stimulated glucose uptake and increased Akt phosphorylation and insulin-stimulated GLUT 4 expression (Mazibuko *et al.*, 2013). Studies have also shown that rooibos and/or its phenolic compounds modulated adipogenesis by decreasing leptin expression (Sanderson *et al*., 2014). The consumption of rooibos (six cups/day for 6 weeks) showed a reduction in serum low-density lipoprotein (LDL) as well as triglycerides in individuals at risk for cardiovascular disease (Marnewick *et al*., 2011) and increased plasma anti-oxidant potential in healthy subjects (Villaño *et al*., 2010). Aspalathin also exhibited anti-inflammatory effects in LPS-stimulated human umbilical vein endothelial cells (HUVECs) where cytokine secretion (IL-6 and TNF-α) was reduced after treatment, furthermore, aspalathin also suppressed NF-κB and ERK1/2 activation by LPS (Lee & Bae, 2015). Aspalathin also improved mitochondrial respiration in palmitate-induced insulin resistant C3A liver cells. Basal respiration was improved after incubation with aspalathin. Aspalathin was shown to increase ATP production, maximal respiration and spare respiratory capacity, suggesting that aspalathin has the ability to improve intracellular energy levels (Mazibuko-Mbeje *et al*., 2019) under metabolic stress conditions.

Afriplex GRT™ (GRT), an aspalathin-rich green rooibos extract, is a pharmaceutical grade product containing 12.8% aspalathin (Patel *et al*., 2016). GRT has been shown to have hypoglycaemic and lipid lowering properties in high-fat diet-induced diabetic primates (Orlando *et al*., 2019). This was supported by the decrease in low-density lipoprotein (LDL) in diabetic monkeys, where as non-diabetic monkeys had increased high-density lipoprotein (HDL) (Orlando *et al*., 2019). The effects of GRT is under investigation to further elucidate its modulating effects on the metabolic syndrome.

2.7 *In vitro* Models

2.7.1 C2C12 myoblast

C2C12 muscle cells, an immortalized myoblast cell line derived from satellite cells, show a typical behaviour that corresponds to that of progenitor lineage (Blau *et al*., 1983; Burattini *et al*., 2004; Wong *et al*., 2020; Yaffe & Saxel, 1977). The C2C12 myoblast cell line is a well-documented *in vitro* model that has facilitated our understanding in the myogenesis pathway (Dedieu *et al*.,

2002), metabolic disease progression (Wong *et al*., 2020) and muscle atrophy (Ono & Sakamoto, 2017; Thomas *et al*., 2000). Multiple studies using this cell line have allowed us to have a comprehensive understanding of the metabolic processes at cellular levels including glucose transport and metabolism, insulin signalling mechanisms, and oxidative stress which have been implicated in insulin resistance (Frisard *et al*., 2015; Jové *et al*., 2006; Luo *et al*., 2019; Mazibuko *et al*., 2013; Muller *et al*., 2012; Ono & Sakamoto, 2017; Thomas *et al*., 2000).

In the undifferentiated state, the myoblasts appear as flat stellate or spindle-shaped mononucleated cells (figure 2.2) (Burattini *et al*., 2004; Kataoka *et al*., 2003; Wong *et al*., 2020). C2C12 myoblasts express MRFs (MyoD, myogenin, Myf5 and MRF-4), proteins known to be exclusively expressed in cells committed to the myogenic lineage (Burattini *et al*., 2004; Dedieu *et al*., 2002; Delgado *et al*., 2003; Krempler & Brenig, 1999). The expression of these MRFs is tightly regulated during myogenesis and each possesses a critical function within the myogenesis pathway (Dedieu *et al*., 2002). This was shown by Dedieu *et al*, (2002) where the transfection of C2C12 cells with an antisense strategy using oligonucleotides against MyoD, myogenin, and Myf-5 significantly affected myoblast fusion compared to the non-treated control, therefore concluding that the fusion of myoblasts is a critical step in the elongation of multinucleated muscle fibres during muscle differentiation. Glucose transporter 4 (GLUT4), predominantly activated by insulin stimulation, is highly expressed in C2C12s, making this cell line useful in studies related to glucose transport/metabolism and insulin signalling in metabolic disease (Luo *et al*., 2019; Mangnall *et al*., 1993; Mazibuko *et al*., 2013; Muller *et al*., 2012). Another characteristic feature of mature muscle fibres is the expression of myosin heavy chain II (MyHC II), which has also been used as a marker for identifying mature multinucleated myotubes upon differentiation of C2C12 myoblasts (Ono & Sakamoto, 2017).

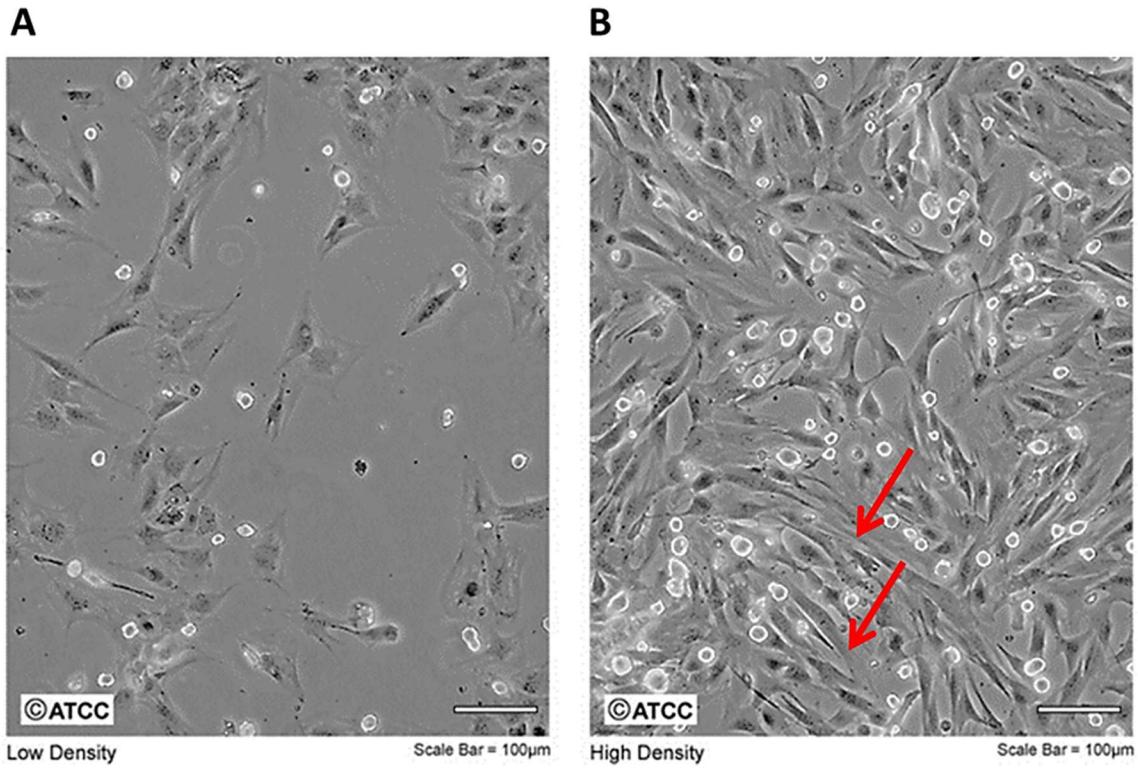

Figure 2.2: Photomicrograph of C2C12 myoblasts viewed under the microscope (Senn, 2006). C2C12 myoblasts at low density appear as flat stellate cells (A). At high density, myoblasts begin to align and elongate to form the characteristic myotubules, as shown by arrows (B). (American Type Culture Collection, 2017) https://www.atcc.org/products/all/CRL-1772.aspx#characteristics

2.7.2 C2C12 myoblast differentiation

The C2C12 cell line is a model of choice in many studies due to its ability to rapidly proliferate and differentiate to form contractile multinucleated myotubes. C2C12 myoblasts are commonly cultured in Dulbecco's modified Eagle's medium (DMEM) containing glucose (4.5 g/L) and supplemented with foetal bovine serum (FBS), usually at 10% final concentration and antibiotics such as gentamycin, amphotericin B and a cocktail of penicillin and streptomycin (PenStrep). To differentiate, the myoblasts are allowed to proliferate to confluence and thereafter fed with differentiation medium containing 2% horse serum (HS). Upon differentiation, C2C12 myoblasts develop myocytes which fuse to form elongated multinucleated fibre-shaped structures (myotubes) within 3 – 7 days after the addition of differentiation medium. (Mazibuko *et al*., 2013; Muller *et al*., 2012; Wong *et al*., 2020). It is worth noting that the differentiation potential of the

myoblasts is dependent on how the cells are subcultured. Thus, to prevent the loss of myoblastic properties during subculturing, it is critical that the cells are not allowed to reach confluence (American Type Culture Collection, 2017).

2.7.3 *In vitro* model of obesity

3T3-L1 is a pre-adipose cell line isolated and expanded from Swiss 3T3 cells. This was based on their ability to accumulate lipids (Green & Kehinde, 1975; Green & Meuth, 1974). 3T3-L1 pre-adipocytes are widely used as an *in vitro* model of white adipocytes to study and understand adipogenesis. It is also a well-established model of obesity (Dludla *et al*., 2018; Jack *et al*., 2017; Mazibuko-Mbeje *et al*., 2020; Sanderson *et al*., 2014). Upon confluency, 3T3-L1 preadipocytes undergo growth arrest and differentiate into mature adipocytes with the use of pro-differentiation treatment/agents such as insulin, synthetic glucocorticoids and 1-methyl-3-isobutyl xanthine (IBMX), a phosphodiesterase inhibitor (Morrison & McGee, 2015).

3 METHODS

3.1 Materials

The materials together with their suppliers and product/catalogue numbers used in this study are listed in the Appendix section.

3.2 General cell culture protocol

3.2.1 Thawing cells

Two cryogenic vials each containing 3T3-L1 ($1x10^6$ cells/mL) and C2C12 ($1x10^6$ cells/mL) in cryopreservation media constituting of DMEM supplemented with 10% FBS and 7% dimethyl sulfoxide (DMSO) was thawed in a pre-warmed water bath (37ºC). One milliliter of the thawed cell suspension was then transferred into a 15 mL centrifuge tube containing 9 mL of pre-warmed growth media (DMEM supplemented with 10% FBS). Cells were pelleted by centrifugation at 800 rpm for 5 minutes. After centrifugation, the supernatant was gently removed by aspiration and the cell pellet was re-suspended in pre-warmed growth media by gently mixing up and down to dislodge pellets into single cells. Thereafter, 1 mL of cell suspension was transferred into T75 cell culture flasks containing 17 mL of pre-warmed growth media in each flask containing 3T3-L1 or C2C12 cells, respectively. The flasks were incubated in a humidified incubator at 37ºC and 5% carbon dioxide (CO_2) until they reached 60 – 70% confluence. Cells were refreshed on day 2 post inoculation by removing spent media and replacing with fresh pre-warmed growth media. After 3 days, cells were then sub-cultured as described in the section below.

3.2.2 Subculture and maintenance

Upon reaching 60 - 70% confluency, sub-cultures of 3T3-L1 and C2C12 cells were produced. Spent growth media was aspirated and cells were washed with 8 mL Dulbecco's phosphate buffered saline (DPBS). Thereafter, cells were incubated with 2 mL of trypsin-versene for 5 minutes at 37ºC. To ensure adequate detachment, cells were observed under an inverted microscope. Trypsinization was inhibited by the addition of pre-warmed growth media. Using a 10 mL serological pipette, cells were gently dissociated by pipetting up and down. The cell suspension was then transferred into a centrifuge tube and pelleted by centrifugation and the supernatant was removed by aspiration. To dislodge the cell pellet into single cells, cells were re-suspended in pre-warmed growth media and the number of viable cells were counted.

Thereafter, 3T3-L1 and C2C12 cells were sub-cultured into T75 cell culture flasks at 1:8 split ratio and incubated in at 37ºC in 5% CO_2 and humidified air. Cells were passaged every 2 - 3 days upon confluency of 60 - 70%. C2C12 myoblasts and 3T3-L1 preadipocytes were used between passages 20 – 28 and 13 – 20, respectively, for all experiments.

3.2.3 Trypan blue exclusion assay

Cell counting was determined by employing the trypan blue exclusion assay (Strober, 2015). The assay allows for light microscopic quantitation of cell viability. The basic principle of the assay relies on the integrity of the cell membrane where, live cells possess an intact cell membrane that excludes the trypan blue dye, whereas non-viable cells do not and therefore absorb the dye (Strober, 2015). To determine the number of viable cells in a cell suspension, 10 µL of 0.4% trypan blue dye was added to 10 µL cell suspension and mixed gently. Subsequently, 10 µL of the trypan blue and cell suspension mixture was loaded on to one chamber of the haemocytometer and viewed under an inverted microscope, where viable and non-viable cells were counted. Thereafter, the percentage and total number of viable cells were calculated as shown in the equations below. Required seeding densities were prepared thereafter (Table 1).

$$viable\ cells\ (\%) = \frac{Total\ number\ of\ viable\ cells}{Total\ number\ of\ cells\ (viable + non\ viable)} \times 100\%$$

$$cells/mL = \frac{total\ number\ of\ viable\ cells \times dilution\ factor \times 10\,000}{no.of\ quadrants}$$

3.2.4 Seeding of 3T3-L1 pre-adipocytes and C2C12 myoblasts

After quantifying the number of viable cells (section 3.2.3), 3T3-L1 pre-adipocytes and C2C12 myoblasts were seeded in respective multiwell plates (Table 1) at 20 000 cells/mL and 25 000 cells/mL for assay purposes, respectively. Thereafter, cells were incubated at 37ºC in 5% CO_2 and humidified air until they reached 90 – 100% confluency.

Table 1: Cell densities for seeding 3T3-L1 pre-adipocytes and C2C12 myoblasts.

Cell line	Multiwell Plate	Cell concentration (cells/mL)	Cell density (cells/well)	Volume
3T3-L1	24 well (Transwell)	$2.0x10^4$	$1.0x10^4$	500 µL
C2C12	96 well	$2.5x10^4$	$5.0x10^3$	200 µL
	24 well	$2.5x10^4$	$2.5x10^4$	1 mL
	6 well	$2.5x10^4$	$7.5x10^4$	2 mL

3.2.5 Differentiation

3.2.5.1 3T3-L1 pre-adipocyte

When cells reached 100% confluence, growth medium was substituted with adipocyte differentiation medium (ADM). The ADM consisted of DMEM, supplemented with 10% FBS, 1 µg/mL insulin, 0.5 mM 3-isobuytl-1-methylxanthine (IBMX) and 1 µM dexamethasone to induce differentiation (day 0). After 72 hours (day 3), ADM was removed from the cells and replaced with adipocyte maintenance medium (AMM) which consisted of DMEM, supplemented with 10% FBS and 1 µg/mL insulin for an additional two days. On the fifth day of differentiation AMM was removed and replaced with growth medium for an additional 2 days. Cells were incubated at 37ºC in 5% CO_2 and humidified air. Thereafter, relevant treatments and assays were performed.

3.2.5.2 C2C12 myoblasts

To induce differentiation, seeded myoblasts were grown to confluence 72 hours post seeding. Growth medium was removed and replaced with differentiation medium (DMEM supplemented with 2% HS) for 3 days, cells were refreshed on the second day from induction of differentiation (day 0). On the third day of differentiation, the myocytes had fused to form mature myotubes as could be observed under the inverted light microscope. Cells were incubated at 37ºC in 5% CO_2 and humidified air.

3.3 Treatment preparation

All final concentrations were prepared in phenol red-free DMEM, containing 33 mM glucose and sodium bicarbonate, supplemented with 2% fatty acid-free bovine serum albumin (BSA) unless otherwise stated. For lipopolysaccharide preparation, 1 mg of LPS was dissolved in 1 mL phosphate buffered saline (PBS) to obtain a stock concentration of 1 mg/mL. Stock solution of LPS was aliquoted and stored at -20ºC until required. A working concentration of 20 µg/mL LPS solution was prepared in DMEM, thereafter appropriate treatment concentrations were prepared from the working LPS solution. A concentrated stock solution of Afriplex GRT™ (GRT) (10 mg/mL) was prepared in 10% DMSO and thereafter a working stock solution of a 1 mg/mL solution was prepared in DMEM.

3.4 Adipocyte-myocyte crosstalk

3.4.1 Adipocyte-skeletal muscle co-culture

3T3-L1 adipocytes and C2C12 skeletal muscle cells were seeded and differentiated as previously described. On the 7th day of post-differentiation, cell culture inserts containing mature 3T3-L1 adipocytes were individually transferred to cell culture plates containing C2C12 myoblasts using sterile forceps. This assembly resulted in a co-culture system where the two cell types shared the same medium but remained separated. C2C12 myoblasts were co-cultured with either 3T3-L1 pre-adipocytes or mature adipocytes in DMEM supplemented with 10% FBS.

3.5 Cell culture treatment

The C2C12 myoblast monoculture and co-culture were washed with pre-warmed DPBS. Thereafter, the cell culture was treated with LPS and/or GRT, prepared as described in section 3.3 for 24 hours. Insulin (1 µM) was added the last 15 minutes of treatment. The concentration of LPS selected was based on preliminary experiments and previously published data (Frost *et al*., 2002, 2003; Hussey *et al*., 2013; Liang *et al*., 2013; Ono & Sakamoto, 2017; Perry *et al*., 2018).

3.6 Inflammation-induced inhibition of myogenesis

3.6.1 Effect of LPS on myoblasts

C2C12 myoblast were seeded in multiwell plates as described in section 3.2.4. After 48 hours, cells were treated with or without LPS (0.1 µg/mL and 1 µg/mL) for 24 hours. Thereafter, 2-deoxyglucose uptake was conducted and media was collected for the measurement of cytokine secretion by enzyme-linked immunosorbent assay (ELISA). Cells were harvested for Western blot analysis and quantitative reverse transcription polymerase chain reaction (qRT-PCR).

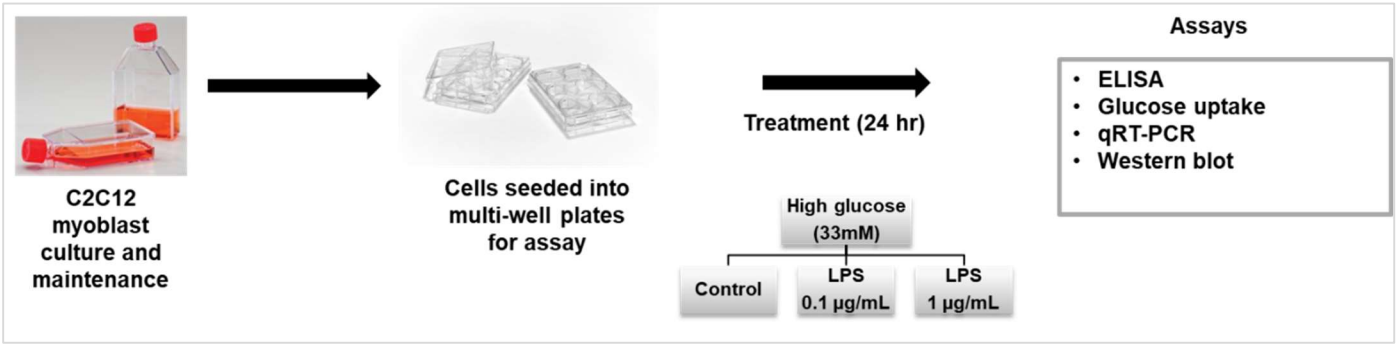

Figure 3.1: Experimental design of *in vitro* C2C12 model.

3.6.2 Effect of LPS on myogenesis study

To determine the effect of LPS on myogenesis, C2C12 myoblasts were seeded in 6 well plates as described in section 3.2.4 with minor modifications. After 48 hours, myoblasts were washed with pre-warmed DPBS and subsequently treated with or without LPS (0.1 µg/mL and 1 µg/mL) in growth media. After 48 hours, the growth medium was removed and replaced with differentiation media to induce myoblast differentiation for a further 48 hours with or without LPS. On the third day (day 3) the formation of myotubes were observed under an inverted light microscope (Figure 3.2.).

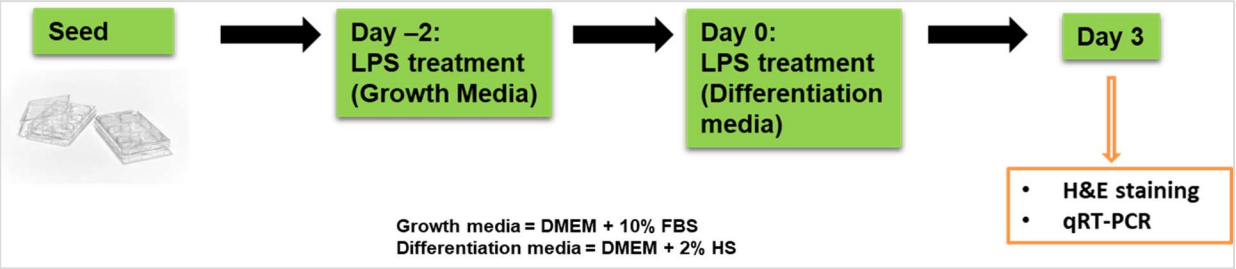

Figure 3.2: C2C12 myogenesis experimental design. C2C12 myoblasts were differentiated in the presence of LPS.

3.7 Cell viability assessment of LPS and GRT in C2C12 model

C2C12 cells were seeded and either differentiated or not in 96 well culture plates mentioned in section 3.2.4. Thereafter, cells were treated with a range of concentrations of LPS (0.05 µg/mL – 1 µg/mL) for 24 hours. For GRT treatments, C2C12 myoblasts were seeded and differentiated in 24 well plates. Cells were then treated with various concentrations of GRT (0.001 µg/mL – 100 µg/mL) at different time points, i.e., 4, 8, 16 and 24 hours.

3.8 3- [4, 5-dimethylthiazol-2-yl]-2, 5 diphenyltetrazolium bromide (MTT) assay

MTT assay is a quantitative colorimetric assay that measures cell metabolic activity as an indicator of cell viability, proliferation and cytotoxicity based on mitochondrial activity. This assay developed by Mosmann, (1983) measures the reduction of the yellow tetrazolium salt (MTT) to water insoluble purple formazan crystals in metabolically active cells by mitochondrial succinate dehydrogenase (Mosmann, 1983).

C2C12 cells were treated as mentioned in section 3.7, thereafter, medium was aspirated. Cells were washed with pre-warmed DPBS and 50 µL of pre-warmed MTT solution (2 mg/mL) was added to each well in both 96 well and 24 well plates, respectively. Thereafter, cells were incubated at 37ºC in 5% CO_2 and humidified air for 30 minutes. The MTT solution was aspirated, and the purple formazan crystals were dissolved in 25 µL Sorenson's glycine buffer and 200 µL of DMSO. Absorbance was measured at 570 nm using the BioTek ELx800® plate reader and Gen5® software for data acquisition.

3.9 Enzyme-linked immunosorbent assay (ELISA)

A mouse IL-6, IL-10 and adiponectin/Acrp30 sandwich ELISA kit was used for detection and quantitation of IL-6, IL-10 and adiponectin secreted by 3T3-L1 and C2C12 (adiponectin was only for 3T3-L1 adipocytes) cells into the media according to the manufacturer's instructions. Briefly, spent culture media was collected from adipocyte-myocyte co-culture and C2C12 mono-culture, after 24 hours of LPS, GRT treatment and the combination thereof. Ninety-six well microplates were coated with primary antibody diluted to working concentration in coating buffer and incubated at room temperature overnight. The plates were washed three times with 1x wash buffer and blocked with 1% BSA solution for 1 hour. Thereafter, prepared standards and thawed media samples were added to the microplates and incubated for 2 hours at room temperature. Bound IL-6 protein was detected using a secondary antibody, streptavidin-horseradish peroxidase, substrate solution (H_2O_2 and tetramethylbenzidine) and 2N sulfuric acid. Absorbance was measured at 450 nm in a multifunction microplate reader. To correct for optical imperfections at 450 nm, OD at 540 nm was subtracted from 450 nm OD readings. A standard curve was generated, and IL-6, IL-10 and adiponectin concentrations were extrapolated thereof. The IL-6 concentrations used for the standard curve were 15.6, 31.3, 62.5, 125, 250, 500 and 1000 pg/mL, and 31.3, 62.5, 125, 250, 500, 1000, and 2000 pg/mL for IL-10 and adiponectin, respectively.

3.10 2-deoxyglucose uptake assay

A glucose uptake kit was used to quantify 2-deoxyglucose (2DG) uptake by C2C12 myoblasts according the manufacturer's instructions and Valley *et al*., (2016), with minor modifications. After treatment, C2C12 myoblasts were washed once with pre-warmed DPBS. Thereafter, 250 µL of 0.1% BSA KRBH was added to each well and cells were serum and glucose starved for 2 hours with insulin (1 µM) added in the last 20 minutes. Twenty-five microliters of 1 mM 2DG in KRBH was added to each well except for the negative control (without 2DG) and incubated for 30 minutes at 37°C in 5% CO_2 and humidified air. To stop the enzymatic reaction, cells were lysed by adding 125 µL of acidic detergent (2% dodecyltrimethylammonium bromide (DTAB) in 0.4M HCl) to each well and placed on a plate shaker for 10 minutes at 60 x 10 rpm for thorough lysing and mixing. Seventy-five microliters of cell lysate were transferred into white walled 96 well microplates and 25 µL of neutralization

buffer (1M Trizma) was added to each well to neutralize the pH. 2-deoxyglucose-6-phosphate (2DG6P) was then detected by adding 100 µL of detection reagent. Luminescence was measured at 15-minute intervals for 1 hour and 30 minutes using the Spectramax i3® multi-mode plate reader. Acidic detergent, neutralization buffer, and 2DG6P detection reagent contain critical components for the detection reaction and thus were also added to the standards. The standard curve was generated using the 1-hour luminescence values to determine 2DG6P concentration. Luminescence signal produced in this assay is proportional to the rate of glucose uptake (Valley *et al*., 2016).

3.11 C2C12 myoblast mitochondrial function

Oxygen consumption rate (OCR) was measured with the Mito Stress assay kit, using the XF96 Extracellular Flux analyzer from Agilent. C2C12 myoblasts were seeded into XF96 cell culture microplates at 12 000 cells per well for 24 hours. After 24 hours, confluent cells were differentiated with differentiation medium for a further 24 hours. Cells were then treated with GRT as previously described. After treatment, cells were washed twice with 180 µL of pre-warmed XF base medium containing 8 mM glucose, 1 mM sodium pyruvate and 2 mM glutamine (pH was adjusted to 7.4), and subsequently incubated with 180 µL of XF assay medium at 37^0C in an incubator (non-CO_2) for 45 min to equilibrate temperature and pH prior to the measurement of OCR. The XF96 microplate plate containing cells was then transferred to the Seahorse XF96® extracellular flux analyzer. The microplate containing cells subjected to a 10-minute equilibration period at three assay cycles, comprising of a 1-minute mix, 3 minutes wait, and 3 minutes measure period cycle. Once equilibration was complete, oligomycin (1 µM) was injected to inhibit ATP synthase. After 3 assay cycles, 0.75 µM carbonyl cyanide-4-trifluoromethoxy-phenylhydrazone (FCCP) was injected to measure maximal respiration. Thereafter, a combination of rotenone (complex I inhibitor) and antimycin (complex III inhibitor) was injected to collapse mitochondrial respiration and enable the calculation of non-mitochondrial respiration. At the end of the incubation period, the protein concentration was assessed using the Bradford protein assay. OCR (pmol/min) was normalized relative to the protein content.

3.12 Histological assessment

Cells were cultured and treated as mentioned in section 3.6.2 and subjected to haematoxylin and eosin (H & E) staining. C2C12 myotubes were washed with PBS and fixed with 1 mL of ice-cold 100% methanol and incubated at 4ºC for 5 minutes. Methanol was removed and cells were again washed with 1 mL PBS. Thereafter, cells were incubated with 1 mL of haematoxylin for 5 minutes at room temperature. The stained cells were rinsed twice with 2 mL of tap water (this allowed the conversion of the bright red colour to blue/purple termed as “Blueing”). Thereafter, 1 mL of eosin was added to each well and allowed to stain for 5 minutes at room temperature. Eosin was removed and stained cells were washed twice with PBS. Stained myotubes were visualized and imaged using the Nikon® microscope using the NIS elements software and five photomicrographs of non-overlapping fields were randomly selected. The width and number of each myotube containing ≥ 3 nuclei was measured and counted using imageJ software. Data is calculated and represented as an average of width and number of myotubes.

3.13 Quantitative reverse transcription polymerase chain reaction (qRT-PCR)

3.13.1 RNA extraction

Following exposure to treatment, cells were washed with cold DPBS. Three hundred microliters of QIAzol® lysis reagent was added per well and cells were scraped with a cell scraper and transferred into clean 1.5 mL Eppendorf tubes. Two hundred microliters of chloroform was added into each sample and mixed by inverting the tubes. The samples were incubated at room temperature for 10 minutes followed by centrifugation at 15 000 g for 20 minutes at 4ºC. The upper aqueous phase containing RNA was gently removed into clean 1.5 mL Eppendorf tubes. Thereafter, 0.5 mL of isopropanol was added to each sample and incubated at 20ºC overnight to precipitate the RNA. After overnight incubation, samples containing precipitated RNA were centrifuged at 15 000 RCF for 20 minutes at 4ºC to pellet the RNA. The supernatant was discarded, and the pellet was washed with 75% (% v/v) ethanol, followed by centrifugation at 15 000 RCF for 10 minutes at 4ºC. The wash step was repeated twice thereafter, the supernatant discarded, and the RNA pellet was air dried. The air-dried RNA pellet was re-dissolved in 50 µL of nuclease-free water and mixed by pipetting up and down several times. Samples were stored at -80ºC until required.

3.13.2 RNA quantification

RNA concentration and purity were assessed using the NanoDrop® spectrophotometer. The absorbance ratios, 260 nm/280 nm ($A_{260/280}$) and 260 nm/230 nm ($A_{260/230}$), are used to indicate the quality and purity of RNA. Ratios greater than 1.8 are accepted as measure of good quality of RNA (Garcia-Elias *et al*., 2017). To quantify the RNA, the spectrophotometer was blanked with 1 µL of RNase-free water. Thereafter, absorbance of each RNA sample was measured in duplicate and the mean value of the two readings were used to calculate the concentration.

3.13.3 Reverse transcription

Total RNA was reverse transcribed into complementary DNA (cDNA) using the QuantiTect Reverse Transcription Kit according to the manufacturer's instructions. RNA samples were thawed on ice and 1 µg of RNA sample was added to nuclease-free water to a total volume of 12 µL in clean 0.2 mL PCR tubes. To DNase treat the samples, 2 µL of gDNA Wipeout buffer was added to the RNA sample to a final volume of 14 µL and mixed by pipetting up and down twice. The RNA samples were then incubated at 42ºC for 2 minutes in a thermal cycler. Thereafter, master mix containing reverse transcriptase, buffer, and RT primer mix was prepared (Table 2) and scaled up to the number of samples requiring to be reverse transcribed. Six microliters of master mix were then added the RNA samples to a final volume of 20 µL and mixed thoroughly by pipetting up and down. The samples were briefly centrifuged (500 rpm) using a bench top microfuge. Subsequently RNA samples were reverse transcribed using a thermal cycler at the following settings: 30 minutes at 42ºC and 3 minutes at 95ºC. The samples were removed from the thermal cycler and diluted 1/10 by adding 180 µL of nuclease-free water and mixed by pipetting up and down several times. Samples were then stored at -20ºC until required.

Table 2: Reaction components for reverse transcription.

Reverse-transcription Master Mix components	Volume/reaction
Quantiscript Reverse Transcriptase*	1 µL
Quantiscript RT buffer+	4 µL
RT Primer Mix	1 µL
Total volume	**6 µL**

* Also contains RNase inhibitor

+ Includes Mg^{2+} and dNTPs

3.13.4 Gene expression analysis

A reaction mixture to a volume of 6 µL containing 5 µL TaqMan™ Fast Advanced Master Mix, 0.5 µL of TaqMan™ Gene Expression Assay and 0.5 µL nuclease-free water was prepared and scaled up according the number of samples to be assayed. Four microliters of each cDNA sample were added in duplicate into each well of a 384-well PCR plate followed by the addition of the reaction mixture to a final volume of 10 µL. A sample substituted with 4 µL of nuclease-free water, a no template control (NTC) sample (sample without cDNA), was designated as a negative control in all PCR reactions. The PCR plates were covered with an adhesive film, centrifuged briefly, and mixed using a plate shaker and followed by brief centrifugation. Thereafter, the PCR plate was analysed using the QuantStudio™ 7 Flex Real-Time PCR System using the QuantStudio™ Real-Time PCR software for data acquisition. The delta-delta Ct ($2^{-\Delta\Delta Ct}$) method was used to analyse the genes of interest.

3.14 Western blot analyses

3.14.1 Protein isolation and quantification

Following exposure of the cells to the stressor and optimized concentration of GRT, cells were washed once with ice cold DPBS (1 mL). Each condition was plated in triplicate and therefore 100 µL of commercial cell lysis buffer (supplemented with protease inhibitor cocktail tablets and 1 µM PMSF) was pipetted into each well. The cells were scraped using a cell scraper (blade width, 20 mm), pooled, and transferred to a 2 mL centrifuge tube to have a final volume of 300 µL. Samples were lysed by adding a stainless-steel bead into each tube and employing the use of the tissue lyser to homogenize the samples. Samples were homogenized at 25 Hz for 1 minute

and rested on ice at 1-minute intervals, this step was performed 5 times. The homogenized cell lysate was centrifuged at 13 000 rpm at 4ºC for 15 minutes and the supernatant, containing the cytoplasmic fraction, was transferred into an empty 1.5 mL centrifuge tube. The RCDC™ (reducing agent and detergent compatible) protein assay kit was used to quantify sample protein concentration. Five microliters of BSA standard concentrations (0.125, 0.25, 0.5, 0.75, 1.0, 1.5, and 2.0 mg/mL) and 5 µL of sample was transferred to a clean 96-well assay plate. Thereafter, 25 µL reagent A' and 200 µL or reagent B were added to each well. The plate was briefly agitated and incubated for 15 minutes at room temperature before measuring absorbance at 630 nm on a multi-mode plate reader. Absorbance readings were used to generate a BSA standard curve, which aided in the subsequent extrapolation of sample protein concentrations.

3.14.2 Preparation of acrylamide gels

The TGX Stain-Free™ FastCast™ Acrylamide kit was used to make 12% polyacrylamide gels. The resolving and stacking gels were prepared according to Table 3. To make the resolving gel solution, equal volumes of resolver A and resolver B solutions were mixed and thereafter, 10% ammonium persulfate (APS) and tetramethylethylenediamine (TEMED) were added and mixed gently. The resolver solution was gently added to 1.5-mm glass plates using a clean 10 mL serological pipette. Glass plates were placed on a casting stand to stabilize the plates during casting (step 1, Figure 2.3). For the stacking gel, equal volumes of stacker A and stacker B were mixed with 10% APS and TEMED. The stacking gel solution was added immediately above the resolving solution (step 2, Figure 2.3). The stacking gel solution was added gently to avoid mixing of the two gel solutions. Gels were allowed to polymerize for 30 – 45 minutes. If not used immediately, gels were covered with a paper towel moistened with deionized water and stored in a sealed plastic bag at 4ºC and used the following day.

Table 3: Hand-casting gel preparation volumes, where n is the number of gels required (Bio-rad).

	1.0 mm Bio-Rad Glass plates (n = gels)		**1.5 mm Bio-Rad Glass plates (n = gels)**	
	Stacker	**Resolver**	**Stacker**	**Resolver**
Resolver A	-	3 mL x n	-	4 mL x n
Resolver B	-	3 mL x n	-	4 mL x n
Stacker A	1 mL x n	-	1.5 mL x n	-
Stacker B	1 mL x n	-	1.5 mL x n	-
Total Volume	**2 mL x n**	**6 mL x n**	**3 mL x n**	**8 mL x n**
TEMED	2 µL x n			
10% APS	10 µL x n	30 µL x n	15 µL x n	40 µL x n

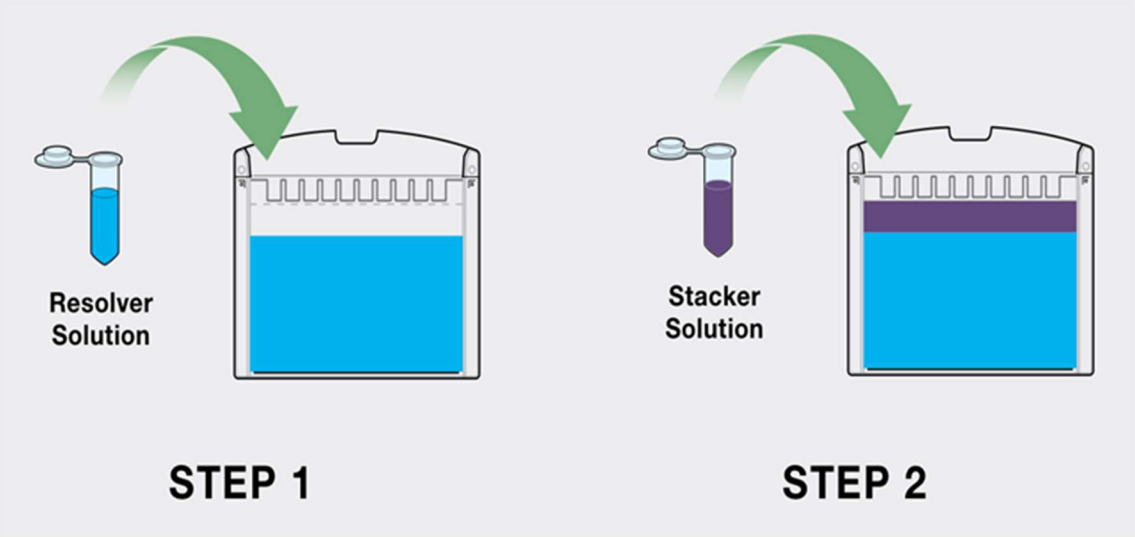

Figure 3.3: Image representing hand casting gels for SDS-PAGE. Resolving and stacking gels were added into 1.5 mm spacer plates.

3.14.3 Separation of proteins by SDS-PAGE

Prepared gels were placed in a mini protein tetra cell tank and filled with running buffer. To denature the proteins, protein samples were diluted 1:3 with 4x Laemmli sample buffer and heated at 95ºC for 5 minutes on a heating block. Thereafter, 30 - 40 µg of protein for each sample was loaded on to a 12% TGX Stain-Free™ polyacrylamide gel electrophoresis (PAGE) gel. A molecular weight standard marker was loaded and was used to monitor the protein separation through the gel. The gels were run for approximately 2 hours at 120V.

3.14.4 Protein transfer

Once proteins were separated, the gels were transferred to pre-cut 0.2 µm nitrocellulose membranes. Briefly, the cassette was removed from the Trans-Blot Turbo system and the transfer sandwich was assembled as illustrated in Figure 2.4. Filter paper (ion reservoir stack) from the Trans-Blot Turbo midi nitrocellulose transfer packs was placed on the cassette base (bottom ion reservoir stack) followed by the nitrocellulose membrane PAGE gel containing separated proteins and the top reservoir stack. Care was taken to remove air bubbles during the process of the sandwich assembly. The cassette lid was place firmly on to the sandwich stack and locked to the cassette base. Thereafter, the cassette was placed in the Trans-Blot Turbo system and the proteins were transferred for 10 minutes at 25V. Ponceau S stain was applied to the membrane for 5 minutes by gentle agitation on an orbital shaker to confirm transfer of proteins. The positively visualized proteins on the membrane were imaged using the ChemiDoc MP™ System. To de-stain the membrane, the nitrocellulose membrane was washed with Tris buffered saline containing Tween 20 (TBS-T) for 5 minutes.

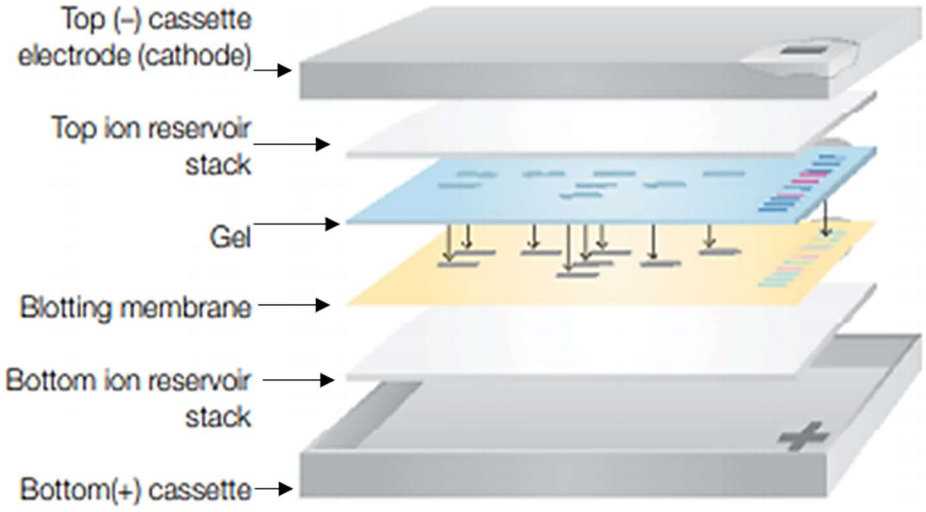

Figure 3.4: Sandwich assembly in the cassette. Proteins separated on SDS-PAGE were transferred to nitrocellulose membranes using the Trans-Blot Turbo system. Image obtained from Bio-rad Trans-Blot® Turbo™ Transfer System Quick Start Guide (https://www.bio-rad.com/sites/default/files/webroot/web/pdf/lsr/literature/10016505E.pdf).

3.14.5 Blocking and labelling of antibodies

To minimize nonspecific antibody binding, the nitrocellulose membrane was blocked with 5% BSA diluted in TBS-T for 1 hour at room temperature with gentle agitation on the orbital shaker. Primary antibody (Table 4) was diluted in TBS-T and was applied to each membrane and subsequently incubated overnight at 4ºC with gentle agitation on an orbital shaker. The membranes were washed three times in TBS-T for 5 minutes by gentle agitation on the orbital shaker. Thereafter, the membranes were incubated with secondary antibody (anti-rabbit or IgG-HRP) at a 1:4000 dilution in 2.5% BSA-TBS-T for 90 minutes with gentle agitation on an orbital shaker. After detection of primary phosphor-proteins, membranes were washed once in TBS-T for 5 minutes and subsequently blocked with 5% non-fat dried milk diluted in TBS-T for 1 hour at room temperature and thereafter washed trice with TBS-T for 5 minutes. Anti-β-actin antibody, diluted 1:1000 in TBS-T, was applied to each membrane and subsequently incubated overnight at 4ºC. Following overnight incubation, membranes were washed three times in TBS-T for 5 minutes with gentle agitation on an orbital shaker and subsequently incubated with secondary antibody (donkey anti-mouse IgG-HRP) at a 1:4000 dilution in 2.5% non-fat milk-TBS-T for 90 minutes. To detect total protein of the respective phosphor-proteins (Table 4), membranes were

stripped of the previously detected proteins by immersing the membranes in stripping buffer for 8 minutes. Thereafter, the membrane was washed twice in PBS by gentle agitation on an orbital shaker for 5 minutes followed by 2 times washes in 1x (Tris buffered saline) TBS for 5 minutes. The membranes were then labelled with primary antibodies as previously mentioned.

Table 4: Primary antibodies.

Primary antibody	Dilution	Catalogue no.	Manufacturer
phospho-Akt	1:2000	ab82183	Abcam
phospho-mTOR	1:800	2971	Cell Signaling Technology
phospho-AMPK	1:800	2535	Cell Signaling Technology
β-actin (housekeeping)	1:1000	Sc-47778	Santa Cruz Biotechnology
Akt	1:1000	9272	Cell Signaling Technology
mTOR	1:800	2972	Cell Signaling Technology
AMPK	1:1000	2532	Cell Signaling Technology

3.14.6 Chemiluminescence detection

A Clarity™ Western ECL Substrate detection kit was used to visualise proteins of interest by adding equal volumes of Clarity Western Peroxide Reagent and Clarity Western Luminol/Enhancer Reagent (detection reagent). The membrane was incubated in chemiluminescent detection reagent for 5 minutes in the dark. Thereafter, images were captured using the ChemiDoc MP™ imaging system. Image Lab 6.1 software was used to analyse proteins of interest. Proteins detected were normalised to β-actin.

3.15 Statistical analysis

Statistical analysis was performed using GraphPad Prism® 8.0.1 (GraphPad Software, La Jolla, California, United States of America). Statistical differences between groups were determined using one-way analysis of variance (ANOVA) followed by Tukey or Dunnett's post hoc tests unless otherwise stated. Data are presented as mean ± standard deviation (SD) and p-values of ≤ 0.05 were considered statistically significant.

4 RESULTS

4.1 C2C12 myoblasts: an *in vitro* model for skeletal muscle development

Murine C2C12 myoblast behavior corresponds with that of activated progenitor cells, and therefore, provide a good model for studying muscle differentiation, function, and regeneration. In culture, C2C12 myoblasts spontaneously differentiate to form contractile, multinucleated myotubules, synonymous with myofibers.

4.2 Effect of LPS on cell viability in C2C12 skeletal muscle cells

C2C12 myoblasts and myotubules were exposed to various concentrations of LPS (0.05 µg/mL to 1 µg/mL) for 24 hours. After 24 hours of exposure to LPS, the myoblasts and myotubules were imaged under brightfield using an Olympus inverted microscope, before performing a MTT cytotoxicity assessment. Visually, the addition of LPS did not induce overt adverse effects on the morphology of the myoblasts (figure 4.2.1 A to C) and myotubules (figure 4.2.1 D to F). In addition, no cytotoxic effects of LPS were detected in both myoblasts and myotubes using the MTT assay (figure 4.2.2 G and H).

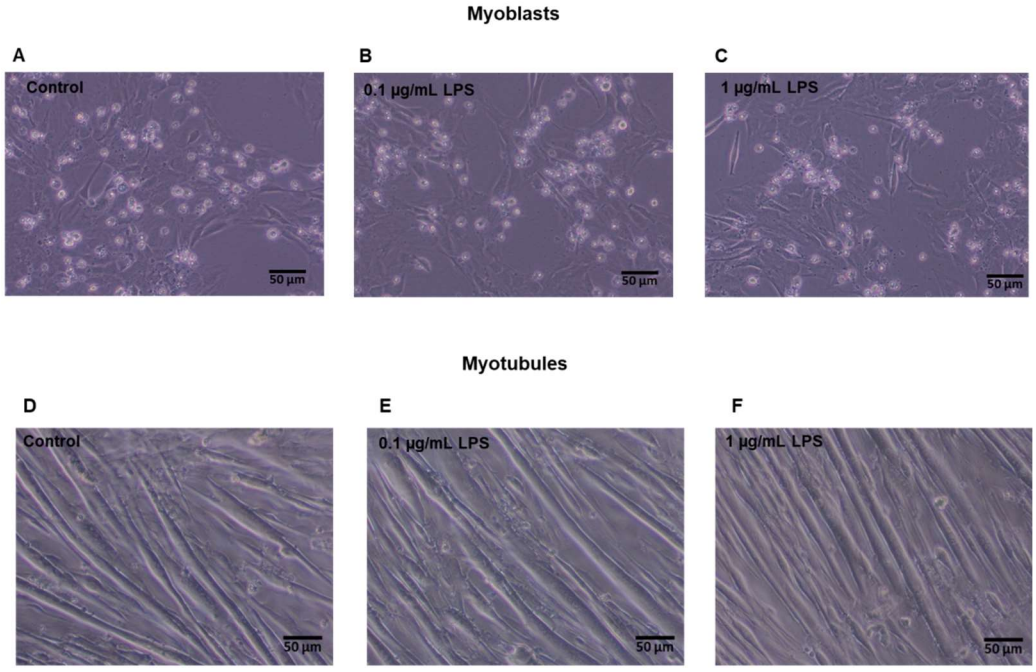

Figure 4.2.1: Comparative assessment of LPS treated C2C12 cell morphology using brightfield microscopy. C2C12 myoblasts (A, B and C) and myotubules (D, E and F) were exposed to LPS (0.05 µg/mL to 1 µg/mL) for 24 hours. Images were obtained at 100x magnification (scale bar = 100 µm).

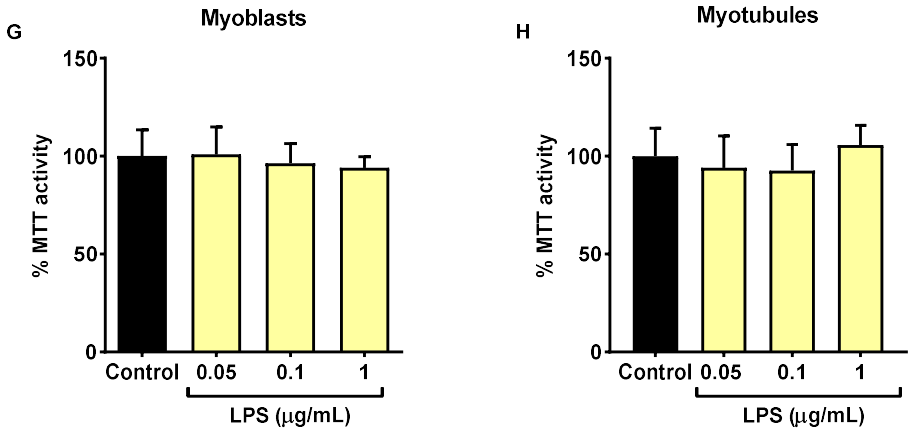

Figure 4.2.2: Effect of LPS on MTT mitochondrial activity of C2C12 cells. C2C12 myoblasts (A) and myotubes (B) were exposed to LPS (0.05 µg/mL to 1 µg/mL) for 24 hours. MTT activity was quantified at 570 nm (O.D.). Results are expressed as mean ± SD of three independent biological repeats (n = 3) relative to the control set at 100%. A one-way Analysis of Variance was performed.

LPS = Lipopolysaccharides, MTT = 3- [4, 5-dimethylthiazol-2-yl]-2, 5 diphenyltetrazolium bromide

4.3 Lipopolysaccharide-induced interleukin-6 secretion is more abundant in myoblasts compared to myotubes

To induce an inflammatory response in C2C12 skeletal muscle cells, we used LPS from *Escherichia coli O127:B8*. C2C12 myoblasts and myotubes were stimulated with 0.1 and 1 µg/mL LPS for 16 and 24 hours, respectively. LPS induced IL-6 secretion in a concentration dependent manner after 16 hours of treatment, with a significant increase observed in myoblasts stimulated with 1 µg/mL LPS (399.4 ± 286.5 pg/mL vs control 71.99 ± 7.68 pg/mL, $p < 0.001$). Moreover, a similar trend was observed after 24 hours of exposure with LPS in C2C12 myoblasts (661.6 ± 444.1 pg/mL vs control 87.06 ± 21.57 pg/mL, $p < 0.001$) (figure 4.3.1 A and B). However, although baseline values were much higher, this effect was not seen in differentiated muscle cells (myotubules) both at 16 and 24 hours (figure 4.3.1 C and D).

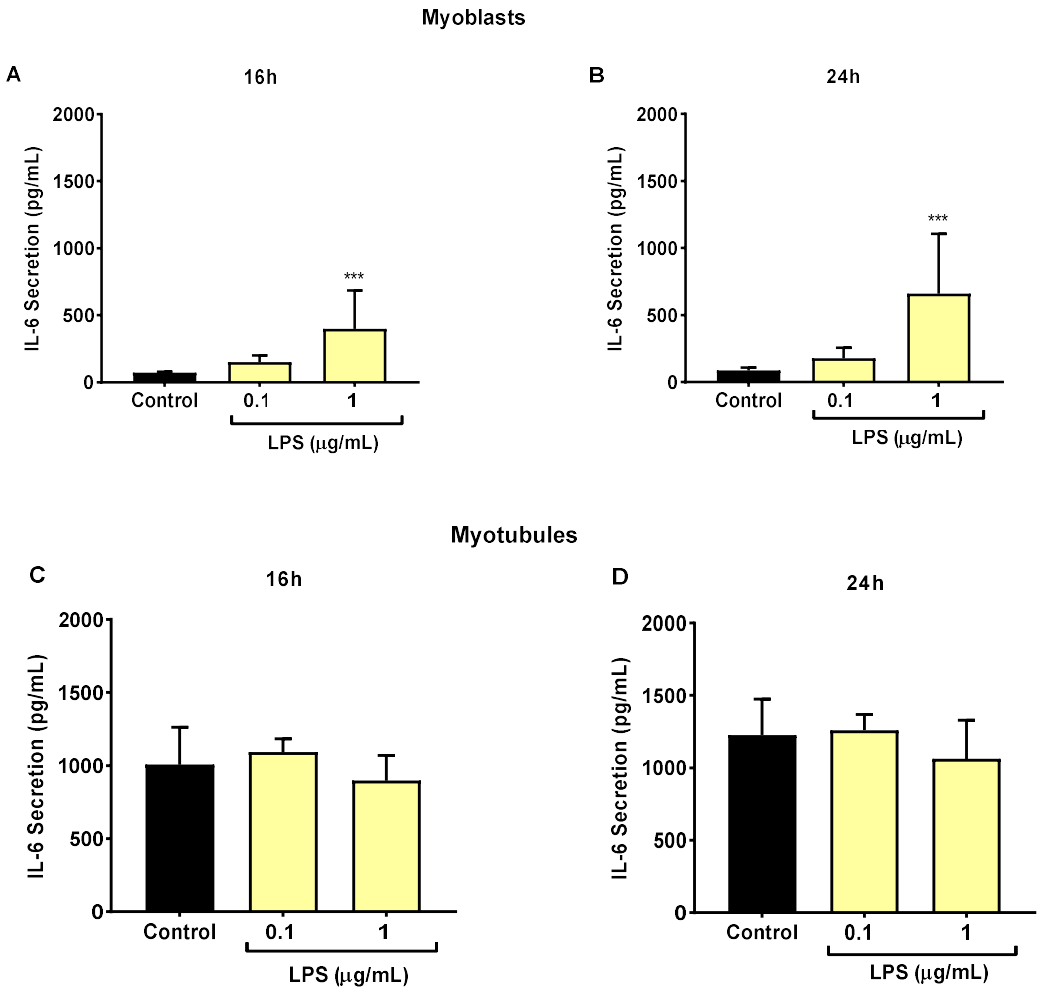

Figure 4.3.1: Effect of LPS on IL-6 secretion of C2C12 cells. C2C12 myoblasts and myotubules were cultured with LPS (0.1 or 1 µg/mL) for 16 h (A and C) and 24 h (B and D). Media was collected and assayed for secreted IL-6 using enzyme-linked immunosorbent assay (ELISA). Data are presented as the mean ± SD of three independent biological repeats (n = 3). A one-way Analysis of Variance was performed with a Dunnett's post hoc test. *** $p < 0.001$ vs control.

LPS = Lipopolysaccharides, IL-6 = Interleukin-6

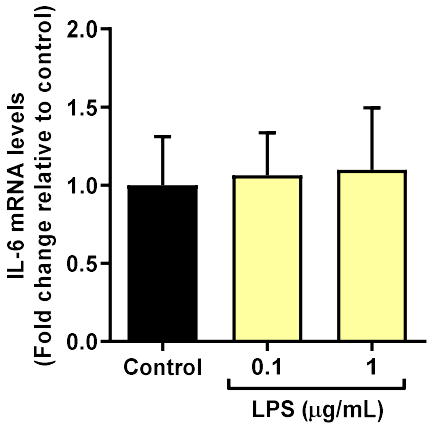

Figure 4.3.2: Effect of LPS on IL-6 mRNA expression of C2C12 cells. C2C12 myoblast IL-6 mRNA was quantified using quantitative real time PCR (q-RT PCR) and IL-6 expression was normalized to the average of beta-2-microglobulin (B2M). Data are presented as the mean ± SD of three independent biological repeats (n = 3) relative to the control. Data were analysed using one-way Analysis of Variance.

LPS = Lipopolysaccharides, IL-6 = Interleukin-6

After exposure to LPS for 24 hours, IL-6 mRNA expression in C2C12 myoblasts remained unchanged compared to the control (figure 4.3.2).

4.4 Lipopolysaccharide-induced Inflammation suppresses glucose uptake in C2C12 myoblasts

The effect of LPS on glucose uptake by C2C12 myoblasts was determined by measuring glucose taken up by the cells from the culture media, and by estimating the intracellular glucose uptake using a 2-deoxyglucose assay after 24 hours. Exposure of C2C12 myoblasts to LPS (0.1 µg/mL) reduced basal glucose uptake from 100 ± 18.7 to 77.5 ± 19.0 mmol/L compared to the control; however, reduction was not significant. At the highest concentration, LPS (1 µg/mL) significantly reduced glucose uptake from 100 ± 18.77 to 56.5 ± 28.4 mmol/L compared to the control set at 100%, $p < 0.01$ (figure 4.4 A). In terms of insulin-stimulated glucose uptake, insulin reversed the LPS effect at both concentrations tested compared to basal levels (figure 4.4 B).

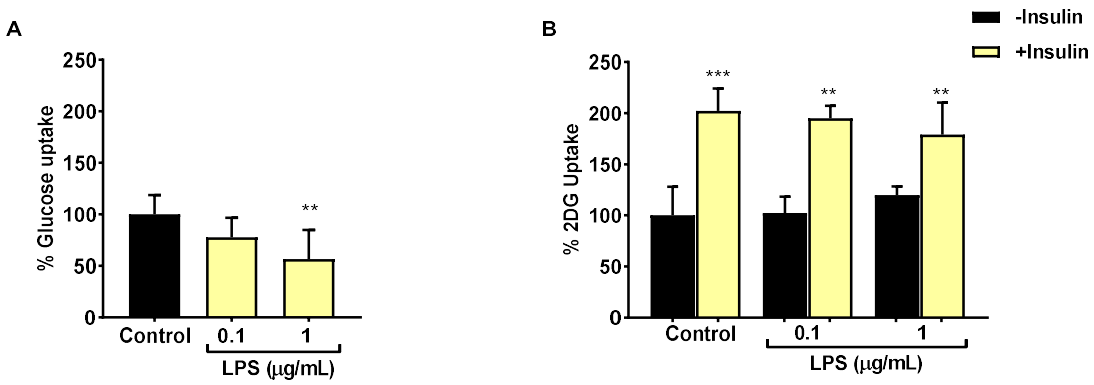

Figure 4.4: Effect of LPS on myoblast glucose utilization. Glucose uptake from the media (A) and insulin-stimulated intracellular 2-deoxyglucose uptake (B) by C2C12 myoblasts exposed to LPS for 24 hours. Media glucose concentration was determined using a glucose oxidase assay. For the insulin stimulated glucose uptake, cells were serum and glucose starved before pulsed with 2-deoxyglucose. Data are presented as the mean ± SD of three independent biological repeats (n = 3), relative to the control set at 100%. A one-way Analysis of Variance was performed with a Tukey post hoc test. ** $p < 0.01$, *** $p < 0.001$ vs control.

LPS = Lipopolysaccharides, 2DG = 2-deoxyglucose

4.5 Lipopolysaccharide-induced inflammation suppresses Akt activation

To investigate the effect of LPS on insulin signalling in C2C12 myoblasts, the expression and activation of Akt by insulin was assessed. Western blot analysis showed that insulin (1 µM) increased Akt phosphorylation by more than 60-fold compared to basal levels (63.55 ± 14.08-fold vs. basal 1.00 ± 0.35-fold, $p < 0.001$) (figure 4.5 A) and that LPS (0.1 and 1 µg/mL) did not significantly alter the activation of Akt by insulin (figure 4.5 A). Western blot analysis with antibodies against total Akt showed that total Akt expression appeared to be reduced by insulin stimulation, both in the insulin stimulated control (0.39 ± 0.13 vs basal 1.00 ± 0.11-fold, $p < 0.01$) and in the LPS treated samples (0.1 µg/mL: 0.46 ± 0.26; 1 µg/mL: 0.41 ± 0.11, vs basal 1.00 ± 0.11-fold, $p < 0.05$) (figure 4.5 B). However, the pAkt/tAkt ratio did not change significantly (figure 4.5 C).

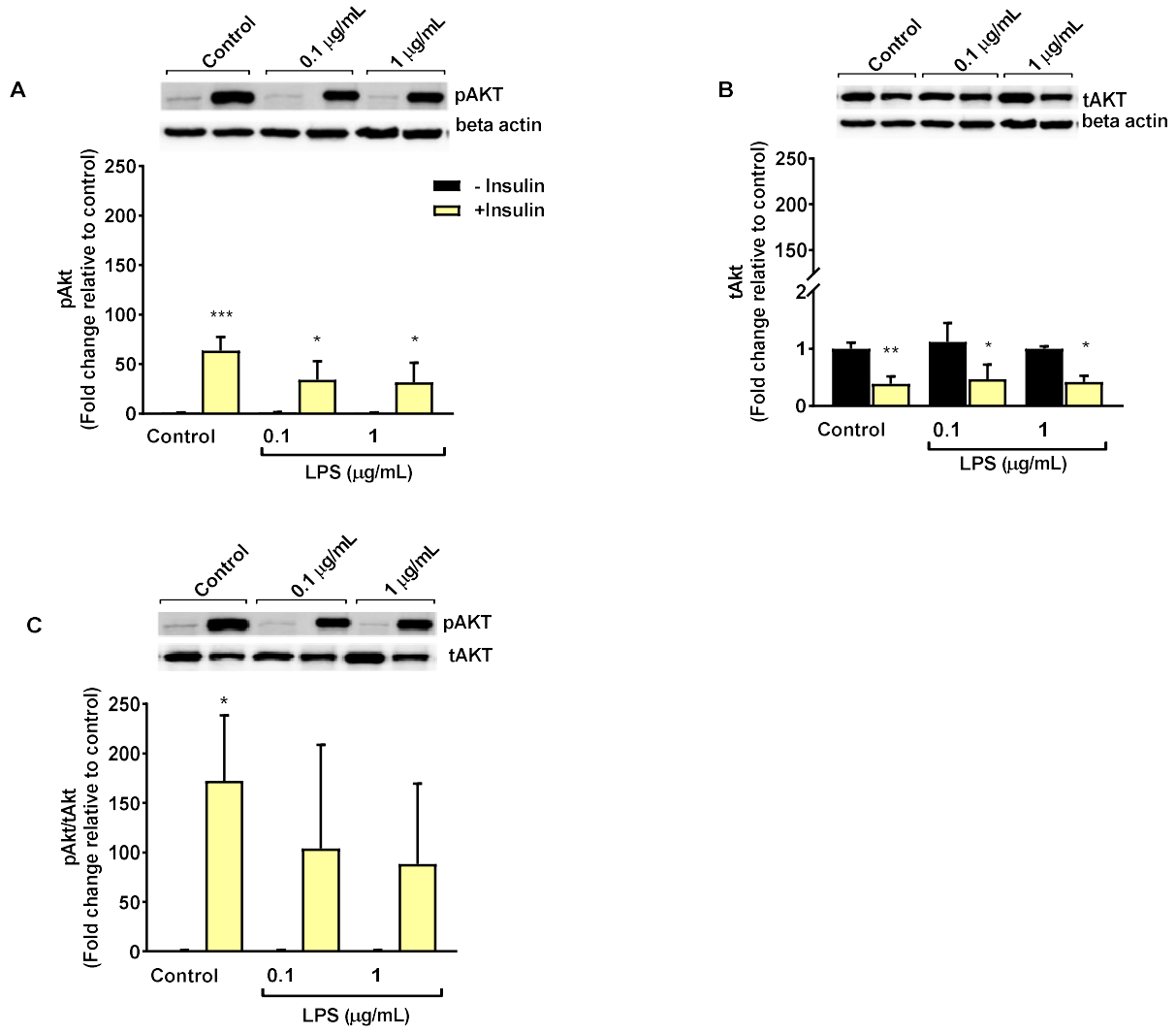

Figure 4.5: LPS-induced inflammation suppresses Akt phosphorylation. C2C12 myoblasts were exposed to LPS for 24 hours and stimulated with insulin (1 µM) for 15 minutes. Cells were lysed and subjected to SDS-PAGE for Western blot analysis. Western blot is a representative image of three independent experiments and data presented as the mean ± SD of three independent biological repeats. A one-way Analysis of Variance was performed with a Tukey post hoc test. * $p < 0.05$, ** $p < 0.01$, *** $p < 0.001$ vs control.

LPS = Lipopolysaccharides, SDS-PAGE = Sodium dodecyl sulphate-polyacrylamide gel electrophoresis

4.6 The effect of LPS on muscle growth and differentiation

To determine the effects of inflammation on myogenesis, C2C12 myoblasts were initially treated with LPS (0.1 and 1µg/mL) for 24 hours, before being subjected to differentiation media to induce

differentiation. At a protein level, LPS had no effect on mTOR compared to the control (figure 4.6.1 A – C) and that LPS did not affect AMPK protein expression and phosphorylation (figure 4.6.2 A - C).

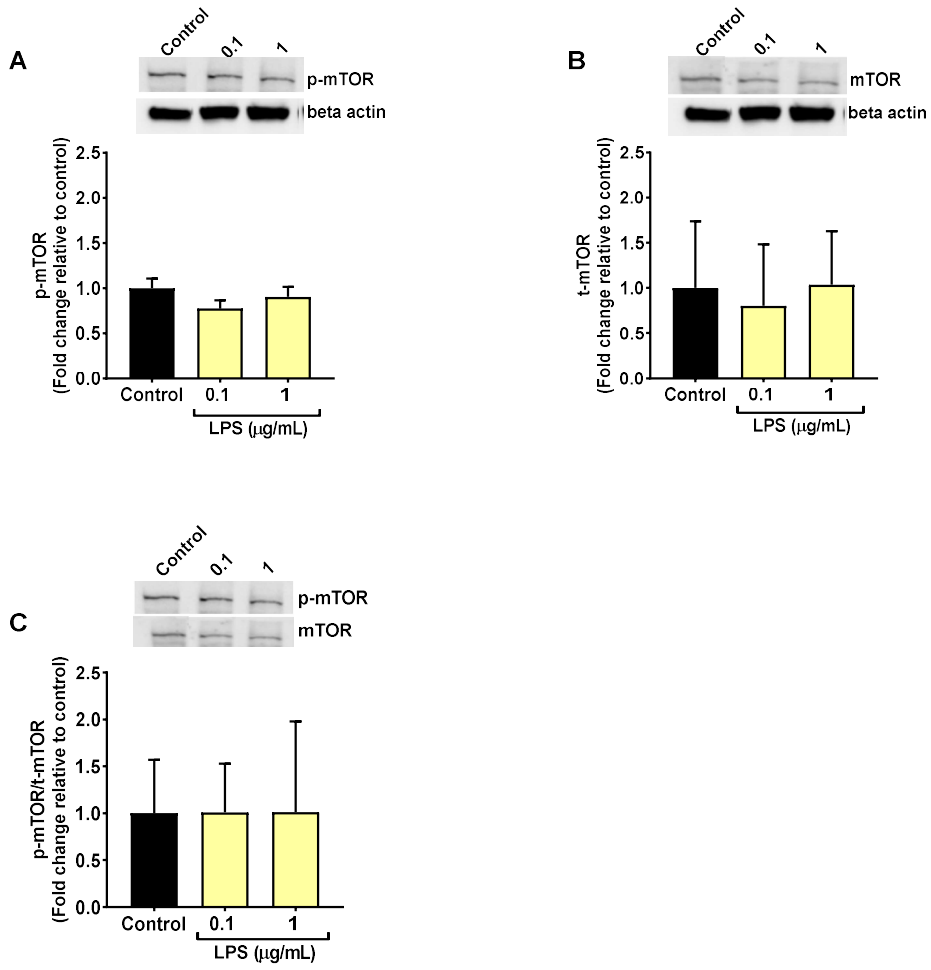

Figure 4.6.1: Effect of LPS on mTOR expression in C2C12 myoblasts. mTOR protein expression in C2C12 myoblasts was quantified by Western blot after LPS exposure for 24 hours (A - C). Western blot is a representative image of three independent experiments and data presented as the mean ± SD of three independent experiments. A one-way Analysis of Variance demonstrated no significant changes of mTOR expression.

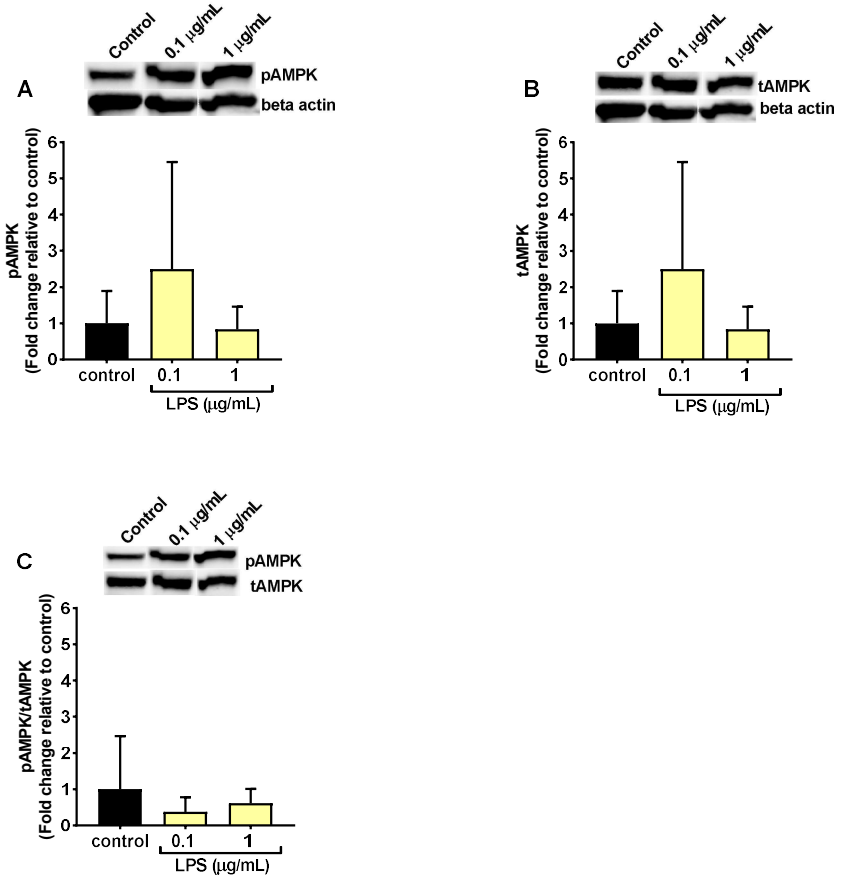

Figure 4.6.2: Effect of LPS on AMPK protein expression of C2C12 myoblasts. C2C12 myoblasts were exposed to LPS for 24 hours. Myoblast AMPK protein expression (A - C) was quantified by Western blot analysis. The Western blot is a representative image of three independent experiments and data presented as the mean ± SD of three independent experiments). A one-way Analysis of Variance demonstrated no significant changes of AMPK expression.

The addition of LPS during C2C12 differentiation induced a strong concentration related IL-6 response during the myoblastic phase of differentiation (day -1 and day 0) (figure 4.6.3). In addition, LPS reduced the formation and width of multinucleated myotubules produced from C2C12 myoblasts as shown in figure 4.6.4 A and D. Histological assessment on H & E stained cells shows decreased myotube formation at the highest concentration of LPS (1 µg/mL) compared to the control (figure 4.6.4 A) and this was confirmed by a decrease in myotube width (figure 4.6.4 B) and number (figure 4.6.4 C). LPS (0.1 and 1 µg/mL) significantly decreased myotube width by 26.5% (27.9 ± 11.5 to 20.5 ± 8.4 µm, $p < 0.0001$) and 35.1% (27.9 ± 11.5 to 18.1 ± 5.6 µm, $p < 0.0001$), respectively compared to the control (figure 4.6.4 B). The higher

concentration of LPS (1 µg/mL) significantly decreased myotube number (14.6 ± 4.5 vs 19.9 ± 4.5, $p < 0.01$) compared to the control, as shown in figure 4.6.4 C.

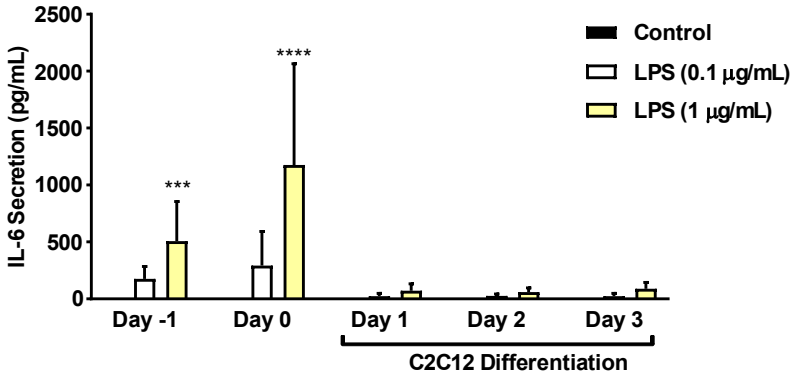

Figure 4.6.3: Effects of LPS on IL-6 secretion in differentiating C2C12 myoblasts. C2C12 myoblasts were differentiated with or without LPS. Media was collected for cytokine analysis using an ELISA kit. Data presented as the mean ± SD of three independent experiments (n = 3). A one-way Analysis of Variance was performed with a Tukey post hoc test. **** $p < 0.0001$ vs control.

LPS = Lipopolysaccharides, ELISA = Enzyme-linked immunosorbent assay.

A

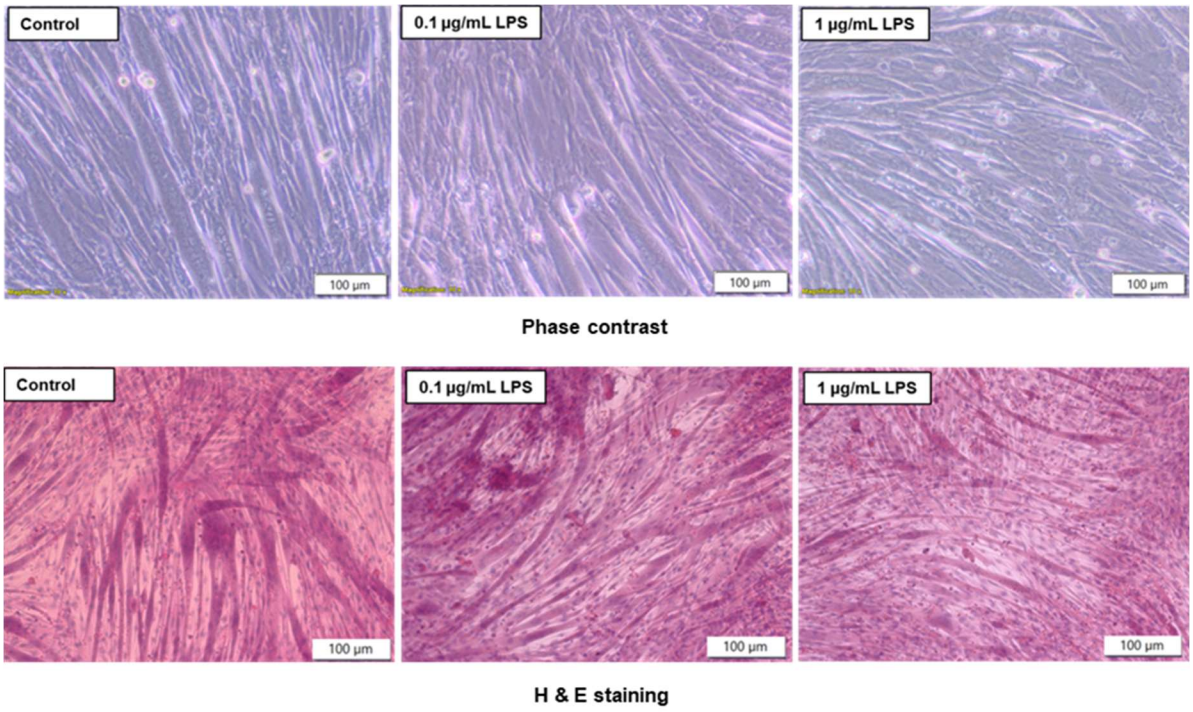

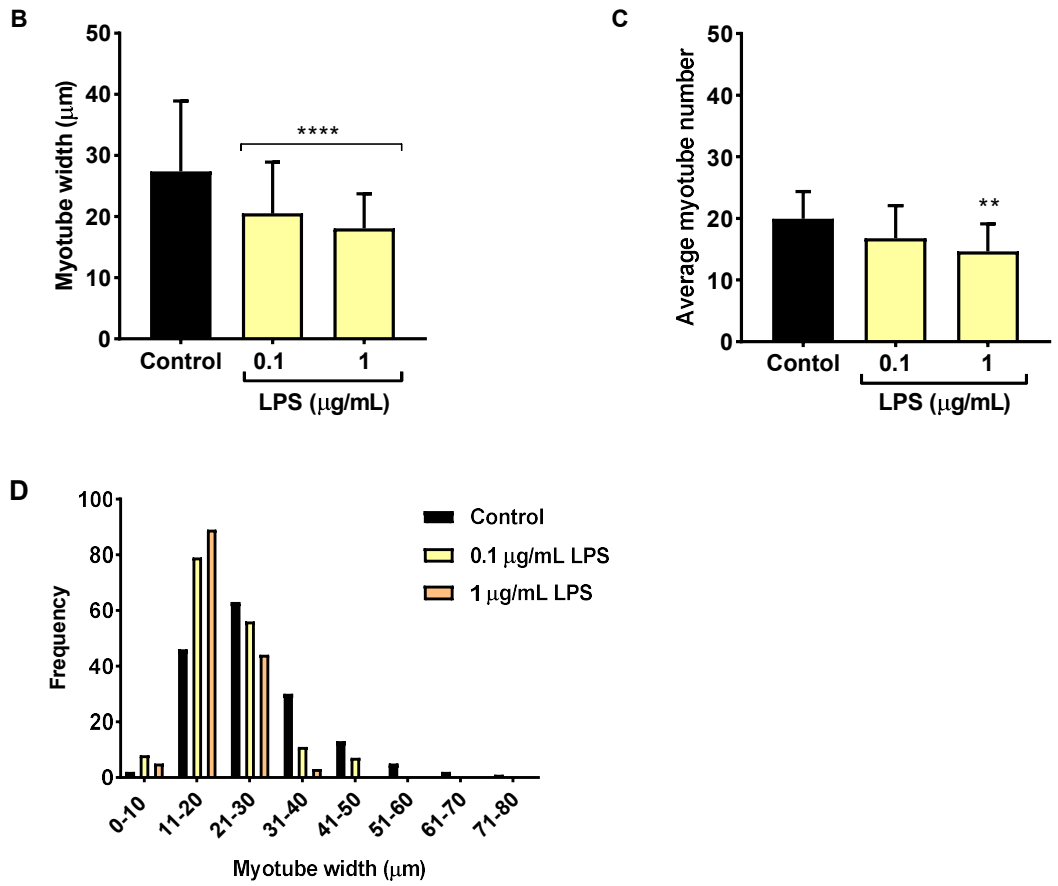

Figure 4.6.4: LPS inhibits myogenesis in C2C12 muscle cells. C2C12 myoblasts were cultured and differentiated with or without LPS. Differentiated myotubes were fixed and subjected to H & E staining (A), thereafter myotube width (B), the myotube number (C) and the distribution of myotube widths (D) were calculated. Images captured at 100X magnification (scale bar = 100 μm). Data are the mean ± SD of 3 independent experiments, each examining 5 randomly selected non-overlapping fields. A one-way Analysis of Variance was performed with a Tukey post hoc test. ** p <0.01, **** p < 0.0001 vs control.

H&E = Haematoxylin and Eosin, LPS = Lipoplysaccharides.

Day 0 represents confluent C2C12 myocytes in growth media before being exposed to differentiation media with or without LPS, and day 1 represents differentiating myocytes after 24 hours culture in differentiation media with or without LPS. As expected, the myogenic genes, myogenin and MyoD mRNA expression increased from day 0 to days 1 and 3 of myotube differentiation (figure 4.6.5 A and B). MyoD expression was not significantly different at day 1 and day 3 of differentiation compared to day 0 (figure 4.6.5 A). However, myogenin expression increased by 88% (1.0 ± 0.6 to 8.8 ± 2.9-fold, p < 0.001) and 87% (1.0 ± 0.6 to 7.9 ± 1.9-fold, p <

0.01) at day 1 and day 3 of differentiation compared to day 0, respectively (figure 4.6.5 B). The expression of myogenin increased after 24-hour exposure to LPS in differentiation media (day 1), but by 72 hours (day 3) exposure to LPS reduced the expression of myogenin compared to day 0 (figure 4.6.5 B). Myostatin gene expression increased by 74% (1.0 ± 0.3 to 3.8 ± 0.9-fold, $p < 0.001$) on the third day of differentiation compared to day 0. LPS concentration-dependently reduced the expression of myostatin on day 1 and day 3 of differentiation (figure 4.6.5 C).

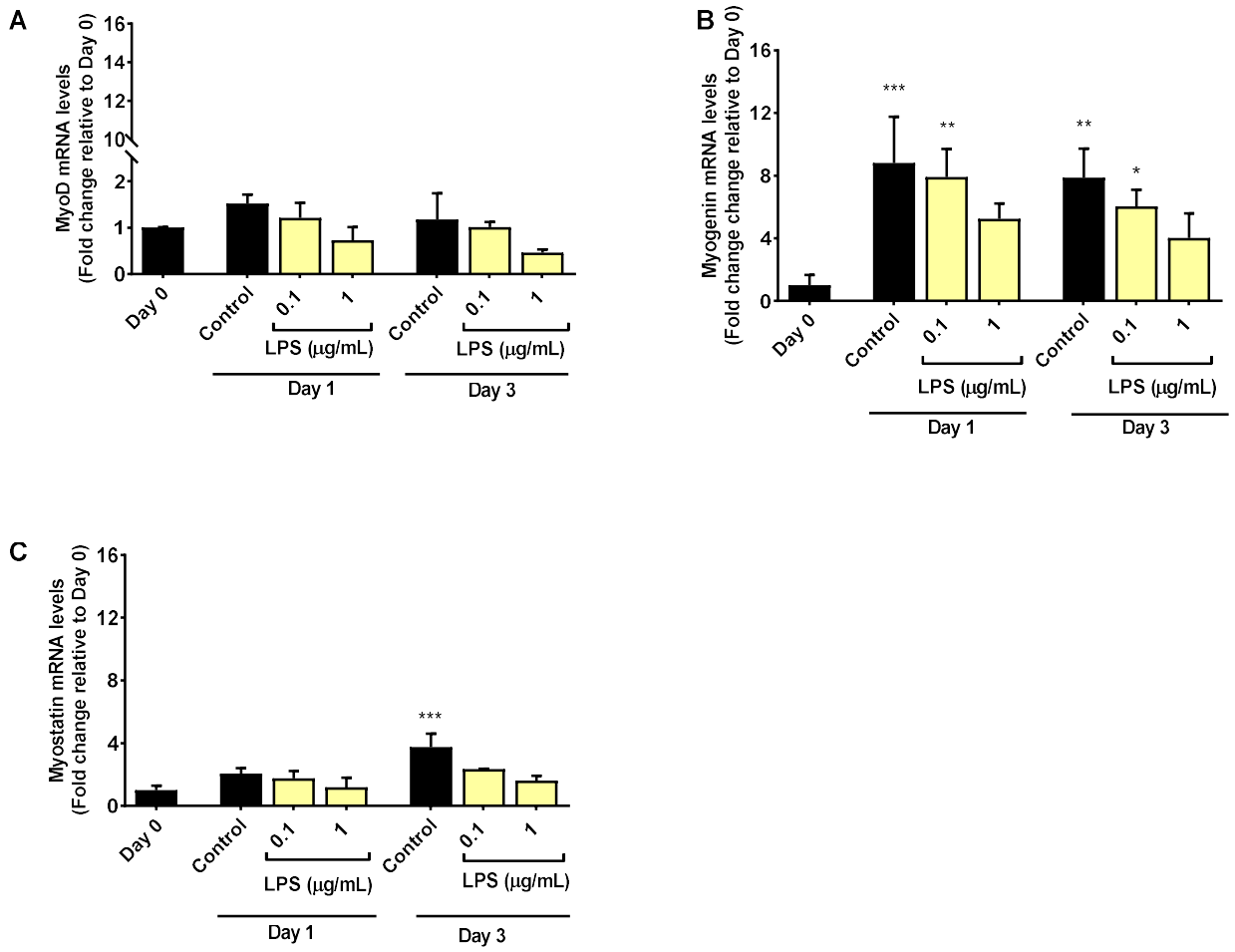

Figure 4.6.5: Effects of LPS on myogenic genes in differentiating C2C12 myoblasts. C2C12 myoblasts were differentiated with or without LPS. Cells were harvested for quantitative reverse transcription polymerase chain reaction (qRT-PCR) where MyoD (A), myogenin (B) and Myostatin (C), mRNA expression was normalized to the average of beta-2-microglobulin (*B2M)*, data expressed as fold change. Data are presented as the mean ± SD of three independent experiments (n = 3). A one-way Analysis of Variance was performed with a Tukey post hoc test. *** $p < 0.001$, ** $p < 0.01$ vs Day 0.

LPS = Lipopolysaccharides.

4.7 Effect of Afriplex GRT™ on MTT (mitochondrial dehydrogenase) activity in C2C12 skeletal muscle cells

A MTT assay was performed to determine the effects of GRT on mitochondrial activity and thus cell viability of C2C12 muscle cells. GRT was tested for cytotoxicity at various concentrations (0.001 µg/mL to 100 µg/mL) at various time points (4, 8, 16, and 24 hours). The study showed that GRT did not decrease MTT activity at the concentrations tested over 24 hours. Interestingly, increases in MTT activity were noted at 4 hours of GRT treatment for concentrations 0.001 µg/mL (8.8%, $p < 0.05$), 0.01 µg/L (16%, $p < 0.001$), 10 µg/mL (14%, $p < 0.001$) and 100 µg/mL (22%, $p < 0.001$) compared to the control, respectively (figure 4.7 A). At 8 hours increased MTT activity was only observed for the 100 µg/mL concentration (19.19%, $p < 0.01$) (Figure 4.7 B). By 16 and 24 hours GRT had no significant measurable effect on mitochondrial activity (Figure 4.7 C and D).

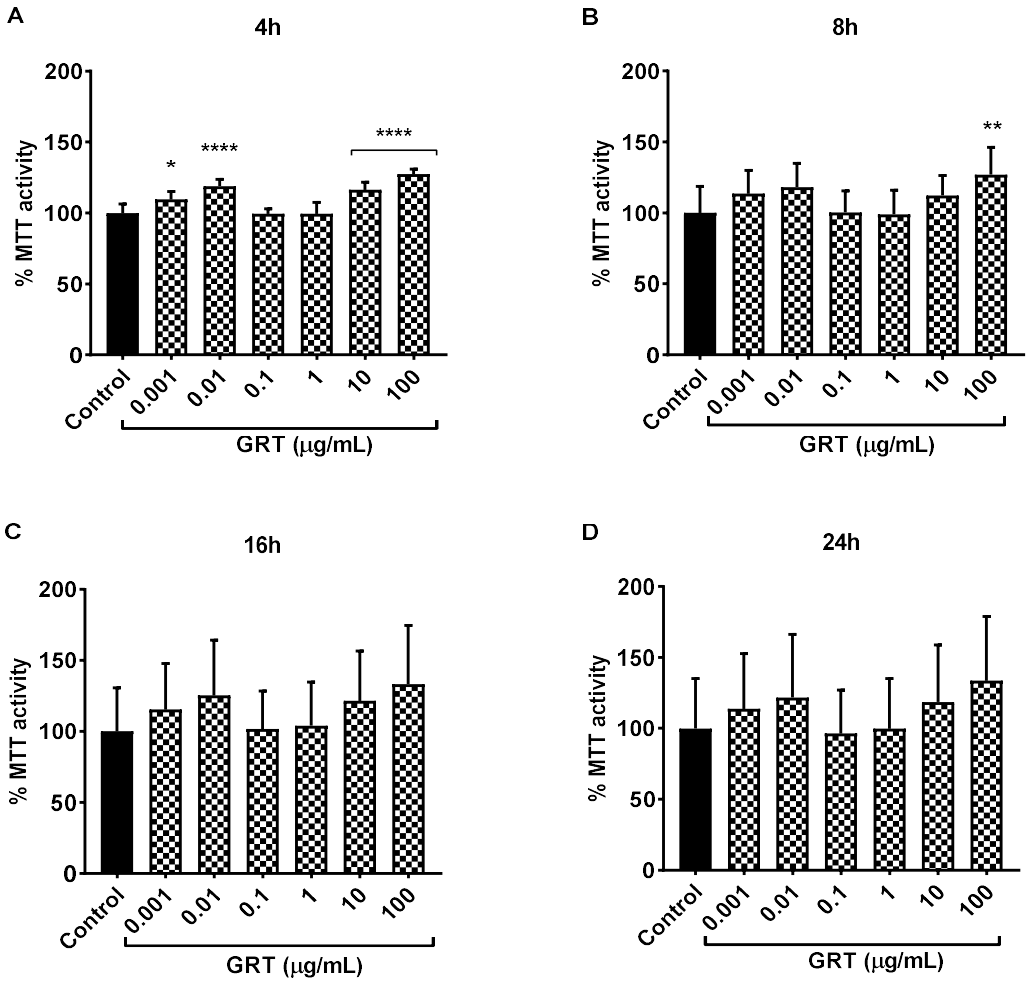

Figure 4.7: MTT activity of C2C12 muscle cells treated with Afriplex GRT for 4 hours (A), 8 hours (B), 16 hours (C) and 24 hours (D). C2C12 myocytes were treated with GRT (0.001 to 100 µg/mL) for 4, 8, 16 and 24 hours, thereafter mitochondrial activity was quantified by MTT assay. Results are expressed as mean ± SD of three independent experiments relative to the control (n = 3). A one-way Analysis of Variance was performed with a Dunnett's post hoc test, * $p < 0.05$, ** $p < 0.01$, **** $p < 0.001$ vs control at 100%.

GRT = Afriplex GRT™ (aspalathin-rich green rooibos extract), MTT = 3- [4, 5-dimethylthiazol-2-yl]-2, 5 diphenyltetrazolium bromide

4.8 Afriplex GRT™ enhances mitochondrial activity in C2C12 muscle cells

The effect of GRT on mitochondrial function was assessed using the Mito stress Seahorse bioenergetics test kit according to manufacturer's instructions. The combined results of the oxygen consumption rate (OCR) after treatment with GRT and positive controls (insulin and metformin) are shown in figure 4.8 A and individual parameters shown in figure 4.8 B - E. GRT significantly increased basal OCR at concentrations of 0.01 µg/mL (72.6 ± 5.4 pmol/min/mg protein), $p < 0.001$), 0.1 µg/mL (74.5 ± 6.2 pmol/min/mg protein, $p < 0.001$), 10 µg/mL (67.3 ± 6.8 pmol/min/mg protein, $p < 0.01$) and 100 µg/mL (65.2 ± 8.8 pmol/min/mg protein, $p < 0.05$) compared to the control (55.1 ± 5.5 pmol/min/mg protein), respectively. The positive control, metformin, also significantly increased basal OCR (64.6 ± 6.0 pmol/min/mg protein, $p < 0.05$) compared to the control. Moreover, GRT significantly increased ATP production at concentrations of 0.01 µg/mL (21.8 ± 3.9 pmol/min/mg protein, $p < 0.01$), 0.1 µg/mL (23.4 ± 2.3 pmol/min/mg protein, $p < 0.001$) and 10 µg/mL (22.8 ± 3.5 pmol/min/mg protein, $p < 0.01$) compared to the control (16.28 ± 2.76 pmol/min/mg protein), respectively (figure 4.8 C). Metformin also showed a significant increase ATP production (22.9 ± 2.3 pmol/min/mg protein, $p < 0.01$) compared to the control (Figure 4.8 C). After the addition of FCCP, an uncoupler of oxidative phosphorylation, both GRT (0.01 µg/mL to 100 µg/mL) and positive controls (insulin and metformin) significantly increased maximal respiration in C2C12 myotubules compared to the control (119.9 ± 17.64 pmol/min/mg protein) (figure 4.8 D). However, GRT did not affect spare respiration capacity (figure 4.8 E).

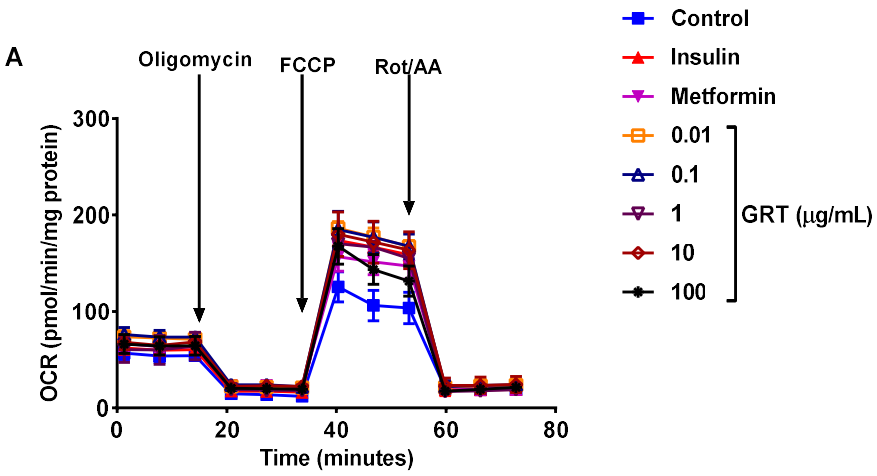

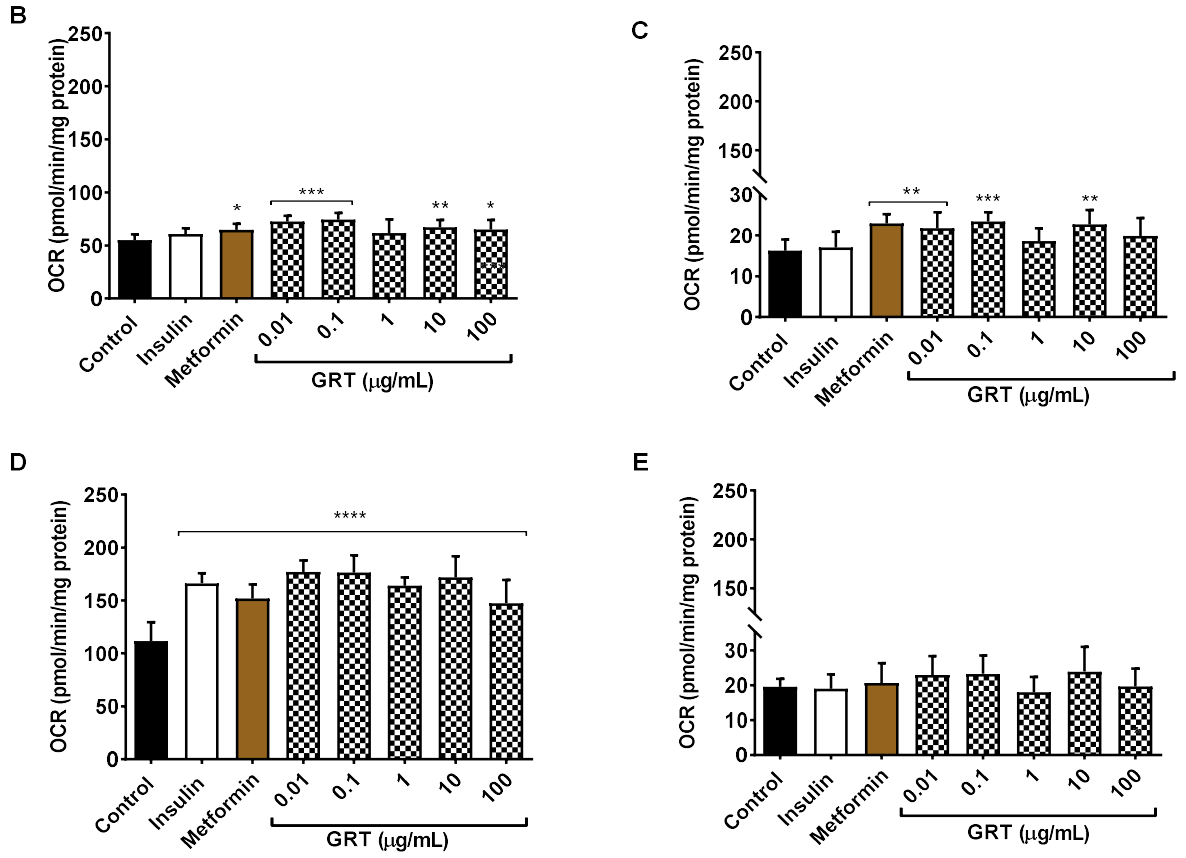

Figure 4.8: Assessment of GRT on C2C12 mitochondrial function. The Mito test assay demonstrated that GRT improved mitochondrial bioenergetics (A), as shown by an increase in basal oxygen consumption rate (OCR) (B), ATP production (C), maximal respiration (D) and spare capacity (E) in differentiated C2C12 skeletal muscle cells exposed to various concentrations of GRT for 24 hours. Cells were also treated with insulin (1 µM) and metformin (1 µM) as positive controls. Results are expressed as mean ± SD of two independent experiments (n = 2). A one-way Analysis of Variance was performed with a Tukey post hoc test. *p < 0.05, **p < 0.01, ***p < 0.001 vs the control.

GRT = Afriplex GRT™ (aspalathin-rich green rooibos extract), FCCP = Trifluoromethoxy carbonyl cyanide phenylhydrazone, Rot = Rotenone, AA = Antimycin A

4.9 Lipopolysaccharide-induced inflammation was not affected by Afriplex GRT™ in C2C12 myoblasts

Myoblast IL-6 secretion was significantly increased in myoblasts stimulated with LPS by 84%, p< 0.0001) (Figure 4.9.1 A). There was no difference between the LPS and GRT (GRT1 = 1 µg/mL) and (GRT10 = 10 µg/mL) combination treatment compared to LPS alone (figure 4.9.1 A).

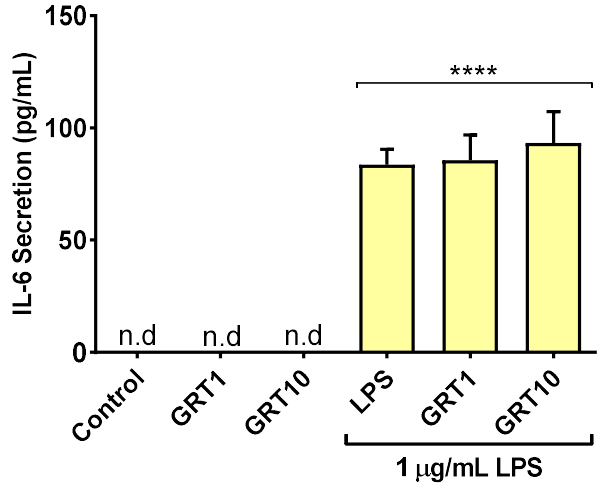

Figure 4.9.1: LPS-induced IL-6 secretion from C2C12 myoblasts. C2C12 myoblasts were cultured with or without LPS and two GRT concentrations (GRT1 = 1 µg/mL and GRT10 = 10 µg/mL) for 24 hours. Thereafter, media was collected and assayed for IL-6 secretion using ELISA. Data presented as the mean ± SD of three independent experiments (n = 3). A one-way Analysis of Variance was performed with a Tukey post hoc test. **** p < 0.0001. n.d = not detectable < 15.6 pg/mL.

GRT = Afriplex™ green rooibos extract, LPS = Lipopolysaccharides, IL-6 = Interluekin 6, ELISA = Enzyme-linked immunosorbent assay.

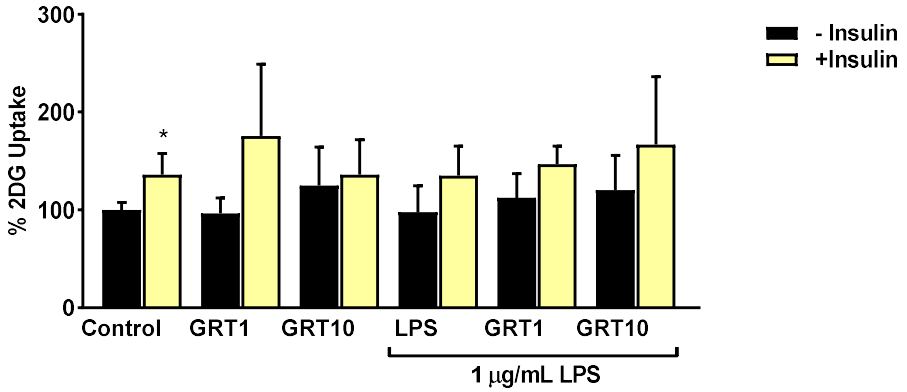

Figure 4.9.2: Effect of GRT on glucose uptake. C2C12 myoblasts stimulated with or without LPS and GRT for 24 hours. Insulin-stimulated 2-deoxyglucose uptake was measured using luminescence. Data presented as the mean ± SD of three independent experiments (n = 3), relative to the control. A one-way Analysis of Variance was performed with a Tukey post hoc test. * $p < 0.05$ vs non-insulin control.
GRT1 = 1 μg/mL and GRT10 = 10 μg/mL, LPS = Lipopolysaccharides, 2DG = 2-deoxyglucose.

GRT did not significantly increase 2DG uptake in LPS stimulated myoblasts, however insulin significantly increased insulin-stimulated 2DG uptake (136.0 ± 21.7% vs 100 ± 7.5%, $p<0.05$) (figure 4.9.2). Akt phosphorylation was increased by insulin stimulation compared to basal levels (1.00 ± 0.85 to 3.66 ± 1.98-fold). The combination of GRT (GRT1 and GRT10) and insulin markedly increased Akt activation (2.75 ± 0.38 and 2.67 ± 0.46-fold, $p < 0.05$; respectively) compared to basal (figure 4.9.3 A). Interestingly, treatment with GRT1 and insulin ameliorated Akt activation in C2C12 myoblasts exposed to LPS (0.25 ± 0.14 to 3.19 ± 0.41-fold) (figure 4.9.3 A). In terms of pAkt/tAkt expression, insulin (7.14 ± 1.61-fold, $p < 0.001$) as well as the combination of insulin and GRT1 (5.04 ± 3.07-fold) significantly affected activation of Akt compared to the non-insulin stimulated control (1.00 ± 0.37-fold) (figure 4.9.3 C).

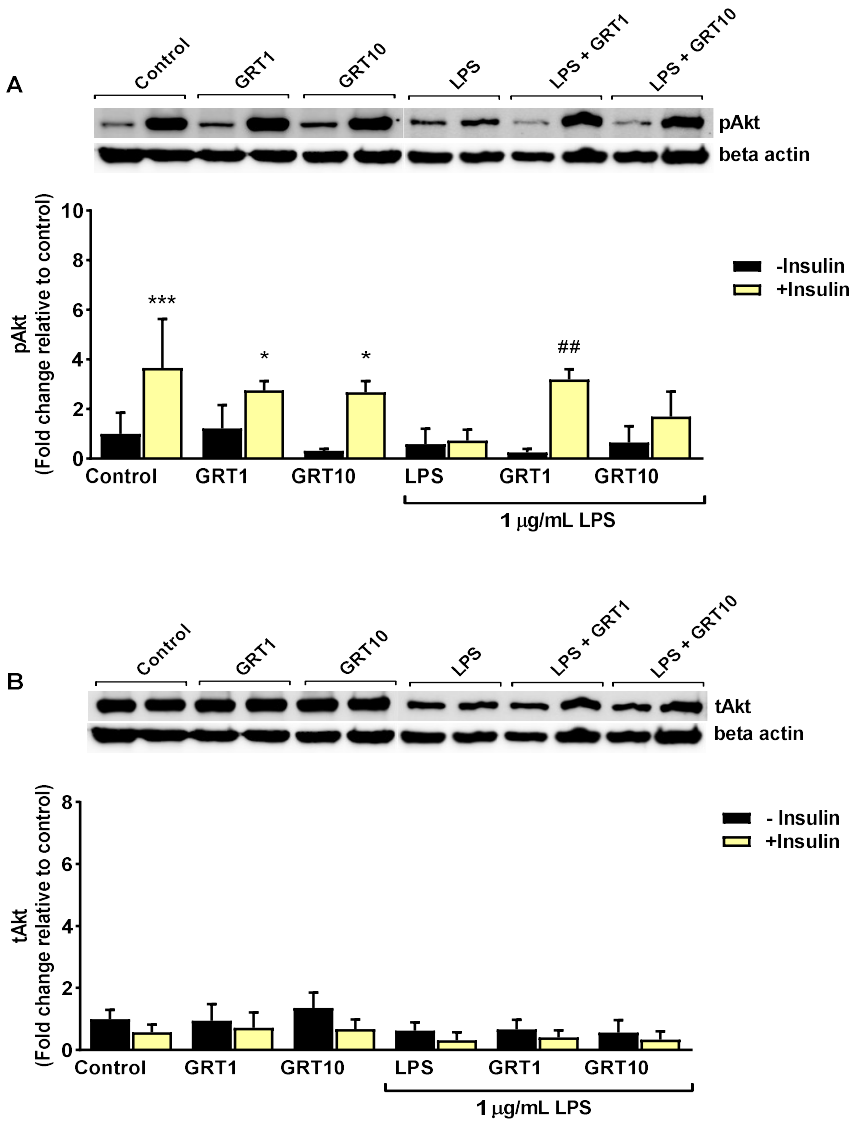

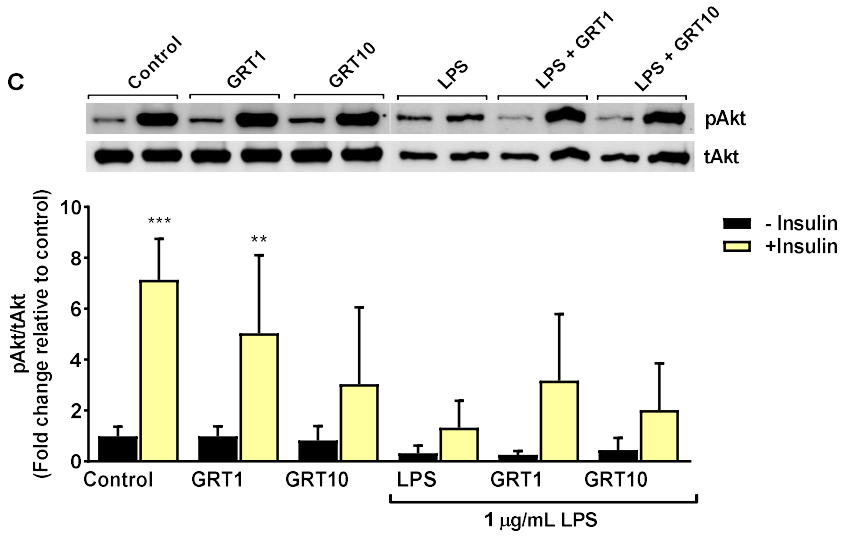

Figure 4.9.3: Effect of GRT on LPS-induced inflammation in C2C12 myoblasts. C2C12 myoblasts treated with LPS and GRT for 24 hours. Akt protein expression and activation was quantified by Western blot (A – C). Western blot is a representative image of two independent experiments and data presented as the mean ± SD of two independent experiments. * $p < 0.05$, ** $p < 0.01$, *** $p < 0.001$ vs non-insulin control. A one-way Analysis of Variance was performed with a Tukey post hoc test. ## $p < 0.01$ vs LPS.

GRT1 = 1 µg/mL, GRT10 = 10 µg/mL, LPS = Lipopolysaccharides.

The incubation of C2C12 myoblasts with LPS combined with GRT did not significantly affect the protein expression of AMPK (figure 4.9.4 A - C).

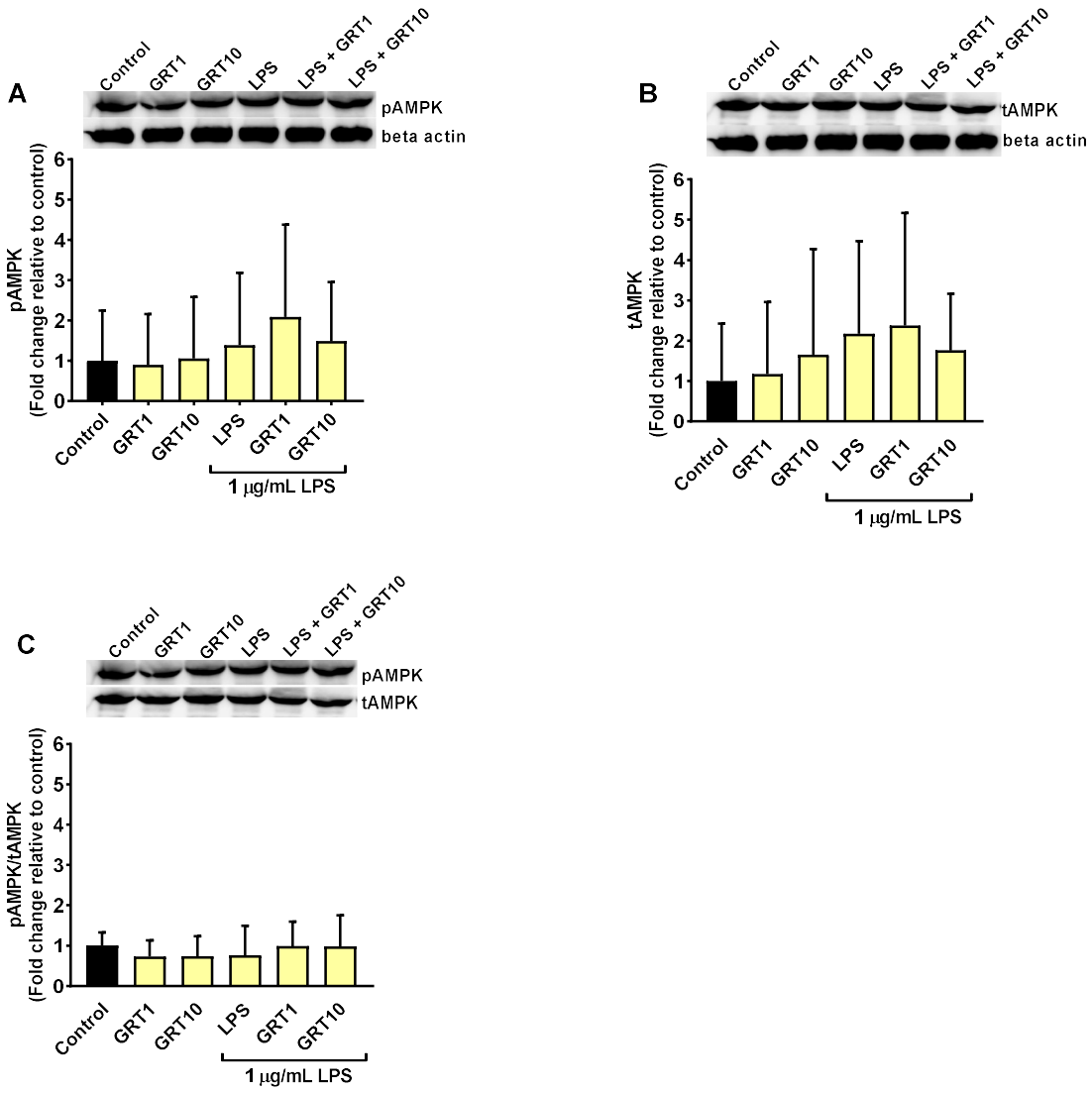

Figure 4.9.4: Effect of GRT on AMPK in LPS-induced inflammation C2C12 myoblasts. C2C12 myoblasts treated with and without LPS and GRT for 24 hours. AMPK protein expression and activation were quantified by Western blot (A – C). Western blot is a representative image of three independent experiments and data are presented as the mean ± SD of three independent experiments. A one-way Analysis of Variance was performed with a Tukey post hoc test. GRT1 = 1 µg/mL, GRT10 = 10 µg/mL, LPS = Lipopolysaccharides.

LPS significantly decreased MyoD (1.01 ± 0.13 to 0.48 ± 0.05-fold, $p < 0.001$) and myogenin (1.01 ± 0.17 to 0.38 ± 0.27-fold, $p < 0.001$) gene expression compared to the controls, respectively (figure 4.9.5 A and B). The addition of GRT did not change the LPS-induced down regulation of MyoD (GRT1: 0.58 ± 0.22-fold, $p < 0.05$; GRT10: 0.46 ± 0.17-fold, $p < 0.001$) compared to the GRT controls (GRT1: 0.86 ± 0.20-fold, GRT10: 0.89 ± 0.40-fold) (Figure 4.9.5 A). The same trend was seen with myogenin, where both concentrations of GRT (GRT1: 0.30 ± 0.21-fold, $p < 0.01$; GRT10: 0.31 ± 0.27-fold, $p < 0.01$) were not able to rescue the down regulation of myogenin by LPS compared to the controls (GRT1: 0.79 ± 0.25-fold, GRT10: 0.85 ± 0.62-fold) (figure 4.9.5 B).

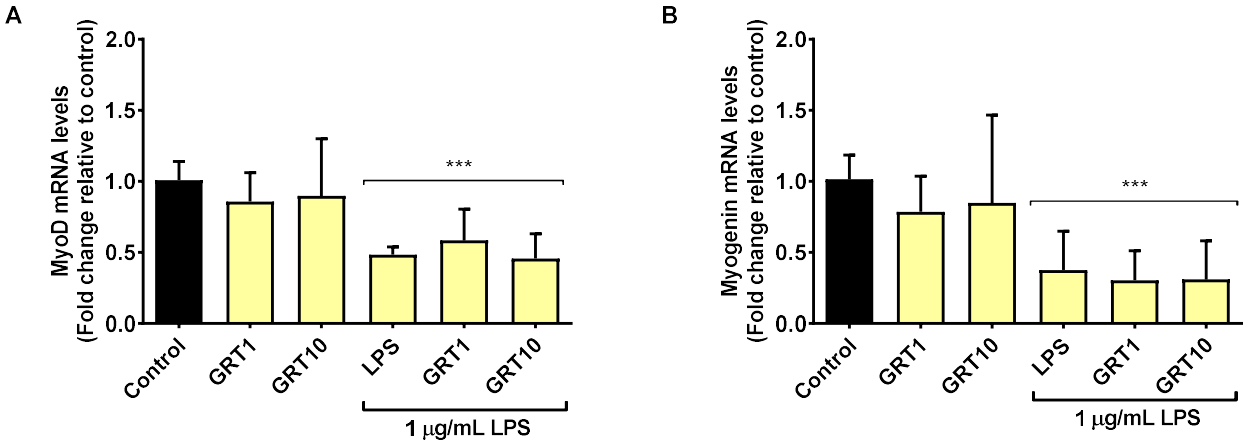

Figure 4.9.5: The effect of LPS on the myogenic genes, MyoD and Myogenin in C2C12 myoblasts. C2C12 myoblasts were treated with LPS and GRT for 24 hours. Thereafter, gene expression of MyoD (A) and myogenin (B) mRNA expression was quantified using quantitative reverse transcription polymerase chain reaction (qRT-PCR) and expression was normalized to the average of *B2M*, data was expressed as fold change. Data presented are the mean ± SD of three independent experiments (n = 3). A one-way Analysis of Variance was performed with a Tukey post hoc test. *** $p < 0.001$ vs Control.

GRT1 = 1 µg/mL, GRT10 = 10 µg/mL, LPS = Lipopolysaccharides, MyoD = myoblast determination protein 1.

4.10 Effect of LPS-induced adipocyte-derived pro-inflammatory cytokines on C2C12 myoblasts

For co-culture studies, C2C12 myoblasts were co-cultured with 3T3-L1 pre-adipocytes and/or differentiated adipocytes. The co-culture was treated with or without LPS or co-treated with GRT for 24 hours. After 24 hours media was collected, and IL-6 secretion was determined. Data shows that the co-culture of 3T3-L1 pre-adipocytes or mature adipocytes did not induce any detectable IL-6 secretion in myoblasts (detection < 15.6 pg/mL) (figure 4.10.1 A and B). The addition of LPS significantly increased IL-6 secretion in the myoblast/pre-adipocyte co-cultures (figure 4.10.1 A). In terms of whether GRT could affect IL-6 secretion, there were no significant differences between the LPS and LPS-GRT1 and LPS-GRT10 treatments. LPS significantly increased IL-6 secretion specifically in the compartment containing the pre-adipocytes (figure 4.10.1 A).

Co-culture of myoblasts with mature adipocytes did not induce IL-6 secretion as seen figure 4.10.1 B (detection limit < 15.6 pg/mL). Myoblast IL-6 secretion was significantly induced in myoblasts (273.27 ± 250.65 pg/mL, $p < 0.001$) compared to the adipocytes (89.63 ± 104.47 pg/mL) in groups exposed to LPS (figure 4.10.1 B). The contribution of IL-6 secretion from the adipocytes to the co-culture was greatly reduced compared that contributed by the pre-adipocytes (figure 4.10.1 A and B). Adiponectin is an anti-inflammatory adipokine and to determine whether adiponectin was the mediating factor in LPS-induced IL-6 secretion in differentiated adipocytes, media from both pre- and differentiated 3T3-L1 adipocytes assayed for adiponectin using and ELISA kit. Data shows that adiponectin was significantly increased in differentiated 3T3-L1 adipocytes ($p < 0.0001$) compared to the pre-adipocytes (figure 4.10.2).

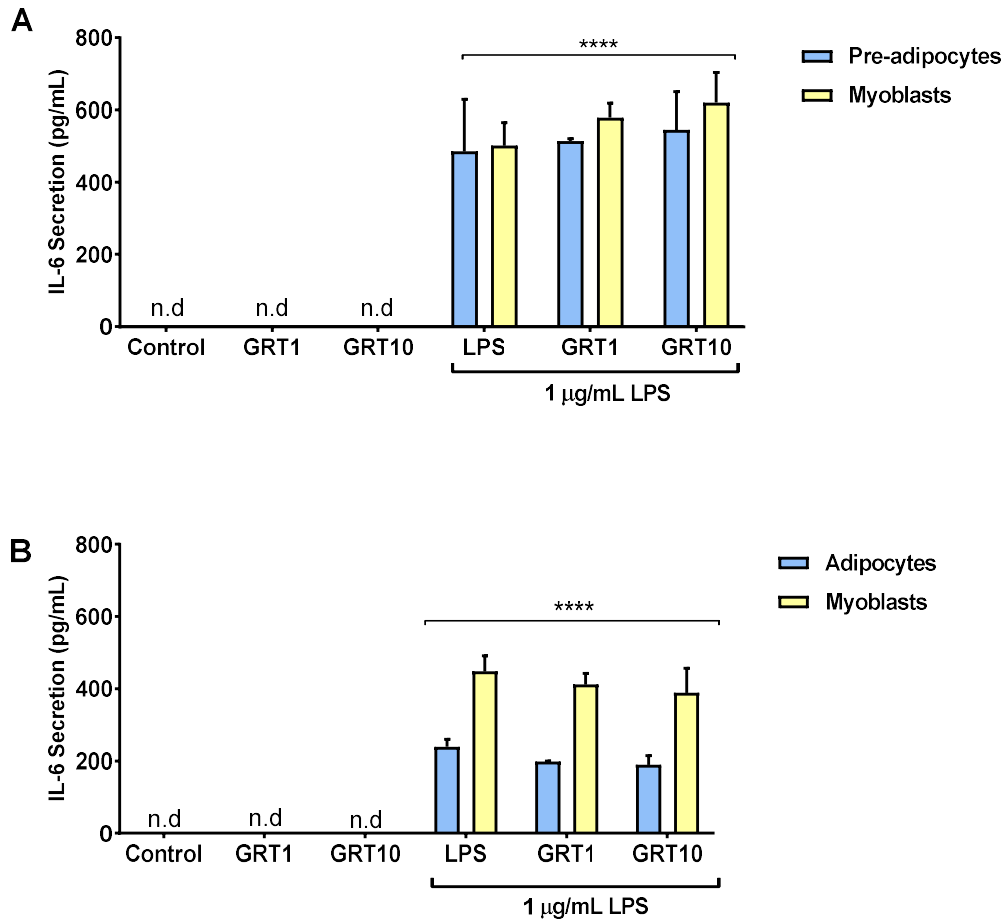

Figure 4.10.1: IL-6 secretion from 3T3-L1 pre-adipocytes, differentiated 3T3-L1 adipocytes and myoblast co-cultures. Co-culture was treated with LPS and two GRT concentrations (GRT1 and GRT10) for 24 hours. Thereafter, media collected from the upper and lower compartments was assayed for IL-6 secretion using ELISA. Data presented are the mean ± SD of three independent experiments (n = 3). A two-way Analysis of Variance was performed with a Tukey post hoc test. **** $p < 0.0001$ vs control. n.d = no detection < 15.6 pg/mL.

GRT1 = 1 µg/mL, GRT10 = 10 µg/mL, LPS = Lipopolysaccharides, IL-6 = Interleukin 6, ELISA = enzyme-linked immunosorbent assay.

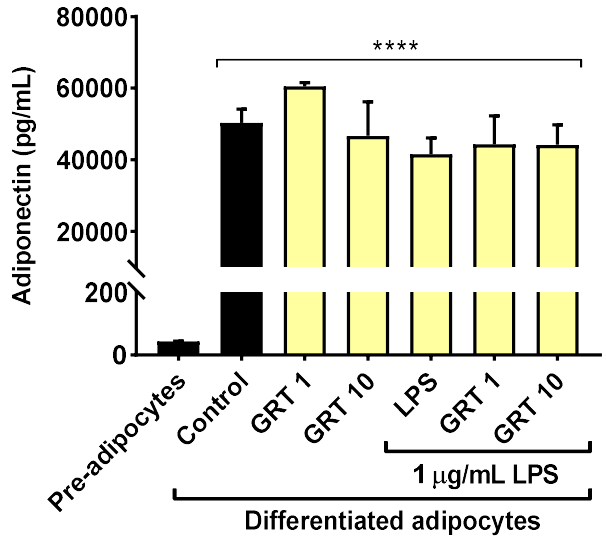

Figure 4.10.2: Adiponectin secretion from 3T3-L1 pre-adipocytes and differentiated 3T3-L1 adipocytes. Media was collected from 3T3-L1 pre-adipocytes and thereafter differentiated. Differentiated 3T3-L1 adipocytes were treated with LPS and two GRT concentrations (GRT1 and GRT10) for 24 hours. Thereafter, media collected from the upper insert compartment was assayed for adiponectin secretion using an ELISA. Data presented are the mean ± SD of three independent experiments (n = 3), relative to pre-adipocytes. A one-way Analysis of Variance was performed with a Tukey post hoc test, **** $p < 0.0001$.

GRT1 = 1 μg/mL, GRT10 = 10 μg/mL, LPS = Lipopolysaccharides, ELISA = enzyme-linked immunosorbent assay.

5 DISCUSSION

5.1 Skeletal muscle plays a crucial role in metabolic homeostasis

In the human, skeletal muscle mass peaks between 25 – 30 years of age attaining an average muscle mass in men of around 44% and women around 33% of body weight (Gallagher & Heymsfield, 1998; Kallman *et al*., 1990; Metter *et al*., 1997, 1999). Apart from movement, skeletal muscle is responsible for peripheral blood glucose and lipid uptake from the circulation in response to various stimuli (Costamagna *et al*., 2015; DeFronzo & Tripathy, 2009; Mukund & Subramaniam, 2019). In terms of glucose, the major glucose transporter, GLUT4 is responsive to insulin stimulation and intracellular signals such as during exercise via the energy sensing signaling system, AMPK triggered by the intracellular AMP/ATP ratio (Kurth-Kraczek *et al*. ,1999; Richter & Hargreaves, 2013). The skeletal muscle also utilizes fatty acids from the circulation that enter the muscle either by passive diffusion or by protein mediated transport where after the lipids are bound to cytoplasmic fatty acid-binding protein and conjugated to coenzyme A for beta-oxidation or fatty acid synthesis (Kelley, 2005). Therefore, muscle and by implication muscle mass plays a crucial role in the body's ability to utilize energy available from various substrates as required by the body during periods of feast, fast and exercise. The role of exercise as a modifiable lifestyle to protect against and prevent the development of metabolic disease is broadly promoted. Exercise has a positive impact on whole body metabolism and is one of the strategies in the management of metabolic diseases (Holten *et al*., 2004) moreover, increased muscle mass has been associated with increased insulin sensitivity (Holten *et al*., 2004; Srikanthan & Karlamangla, 2011). It is also well known that the skeletal muscle is a metabolically active tissue that secretes various myokines especially during periods of exercise (Carey *et al*., 2006; Hartwig *et al*., 2014) therefore, a sedentary lifestyle would result in a lack of these contraction-induced myokines which have beneficial effects on energy metabolism with the muscle tissue and other body organs or tissues (Huh *et al*., 2014; Li *et al*., 2017; Pedersen *et al*., 2007; Zhang *et al*., 2014).

Metabolic syndrome has been associated with a decrease in muscle mass, resulting in a loss of insulin mediated glucose uptake in prediabetic individuals (Jeon *et al*., 2020; Srikanthan & Karlamangla, 2011). As skeletal muscle accounts for ca. 70 - 80% of the glucose uptake from the circulation, loss of insulin responsiveness can result in persistent hyperglycaemia (DeFronzo, 1992; DeFronzo *et al*., 1979; DeFronzo, 2004; DeFronzo & Tripathy, 2009; Tripathy & Chavez, 2010). Chronic insulin resistance is a serious condition that affects the ability of insulin responsive tissues, especially skeletal muscles, to remove post-prandial glucose from the circulation. A major cause of insulin resistance in muscle is attributable to chronic inflammation primarily

resulting from the gut and perpetuated by the adipose tissue (Cani *et al*., 2007; Guerville *et al*., 2017).

In the gut, diet and dysbiosis (unhealthy gut microbiota) induce an inflammatory state driven by release of inflammatory mediators such as lipopolysaccharides (LPS) derived from nefarious gram-negative gut bacteria (Boulangé *et al*., 2016). In the circulation, LPS interacts with peripheral tissue and the innate immune system thereby, contributing to a state of chronic low-grade inflammation (Ferrante, 2007; Weisberg *et al*., 2003; Wu & Ballantyne, 2017). As obese and T2DM individuals have higher circulating plasma LPS levels (metabolic endotoxemia) this has been attributed to 'leaky gut' syndrome. Subjects with metabolic syndrome have altered intestinal wall permeability therefore allowing the translocation of endotoxin into the circulation where it interacts with peripheral tissues, particularly adipose and muscle tissue (Gomes *et al*., 2017; Jayashree *et al*., 2014).

In adipose tissue, LPS-induced metabolic endotoxemia results in the up-regulation and secretion of various pro-inflammatory cytokines, including IL-6, TNF-α, MCP-1, of which are associated with the metabolic syndrome (Clemente-Postigo *et al*., 2019; Hotamisligil *et al*., 1993; Pereira & Alvarez-Leite, 2014). Chronic elevation of these cytokines have a detrimental effect on skeletal muscle insulin sensitivity and underlie the development of insulin resistance and glucose intolerance, and are risk factor for a series of metabolic diseases such as T2DM (Feinstein *et al*., 1993; Kern *et al*., 2001; Rasouli & Kern, 2008; Shoelson, 2006). What is generally not considered is the cytokine response of skeletal muscle in response to metabolic endotoxemia. IL-6 and TNF-α are up-regulated in response to metabolic endotoxemia, and results in a decrease in insulin sensitivity (Sell *et al*., 2006, 2008). IL-10, a well-known anti-inflammatory cytokine is reduced in skeletal muscle in obese individuals (Wu & Ballantyne, 2017). In skeletal muscle the inflammatory response could either be modulated or worsened by the paracrine effect of adiponectin and IL-6 (Christiansen *et al*., 2010; Nicholson *et al*., 2018). Franckhauser *et al* (2008) showed that chronic elevation of circulating IL-6 promoted insulin resistance characterised by hyperinsulinaemia, impaired insulin-stimulated glucose uptake by the skeletal muscle and hepatic inflammation in mice overexpressing IL-6 (Franckhauser *et al*., 2008).

This study investigated the effect of LPS on C2C12 myoblasts and specifically, their ability to differentiate and form myotubules as a surrogate *in vitro* model for myogenesis. As an inflammatory marker the pro-inflammatory cytokine IL-6 was selected. The effect of LPS on the myogenic genes myogenin, MyoD and myostatin, as well as other signaling pathway effectors such as Akt, AMPK and mTOR were investigated to better understand the underlying

mechanisms as well as the phenotypic effect on myoblast to myotubule differentiation. The effect of LPS on insulin sensitivity and glucose uptake was also measured. The study also included an *in vitro* co-culture model, using 3T3-L1 pre-adipocytes and differentiated 3T3-L1 adipocytes cultured on an insert membrane into a well containing C2C12 myoblasts.

5.2 Lipopolysaccharide was not cytotoxic to C2C12 skeletal muscle cells

In this study a MTT assay confirmed that LPS at the concentrations tested (0.05, 0.1 and 1 µg/mL) was not cytotoxic to either the C2C12 myoblast nor the differentiated myotubules (figure 4.2.2). This was further confirmed by an unchanged morphology of the myoblasts and myotubules after 24-hour exposure to LPS (figure 4.2.1). In agreement with our findings, Podbregar and colleagues found LPS (100 ng/mL) was not cytotoxic to myoblasts or myotubes (Podbregar *et al*., 2013). In addition a study by Shang *et al* (2015) reported that incubation with LPS for 24 hours at concentrations up to 50 µg/mL were not toxic to C2C12 myoblasts and only high concentrations (100 – 150 µg/mL) affected myoblast morphology (Shang *et al*., 2015).

5.3 Lipopolysaccharide induces Interleukin-6 secretion in myoblasts but not in myotubules

LPS is a potent inducer of pro-inflammatory cytokine IL-6 and strongly induces pro-inflammatory cytokine IL-6 secretion in murine C2C12 myoblasts (Frost *et al*., 2002; Frost *et al*., 2003; Liang *et al*., 2013; Podbregar *et al*., 2013). The role of the pro-inflammatory cytokine IL-6 is well described and is identified as a major driver of insulin resistance, obesity and the development of T2DM (Kim, Bachmann, & Chen, 2009). Although approximately 35% of IL-6 is secreted by the adipose tissue, including resident adipose tissue macrophages, IL-6 is also produced by muscle during strenuous exercise and thus can also be regarded as a myokine, owing to the fact that IL-6 deficient (IL-$6^{-/-}$) mice have reduced endurance and energy expenditure during exercise (Fäldt *et al*., 2004; Helge *et al*., 2003; Pedersen *et al*., 2004; Pedersen & Fischer, 2007). Paradoxically, in skeletal muscle, IL-6 appears to have an insulin sensitizing effect and plays an active role in muscle repair of skeletal muscle (Carey *et al*., 2006; Pedersen *et al*., 2004). Conversely IL-6 has also been associated with muscle atrophy and wasting (Haddad *et al*., 2005).

This study confirmed that C2C12 myoblasts produce and secrete significant amounts of IL-6 in response to LPS (figure 4.3.1 A and B, $p < 0.001$), whilst differentiated myotubules where unresponsive to LPS (figure 4.3.1 C and D). This corresponds to findings from studies on isolated human skeletal muscle cells that showed a significant increase in myoblast IL-6 secretion compared to myotubes (Podbregar *et al*., 2013). Using the C2C12 myoblast cell line, Frost *et al* (2003) demonstrated that both cell types (myoblasts and myotubules) had a similar increase in IL-6 mRNA after 4 hours of exposure to LPS, however, IL-6 protein secretion by myotubules was significantly reduced compared to myoblasts (Frost *et al*., 2003) suggesting that IL-6 gene expression may be differentially regulated between the two cell types. In C2C12 myoblasts, LPS concentration dependently (0.01 to 10 µg/mL) increased IL-6 mRNA expression after 4 hours and was elevated nearly 5-fold above basal levels after 18 hours in myoblasts exposed to 1 µg/mL LPS (Frost *et al*., 2002). In a follow up study Frost *et al*, (2003) again demonstrated a strong LPS stimulated IL-6 secretion response by myoblasts up to 16 hours. Western blot analysis showed maximum protein expression for IL-6 occurred at 2 - 3 hours and IL-6 mRNA expression was also seen maximally expressed (~ 9-fold) at 3 hours but had decreased to baseline by 16 hours (Frost *et al*., 2003). These findings could explain why we did not see increased IL-6 mRNA expression in the C2C12 myoblasts after 24 hours (figure 4.3.2).

5.4 Lipopolysaccharide partially suppresses insulin signalling

To determine whether LPS affects glucose uptake in skeletal muscle and whether it in fact could sensitize muscle to insulin, was investigated by exposing myoblasts with LPS for 24 hours. Glucose removal by the C2C12 myoblasts from the media as well as the intracellular glucose uptake using 2-deoxyglucose as an indicator of insulin stimulated intracellular glucose uptake was evaluated. Interestingly, LPS concentration dependently decreased the removal of glucose from the media (figure 4.4 A, $p < 0.01$), whilst both basal and insulin stimulated intracellular uptake as measured by 2-deoxyglucose uptake, were not affected by LPS (figure 4.4 B). This suggests that although the LPS has some downstream effect on glucose metabolism, the insulin responsiveness of the C2C12 myoblast was not affected by LPS. Supporting the notion that in skeletal muscle derived IL-6 does not induce insulin resistance. Although the activation of Akt of C2C12 myoblasts by insulin was attenuated by LPS (figure 4.5 A and C), suggesting that insulin signalling was affected, this was further supported by Liang *et al*, (2013), where LPS (100 ng/mL) reduced insulin-stimulated Akt phosphorylation (Liang *et al*., 2013). The mechanistic target of

rapamycin is a well-known kinase involved in the regulation of muscle mass, thereby controlling protein translation; however, AMPK is a negative regulator of mTOR gearing the cellular processes toward a catabolic state (Sukumaran *et al*., 2020). In this study, protein expression or activation of mTOR was not affected by LPS suggesting that the skeletal muscle anabolic and catabolic processes were not affected (figure 4.6.1 A – C). Neither was AMPK protein expression and activation affected, suggesting that cellular AMP/ATP levels were not affected by the LPS (figure 4.6.2 A – C).

5.5 Lipopolysaccharide inhibits myogenesis

Murine C2C12 myoblasts readily differentiate into myocytes that fuse to form myotubules when the FBS serum content of the media is reduced from 10% to 0.5%, or the 10% FBS is replaced by 2% HS (Langen *et al*., 2003). In this study the latter method of differentiation was used once the myoblast cultures were ca. 80% confluent. Three days after differentiation, multiple elongated myotubules had formed and in this study, these were used to study the effects of LPS on differentiated skeletal muscle. A major issue in the maintenance of muscle mass revolves around a balance between skeletal muscle damage, muscle repair and the building of new muscle fibers from muscle satellite cells in response to myogenic stimuli (Costamagna *et al*., 2015; Frontera & Ochala, 2015; Gordon *et al*., 2013; Gransee *et al*., 2012; Mukund & Subramaniam, 2019). Interestingly IL-6 secretion during vigorous exercise and muscle damage/injury plays an important role in the repair process (Belizário, Fontes-Oliveira, Borges, Kashiabara, & Vannier, 2016; Muñoz-Cánoves, Scheele, Pedersen, & Serrano, 2013; Serrano *et al*., 2008). In this study we investigated the effect that LPS has on the differentiation of C2C12 myotubules from myoblasts. In this experiment myoblast differentiation was induced by replacing the 10% FBS in the media with 2% HS for three days, with or without exposure to LPS. After three days the number and width of the myotubules were measured using a digitized image and imaging software by using point-to-point measurements. Based on the morphology and measurements, LPS did reduce the number of myotubules that formed during differentiation (figure 4.6.4 C, $p < 0.01$). In addition, the width of the myotubules was also reduced, when differentiated in the presence of LPS (figure 4.6.4 B, $p < 0.0001$). This finding is in agreement with a study by Ono *et al*, (2017) where LPS reduced myotubule width and fusion index in C2C12 myoblasts differentiated in the presence of LPS (Ono & Sakamoto, 2017). In a follow up study, Ono *et al*, (2020) demonstrated that LPS induced muscle mass loss in a mouse model of endotoxemia-associated muscle weakness, and

was confirmed by the histological examination of the tibialis anterior muscle sections which showed that LPS induced shrinkage of muscle fibres (Ono *et al*., 2020).

Interestingly, IL-6 secretion peaked just before differentiation (figure 4.6.3, $p < 0.0001$) and reduced to near control levels once the differentiating media containing the 2% horse serum was added. This suggests that the reduction in myotubule formation was the result of the LPS and not IL-6. In terms of myogenic gene expression LPS suppressed myogenin mRNA expression (figure 4.6.5 B) the myogenic factor that is activated during serum deprivation as is the case for reducing the 10% FBS to 2% HS in the C2C12 differentiation media. Myogenin induces cell cycle arrest and commits the myoblast to the myocyte lineage (Andrés & Walsh, 1996). The other myogenic gene MyoD, plays an important role in the proliferation of myoblasts and regulation of other myogenic regulatory factors (Almeida *et al*., 2016; Burattini *et al*., 2004; Dedieu *et al*., 2002). In this case, the C2C12 myoblasts were almost 80% confluent when differentiation was initiated and therefore these cells were already approaching senescence, explaining the low levels of MyoD expression (figure 4.6.5 A) (Moran *et al*., 2002).

Myostatin protein expression was also investigated during differentiation. Although myostatin is generally associated with muscle catabolism and muscle wasting (Lautaoja *et al*., 2020; Ono & Sakamoto, 2017; Ríos *et al*., 2002; Taylor *et al*., 2001; Thomas *et al*., 2000). In this study myostatin expression increased during C2C12 myoblast differentiation (figure 4.6.5 C) suggesting that it could play a role in the regulation of myoblast proliferation and the cell survival (Artaza *et al*., 2002; Ríos *et al*., 2001). However, myostatin expression was down regulated in differentiating myoblasts exposed to LPS and this was also seen for myogenin and MyoD. These findings were also demonstrated by Ono *et al* (2017), where LPS down regulated myogenin and MyoD, in C2C12 myoblasts differentiated in the presence of LPS, but not myostatin. Myostatin expression was increased in the presence of LPS both at mRNA and protein level (Ono & Sakamoto, 2017). Weber *et al* (2005) showed that LPS injection decreased the MyoD and myostatin mRNA expression after 24 hours in muscle samples from channel catfish (Ictalurus punctatus) (Weber *et al*., 2005). A study by Lang *et al* (2001) showed that myostatin mRNA expression was not altered 24 hours post LPS injection in their rat model (Lang *et al*., 2001), whereas a study by Smith *et al* (2010) showed reduced myostatin mRNA expression and unchanged protein levels in cecal ligation and puncture sepsis-induced rats (Smith *et al*., 2010). Although there is contradicting data in the regulation of myostatin, this study confirms that MyoD and myogenin are actively involved in myogenesis and their regulation is critical for myotube size and number as denoted in the study by Dedieu *et al* (2002).

5.6 Potential properties of Afriplex GRT^{TM} in modulating mitochondrial metabolism

After establishing the *in vitro* C2C12 skeletal model and the effects of LPS on the IL-6 production, glucose utilization, insulin sensitivity and myoblast differentiation into myotubules. The effects of an aspalathin-rich green rooibos extract GRT, previously shown to enhance glucose metabolism, was evaluated on LPS treated C2C12 myoblasts. GRT was not cytotoxic to C2C12 myoblasts up to a concentration of 100 µg/mL, after 24 hours of treatment (figure 4.7 D). This is in agreement with a study conducted by Millar *et al* (2020), where GRT at 10 and 100 µg/mL showed no cytotoxic effect on C3A liver cells (Millar *et al*., 2020). To further assess the effect of GRT on mitochondrial bioenergetics, we performed a Seahorse XF Cell Mito Stress Test assay. In agreement with the MTT data, that demonstrated GRT increased MTT activity, we observed that GRT increased OCR capacity in terms of basal, maximal respiration and ATP production (figure 4.8 B - D). This suggests that GRT has the potential to improve or enhance mitochondrial respiratory capacity and therefore increase energy output of the cells, and to maintain cellular functions under stress conditions as energy demands increase (Hill *et al*., 2012). This corresponds with a previous study by Uličná *et al*, (2019) showing that an aqueous extract of green rooibos improved ATP production in isolated mitochondria from carbon tetrachloride (CCl4)-induced liver damage rats (Uličná *et al*., 2019). Spare respiratory capacity is hypothesized as the compensatory mechanism available to the cells in response to increased energy demand or stress (Brand & Nicholls, 2011; Decleer *et al*., 2018). The exposure of C2C12 cells to GRT did not affect spare respiratory capacity (calculated as the difference between basal and maximal respiration) (figure 4.8 E). This suggests that GRT enhances mitochondrial respiration i.e., increasing both basal and maximal respiration without depleting spare respiratory capacity, leaving the cells reserve to produce additional ATP in case of extra need intact. Taking it all together, this provides evidence of the potential properties of GRT in its ability to modulate and ameliorate mitochondrial metabolism in insulin resistant tissues.

5.7 Lipopolysaccharide-induced Inflammation is not affected by rooibos extract

Although previous studies have suggested that rooibos reduced IL-6 plasma concentrations *in vivo*, *in vitro* blood cultures in fact increased IL-6 secretion (Smith & Swart, 2016). However, in this study treatment of C2C12 myoblasts with GRT did not influence LPS-induced IL-6 secretion

over a 24-hour period (figure 4.9.1). In terms of intracellular glucose uptake rate as determined by intracellular 2-deoxyglucose, GRT did not significantly affect basal, or insulin stimulated uptake rates in the presence LPS (figure 4.9.2). Although GRT did not have a significant effect on the insulin-stimulated Akt protein expression and activation except for the low GRT concentration (GRT1), which significantly affected the expression of and activation of insulin-Akt expression compared to the non-stimulated control (figure 4.9.3 A - C). Interestingly, the low concentration of GRT significantly improved insulin stimulated Akt activation blunted by the LPS (figure 4.9.3 A). This is in keeping with several other *in vitro* and *in vivo* studies have been conducted to evaluate the glucose lowering ability of rooibos extracts or rooibos components. The mechanisms proposed by these studies constantly involved increased activation of Akt and AMPK (Dludla *et al*., 2017; Kawano *et al*., 2009; Mazibuko *et al*., 2013; Muller *et al*., 2012). Unfortunately, the AMPK results were inconclusive and could not support such a hypothesis (figure 4.9.4 A – C). Interestingly LPS reduced the mRNA expression of the myogenic genes myogenin and MyoD in the C2C12 myoblast after 24 hours. GRT appeared not to affect the expression of these myogenic genes either with or without LPS treatment (figure 4.9.5 A and B).

5.8 Lipopolysaccharide-induced interleukin-6 secretion in C2C12 co-cultured with 3T3-L1 adipocytes

Next, we investigated the effect of LPS in a co-culture model of 3T3-L1 pre-adipocytes or differentiated 3T3-L1 adipocyte culture on a membrane insert to establish the relative contribution of IL-6 from the adipose cells on the apical side of the membrane to the IL-6 secreted by the C2C12 myoblasts in the basolateral compartment. Interleukin-6 secretion by the pre-adipocytes (figure 4.10.1 A, $p < 0.0001$) was significantly higher into apical compartment than that by the differentiated 3T3-L1 adipocytes (figure 4.10.1 B). This finding corresponded to that of Harkins *et al*, (2004), showing that the 3T3-L1 pre-adipocytes expressed higher levels of LPS-induced IL-6 mRNA and secreted IL-6 than the differentiated cells. In addition, *ob/ob* mice stromal adipose tissue secreted more IL-6 than mature fully differentiated adipocytes (Harkins *et al*., 2004).

In this study, it was also interesting to note that in the 3T3-L1 pre-adipocytes, the IL-6 concentrations were similar in both compartments (apical and basolateral) (figure 4.10.1 A), whilst in the co-culture with the differentiated adipocytes, the contribution from the adipocytes was less and indeed the IL-6 secretion by the C2C12 myoblasts was also attenuated (figure 4.10.1 B).

Seyoum *et al* (2011) also demonstrated that the addition of LPS (1 µg/mL) increased IL-6 mRNA expression in L6 myocytes co-cultured with 3T3-L1 pre-adipocytes by 9.5-fold compared to a 8.2-fold increase when co-cultured with differentiated 3T3-L1 adipocytes. In addition IL-6 secretion was increased in L6 myocytes co-cultured with 3T3-L1 pre-adipocytes (Seyoum *et al*., 2011) as is confirmed in this study, and is in agreement with that of Harkins *et al* (2004). This suggests that some crosstalk could exist and that differentiated adipocytes could have some anti-inflammatory properties. Mediators of such anti-inflammatory effects by adipocytes could include adipokines such as adiponectin and cytokines such as IL-10 (Lira *et al*., 2012). Indeed, this study supported the aforementioned, as adiponectin was highly secreted by differentiated 3T3-L1 adipocytes compared to the minimal secretion observed in 3T3-L1 pre-adipocytes (figure 4.10.2). This finding confirmed the observations by Körner and colleagues (2005) where they observed that adiponectin protein was not expressed by human pre-adipocytes and expression was only observed in mature adipocytes (differentiated adipocytes) (Körner *et al*., 2005).

A study by Zoico *et al*, (2009) showed that adiponectin significantly suppressed LPS-induced expression of IL-6 mRNA expression and protein secretion in differentiated 3T3-L1 adipocytes exposed to LPS (1 µg/mL), the same was observed with MCP-1 expression, therefore showing that adiponectin acts as a modulator of the inflammatory response by suppressing the expression of pro-inflammatory cytokines (Zoico *et al*., 2009). Chirumbolo *et al* (2014) demonstrated that IL-10 expression was increased at low concentrations (1 to 10 ng/mL) but was downregulated with increasing LPS concentration (up to 10 000 ng/mL) and incubation times in differentiated 3T3-L1 adipocytes (Chirumbolo *et al*., 2014). In this study, however, IL-10 secretion was not detected in the media collected from C2C12 myoblasts as well as the 3T3-L1 pre-adipocytes and the mature adipocytes (data not shown).

6 CONCLUSIONS

6.1 Concluding Remarks

Lipopolysaccharide (LPS) proved to be a formidable inducer of IL-6 cytokine inflammatory response in C2C12 myoblasts compared to myotubules. Although, LPS had no effect on myoblast morphology, myotubule formation was significantly reduced with a concurrent decrease in myogenic regulatory factors, MyoD and myogenin, as well as a decrease in myotube width. In terms of energy metabolism, C2C12 myoblasts were still responsive to insulin stimulation. GRT was able to increase C2C12 skeletal muscle maximal oxidation consumption, suggesting a protective effect on mitochondrial bioenergetics and energy modulatory properties, however this was not seen in combination with LPS. Further, in this study GRT did not modulate the inflammatory response nor alter the cellular energy status of the cells in terms of AMPK and mTOR activation.

Adipokine-myocyte crosstalk is particularly important in maintaining healthy whole-body metabolism. This study suggests that in co-culture the LPS-induced inflammatory IL-6 response by myoblasts was modulated by differentiated 3T3-L1 adipocytes, and this was accommodated by a dramatic increase of adiponectin but not IL-10. The co-culture model established in this study allows for further investigation on the role of such adipokine crosstalk in between adipocytes and muscle into paracrine/endocrine function.

6.2 Limitations of the study

Mitochondrial bioenergetics of myoblasts exposed to LPS and GRT were not conducted due to time and budget constraints. Determining the OCR parameters to access the energy status of the myoblasts following LPS exposure, and if the rooibos extract was able to decrease or enhance mitochondrial energy capacity under stress. The extracellular cytoplasmic acidification rates (ECAR) were not determined, and these would have been beneficial to understand the effect of LPS and GRT on glycolysis.

This study also showed that LPS inhibits myogenesis through a decrease in myotube size and width. As the Western blot protein expression of mTOR and AMPK was inconclusive, assessing these and other insulin signaling genes such as AKT, AS160 and GLUT4 would have contributed

to a better understanding of how LPS impacts on myoblast differentiation and the mechanism(s) involved in glucose metabolism and cellular energy homeostasis in atrophying muscle.

6.3 Future work

To address the limitations of the study, proposed future experiments will include the assessment of glucose metabolism in myoblasts differentiated in the presence of LPS as well as PCR array to access and/or identify genes related to disease progression in metabolic syndrome and muscle wasting.

Agilent Seahorse XF Analyzer will be used to access the mitochondrial bioenergetics in myoblasts fully differentiated in the presence of LPS (OCR and ECAR). Determining OCR and ECAR of the myoblasts following LPS exposure will establish if the rooibos extract was able to decrease or enhance mitochondrial energy capacity.

Furthermore, adiponectin was significantly secreted in differentiated adipocytes, potentially offering protective anti-inflammatory effects as seen by a reduced IL-6 secretion in differentiated adipocytes compared to the 3T3-L1 pre-adipocytes. Therefore, further gene expression and protein analysis of adipocyte-myocyte co-culture can elucidate the effects of adipocytes on myoblast gene expression and the mechanisms involved.

6.4 Contributions to the study

Prof C.J.F. Muller contributed to the conception and design of the study. Nnini Obonye contributed to the data collection. Nnini Obonye and Prof S.E. Mazibuko-Mbeje provided data analysis and interpretation. The drafting of the thesis was provided by Nnini Obonye and Prof C.J.F. Muller. Prof C.J.F. Muller, Nnini Obonye, Prof S.E. Mazibuko-Mbeje and Prof H. Strijdom contributed to the critical revision of the thesis and final approval of the version to be submitted.

7 REFERENCES

Ahmad, M., Wolberg, A., & Kahwaji, C. I. (2021). Biochemistry, Electron Transport Chain. In *StatPearls*. StatPearls Publishing. http://www.ncbi.nlm.nih.gov/pubmed/30252361

Allen, D. L., Hittel, D. S., & McPherron, A. C. (2011). Expression and function of myostatin in obesity, diabetes, and exercise adaptation. *Medicine and Science in Sports and Exercise*, *43*(10), 1828–1835. https://doi.org/10.1249/MSS.0b013e3182178bb4

Almeida, C. F., Fernandes, S. A., Ribeiro Junior, A. F., Keith Okamoto, O., & Vainzof, M. (2016). Muscle Satellite Cells: Exploring the Basic Biology to Rule Them. *Stem Cells International*, *2016*, 1–14. https://doi.org/10.1155/2016/1078686

American Type Culture Collection. (2017). *C2C12 ATCC ® CRL-1772™ Mus musculus muscle*. https://www.atcc.org/products/all/CRL-1772.aspx#characteristics

Amor, M., Itariu, B. K., Moreno-Viedma, V., Keindl, M., Jürets, A., Prager, G., Langer, F., Grablowitz, V., Zeyda, M., & Stulnig, T. M. (2019). Serum Myostatin is Upregulated in Obesity and Correlates with Insulin Resistance in Humans. *Experimental and Clinical Endocrinology & Diabetes*, *127*(08), 550–556. https://doi.org/10.1055/a-0641-5546

Andrés, V., & Walsh, K. (1996). Myogenin expression, cell cycle withdrawal, and phenotypic differentiation are temporally separable events that precede cell fusion upon myogenesis. *The Journal of Cell Biology*, *132*(4), 657–666. https://doi.org/10.1083/jcb.132.4.657

Arnold, L., Henry, A., Poron, F., Baba-Amer, Y., van Rooijen, N., Plonquet, A., Gherardi, R. K., & Chazaud, B. (2007). Inflammatory monocytes recruited after skeletal muscle injury switch into antiinflammatory macrophages to support myogenesis. *Journal of Experimental Medicine*, *204*(5), 1057–1069. https://doi.org/10.1084/jem.20070075

Artaza, J. N., Bhasin, S., Mallidis, C., Taylor, W., Ma, K., & Gonzalez-Cadavid, N. F. (2002). Endogenous expression and localization of myostatin and its relation to myosin heavy chain distribution in C2C12 skeletal muscle cells. *Journal of Cellular Physiology*, *190*(2), 170–179. https://doi.org/10.1002/jcp.10044

Ato, S., Kido, K., Sato, K., & Fujita, S. (2019). Type 2 diabetes causes skeletal muscle atrophy but does not impair resistance training-mediated myonuclear accretion and muscle mass gain in rats. *Experimental Physiology*, *104*(10), 1518–1531. https://doi.org/10.1113/EP087585

Austin, L., Bower, J., Kurek, J., & Vakakis, N. (1992). Effects of leukaemia inhibitory factor and

other cytokines on murine and human myoblast proliferation. *Journal of the Neurological Sciences*, *112*(1–2), 185–191. https://doi.org/10.1016/0022-510X(92)90149-F

Baker, J. S., McCormick, M. C., & Robergs, R. A. (2010). Interaction among Skeletal Muscle Metabolic Energy Systems during Intense Exercise. *Journal of Nutrition and Metabolism*, *2010*, 1–13. https://doi.org/10.1155/2010/905612

Baker, R. G., Hayden, M. S., & Ghosh, S. (2011). NF-κB, inflammation, and metabolic disease. In *Cell Metabolism* (Vol. 13, Issue 1, pp. 11–22). NIH Public Access. https://doi.org/10.1016/j.cmet.2010.12.008

Bays, H., Mandarino, L., & DeFronzo, R. A. (2004). Role of the Adipocyte, Free Fatty Acids, and Ectopic Fat in Pathogenesis of Type 2 Diabetes Mellitus: Peroxisomal Proliferator-Activated Receptor Agonists Provide a Rational Therapeutic Approach. In *Journal of Clinical Endocrinology and Metabolism* (Vol. 89, Issue 2, pp. 463–478). Oxford Academic. https://doi.org/10.1210/jc.2003-030723

Belizário, J. E., Fontes-Oliveira, C. C., Borges, J. P., Kashiabara, J. A., & Vannier, E. (2016). Skeletal muscle wasting and renewal: a pivotal role of myokine IL-6. *SpringerPlus*, *5*(1), 619. https://doi.org/10.1186/s40064-016-2197-2

Bjornson, C. R. R., Cheung, T. H., Liu, L., Tripathi, P. V., Steeper, K. M., & Rando, T. A. (2012). Notch Signaling Is Necessary to Maintain Quiescence in Adult Muscle Stem Cells. *STEM CELLS*, *30*(2), 232–242. https://doi.org/10.1002/stem.773

Blau, H. M., Chiu, C. P., & Webster, C. (1983). Cytoplasmic activation of human nuclear genes in stable heterocaryons. *Cell*, *32*(4), 1171–1180. https://doi.org/10.1016/0092-8674(83)90300-8

Boden, G., She, P., Mozzoli, M., Cheung, P., Gumireddy, K., Reddy, P., Xiang, X., Luo, Z., & Ruderman, N. (2005). Free fatty acids produce insulin resistance and activate the proinflammatory nuclear factor-Kb pathway in rat liver. *Diabetes*, *54*(12), 3458–3465. https://doi.org/10.2337/diabetes.54.12.3458

Bodine, S. C., Stitt, T. N., Gonzalez, M., Kline, W. O., Stover, G. L., Bauerlein, R., Zlotchenko, E., Scrimgeour, A., Lawrence, J. C., Glass, D. J., & Yancopoulos, G. D. (2001). Akt/mTOR pathway is a crucial regulator of skeletal muscle hypertrophy and can prevent muscle atrophy in vivo. *Nature Cell Biology*, *3*(11), 1014–1019. https://doi.org/10.1038/ncb1101-1014

Bortolotto, S. K., Morrison, W. A., Han, X., & Messina, A. (2004). Mast cells play a pivotal role in ischaemia reperfusion injury to skeletal muscles. *Laboratory Investigation*, *84*(9), 1103–1111. https://doi.org/10.1038/labinvest.3700126

Boström, P., Wu, J., Jedrychowski, M. P., Korde, A., Ye, L., Lo, J. C., Rasbach, K. A., Boström, E. A., Choi, J. H., Long, J. Z., Kajimura, S., Zingaretti, M. C., Vind, B. F., Tu, H., Cinti, S., Højlund, K., Gygi, S. P., & Spiegelman, B. M. (2012). A PGC1-α-dependent myokine that drives brown-fat-like development of white fat and thermogenesis. *Nature*, *481*(7382), 463–468. https://doi.org/10.1038/nature10777

Boulangé, C. L., Neves, A. L., Chilloux, J., Nicholson, J. K., & Dumas, M.-E. (2016). Impact of the gut microbiota on inflammation, obesity, and metabolic disease. *Genome Medicine*, *8*(1), 42. https://doi.org/10.1186/s13073-016-0303-2

Boutagy, N. E., McMillan, R. P., Frisard, M. I., & Hulver, M. W. (2016). Metabolic endotoxemia with obesity: Is it real and is it relevant? *Biochimie*, *124*, 11–20. https://doi.org/10.1016/j.biochi.2015.06.020

Brand, M. D., & Nicholls, D. G. (2011). Assessing mitochondrial dysfunction in cells. *Biochemical Journal*, *435*(2), 297–312. https://doi.org/10.1042/BJ20110162

Brody, T. (1999). Energy Requirement. In *Nutritional Biochemistry* (pp. 273–309). Elsevier. https://doi.org/10.1016/B978-012134836-6/50008-1

Bryner, R. W., Woodworth-Hobbs, M. E., Williamson, D. L., & Alway, S. E. (2012). Docosahexaenoic Acid Protects Muscle Cells from Palmitate-Induced Atrophy. *ISRN Obesity*, *2012*, 1–14. https://doi.org/10.5402/2012/647348

Buckingham, M. (2007). Skeletal muscle progenitor cells and the role of Pax genes. *Comptes Rendus - Biologies*, *330*(6–7), 530–533. https://doi.org/10.1016/j.crvi.2007.03.015

Buckingham, M., & Relaix, F. (2015). PAX3 and PAX7 as upstream regulators of myogenesis. In *Seminars in Cell and Developmental Biology* (Vol. 44, pp. 115–125). Academic Press. https://doi.org/10.1016/j.semcdb.2015.09.017

Burattini, S., Ferri, R., Battistelli, M., Curci, R., Luchetti, F., & Falcieri, E. (2004). C2C12 murine myoblasts as a model of skeletal muscle development: Morpho-functional characterization. *European Journal of Histochemistry*, *48*(3), 223–234. https://doi.org/10.4081/891

Burks, T. N., & Cohn, R. D. (2011). Role of TGF-β signaling in inherited and acquired

myopathies. *Skeletal Muscle*, *1*(1), 19. https://doi.org/10.1186/2044-5040-1-19

Canda, B. D., Oguntibeju, O. O., & Marnewick, J. L. (2014). Effects of consumption of rooibos (Aspalathus linearis) and a rooibos-derived commercial supplement on hepatic tissue injury by tert -butyl hydroperoxide in wistar rats. *Oxidative Medicine and Cellular Longevity*, *2014*. https://doi.org/10.1155/2014/716832

Cani, P. D., Amar, J., Iglesias, M. A., Poggi, M., Knauf, C., Bastelica, D., Neyrinck, A. M., Fava, F., Tuohy, K. M., Chabo, C., Waget, A., Delmee, E., Cousin, B., Sulpice, T., Chamontin, B., Ferrieres, J., Tanti, J.-F., Gibson, G. R., Casteilla, L., … Burcelin, R. (2007). Metabolic Endotoxemia Initiates Obesity and Insulin Resistance. *Diabetes*, *56*(7), 1761–1772. https://doi.org/10.2337/db06-1491

Cani, P. D., Bibiloni, R., Knauf, C., Waget, A., Neyrinck, A. M., Delzenne, N. M., & Burcelin, R. (2008). Changes in Gut Microbiota Control Metabolic Endotoxemia-Induced Inflammation in High-Fat Diet-Induced Obesity and Diabetes in Mice. *Diabetes*, *57*(6), 1470–1481. https://doi.org/10.2337/db07-1403

Carey, A. L., Steinberg, G. R., Macaulay, S. L., Thomas, W. G., Holmes, A. G., Ramm, G., Prelovsek, O., Hohnen-Behrens, C., Watt, M. J., James, D. E., Kemp, B. E., Pedersen, B. K., & Febbraio, M. A. (2006). Interleukin-6 Increases Insulin-Stimulated Glucose Disposal in Humans and Glucose Uptake and Fatty Acid Oxidation In Vitro via AMP-Activated Protein Kinase. *Diabetes*, *55*(10), 2688–2697. https://doi.org/10.2337/db05-1404

Caroff, M., & Karibian, D. (2003). Structure of bacterial lipopolysaccharides. *Carbohydrate Research*, *338*(23), 2431–2447. https://doi.org/10.1016/j.carres.2003.07.010

Chatterjee, M., & Scobie, I. (2002). The pathogenesis of type 2 diabetes mellitus. *Practical Diabetes International*, *19*(8), 255–257. https://doi.org/10.1002/pdi.385

Chavez, J. A., & Summers, S. A. (2003). Characterizing the effects of saturated fatty acids on insulin signaling and ceramide and diacylglycerol accumulation in 3T3-L1 adipocytes and C2C12 myotubes. *Archives of Biochemistry and Biophysics*, *419*(2), 101–109. https://doi.org/10.1016/j.abb.2003.08.020

Chavez, J. A., & Summers, S. A. (2010). Lipid oversupply, selective insulin resistance, and lipotoxicity: Molecular mechanisms. *Biochimica et Biophysica Acta - Molecular and Cell Biology of Lipids*, *1801*(3), 252–265. https://doi.org/10.1016/j.bbalip.2009.09.015

Chazaud, B., Sonnet, C., Lafuste, P., Bassez, G., Rimaniol, A.-C., Poron, F., Authier, F.-J., Dreyfus, P. A., & Gherardi, R. K. (2003). Satellite cells attract monocytes and use macrophages as a support to escape apoptosis and enhance muscle growth. *Journal of Cell Biology*, *163*(5), 1133–1143. https://doi.org/10.1083/jcb.200212046

Chen, L., Chen, R., Wang, H., & Liang, F. (2015). Mechanisms Linking Inflammation to Insulin Resistance. *International Journal of Endocrinology*, *2015*, 1–9. https://doi.org/10.1155/2015/508409

Chirumbolo, S., Franceschetti, G., Zoico, E., Bambace, C., Cominacini, L., & Zamboni, M. (2014). LPS response pattern of inflammatory adipokines in an in vitro 3T3-L1 murine adipocyte model. *Inflammation Research*, *63*(6), 495–507. https://doi.org/10.1007/s00011-014-0721-9

Chiva-Blanch, G., & Badimon, L. (2017). Effects of Polyphenol Intake on Metabolic Syndrome: Current Evidences from Human Trials. *Oxidative Medicine and Cellular Longevity*, *2017*, 1–18. https://doi.org/10.1155/2017/5812401

Christiansen, T., Paulsen, S. K., Bruun, J. M., Pedersen, S. B., & Richelsen, B. (2010). Exercise training versus diet-induced weight-loss on metabolic risk factors and inflammatory markers in obese subjects: a 12-week randomized intervention study. *American Journal of Physiology. Endocrinology and Metabolism*, *298*(4), E824-31. https://doi.org/10.1152/ajpendo.00574.2009

Chu, W., Wei, W., Yu, S., Han, H., Shi, X., Sun, W., Gao, Y., Zhang, L., & Chen, J. (2016). C2C12 myotubes inhibit the proliferation and differentiation of 3T3-L1 preadipocytes by reducing the expression of glucocorticoid receptor gene. *Biochemical and Biophysical Research Communications*, *472*(1), 68–74. https://doi.org/10.1016/j.bbrc.2016.02.063

Cinti, S., Mitchell, G., Barbatelli, G., Murano, I., Ceresi, E., Faloia, E., Wang, S., Fortier, M., Greenberg, A. S., & Obin, M. S. (2005). Adipocyte death defines macrophage localization and function in adipose tissue of obese mice and humans. *Journal of Lipid Research*, *46*(11), 2347–2355. https://doi.org/10.1194/jlr.M500294-JLR200

Clarke, B. A., Drujan, D., Willis, M. S., Murphy, L. O., Corpina, R. A., Burova, E., Rakhilin, S. V., Stitt, T. N., Patterson, C., Latres, E., & Glass, D. J. (2007). The E3 Ligase MuRF1 Degrades Myosin Heavy Chain Protein in Dexamethasone-Treated Skeletal Muscle. *Cell Metabolism*, *6*(5), 376–385. https://doi.org/10.1016/j.cmet.2007.09.009

Cleasby, M. E., Jarmin, S., Eilers, W., Elashry, M., Andersen, D. K., Dickson, G., & Foster, K. (2014). Local overexpression of the myostatin propeptide increases glucose transporter expression and enhances skeletal muscle glucose disposal. *American Journal of Physiology-Endocrinology and Metabolism*, *306*(7), E814–E823. https://doi.org/10.1152/ajpendo.00586.2013

Clemente-Postigo, M., Oliva-Olivera, W., Coin-Aragüez, L., Ramos-Molina, B., Giraldez-Perez, R. M., Lhamyani, S., Alcaide-Torres, J., Perez-Martinez, P., El Bekay, R., Cardona, F., & Tinahones, F. J. (2019). Metabolic endotoxemia promotes adipose dysfunction and inflammation in human obesity. *American Journal of Physiology-Endocrinology and Metabolism*, *316*(2), E319–E332. https://doi.org/10.1152/ajpendo.00277.2018

Cline, G. W., Jucker, B. M., Trajanoski, Z., Rennings, A. J. M., & Shulman, G. I. (1998). A novel 13C NMR method to assess intracellular glucose concentration in muscle, in vivo. *American Journal of Physiology - Endocrinology and Metabolism*, *274*(2 37-2), E381–E389. https://doi.org/10.1152/ajpendo.1998.274.2.e381

Cohen, S., Brault, J. J., Gygi, S. P., Glass, D. J., Valenzuela, D. M., Gartner, C., Latres, E., & Goldberg, A. L. (2009). During muscle atrophy, thick, but not thin, filament components are degraded by MuRF1-dependent ubiquitylation. *Journal of Cell Biology*, *185*(6), 1083–1095. https://doi.org/10.1083/jcb.200901052

Costamagna, D., Costelli, P., Sampaolesi, M., & Penna, F. (2015). Role of Inflammation in Muscle Homeostasis and Myogenesis. *Mediators of Inflammation*, *2015*, 1–14. https://doi.org/10.1155/2015/805172

Cusi, K., Maezono, K., Osman, A., Pendergrass, M., Patti, M. E., Pratipanawatr, T., DeFronzo, R. A., Kahn, C. R., & Mandarino, L. J. (2000). Insulin resistance differentially affects the PI 3-kinase- and MAP kinase-mediated signaling in human muscle. *Journal of Clinical Investigation*, *105*(3), 311–320. https://doi.org/10.1172/JCI7535

de Carvalho, C., & Caramujo, M. (2018). The Various Roles of Fatty Acids. *Molecules*, *23*(10), 2583. https://doi.org/10.3390/molecules23102583

Decleer, M., Jovanovic, J., Vakula, A., Udovicki, B., Agoua, R.-S., Madder, A., De Saeger, S., & Rajkovic, A. (2018). Oxygen Consumption Rate Analysis of Mitochondrial Dysfunction Caused by Bacillus cereus Cereulide in Caco-2 and HepG2 Cells. *Toxins*, *10*(7), 266. https://doi.org/10.3390/toxins10070266

Dedieu, S., Mazères, G., Cottin, P., & Brustis, J. J. (2002). Involvement of myogenic regulator factors during fusion in the cell line C2C12. *International Journal of Developmental Biology*, *46*(2), 235–241. https://doi.org/10.1387/ijdb.11934152

DeFronzo, R. A. (1992). Pathogenesis of Type 2 (non-insulin dependent) diabetes mellitus: a balanced overview. *Diabetologia*, *35*(4), 389–397. https://doi.org/10.1007/BF00401208

DeFronzo, R. A., Tobin, J. D., & Andres, R. (1979). Glucose clamp technique: A method for quantifying insulin secretion and resistance. *American Journal of Physiology Endocrinology Metabolism and Gastrointestinal Physiology*, *6*(3), E214-23. https://doi.org/10.1152/ajpendo.1979.237.3.e214

DeFronzo, Ralph A. (2004). Pathogenesis of type 2 diabetes mellitus. *Medical Clinics of North America*, *88*(4), 787–835. https://doi.org/10.1016/j.mcna.2004.04.013

DeFronzo, Ralph A., & Tripathy, D. (2009). Skeletal Muscle Insulin Resistance Is the Primary Defect in Type 2 Diabetes. *Diabetes Care*, *32*(suppl_2), S157–S163. https://doi.org/10.2337/dc09-S302

Dehoux, M., Van Beneden, R., Pasko, N., Lause, P., Verniers, J., Underwood, L., Ketelslegers, J. M., & Thissen, J. P. (2004). Role of the insulin-like growth factor I decline in the induction of atrogin-1/MAFbx during fasting and diabetes. *Endocrinology*, *145*(11), 4806–4812. https://doi.org/10.1210/en.2004-0406

Delgado, I., Huang, X., Jones, S., Zhang, L., Hatcher, R., Gao, B., & Zhang, P. (2003). Dynamic gene expression during the onset of myoblast differentiation in vitro. *Genomics*, *82*(2), 109–121. https://doi.org/10.1016/S0888-7543(03)00104-6

Diagnosis and Classification of Diabetes Mellitus. (2010). *Diabetes Care*, *33*(Supplement_1), S62–S69. https://doi.org/10.2337/dc10-S062

Dietze-Schroeder, D., Sell, H., Uhlig, M., Koenen, M., & Eckel, J. (2005). Autocrine action of adiponectin on human fat cells prevents the release of insulin resistance-inducing factors. *Diabetes*, *54*(7), 2003–2011. https://doi.org/10.2337/diabetes.54.7.2003

Dietze, D., Köenen, M., Röhrig, K., Horikoshi, H., Hanner, H., & Eckel, J. (2002). Impairment of insulin signaling in human skeletal muscle cells by co-culture with human adipocytes. *Diabetes*, *51*(8), 2369–2376. https://doi.org/10.2337/diabetes.51.8.2369

Dirks, M. L., Wall, B. T., Van De Valk, B., Holloway, T. M., Holloway, G. P., Chabowski, A.,

Goossens, G. H., & Van Loon, L. J. (2016). One week of bed rest leads to substantial muscle atrophy and induces whole-body insulin resistance in the absence of skeletal muscle lipid accumulation. *Diabetes*, *65*(10), 2862–2875. https://doi.org/10.2337/db15-1661

Distefano, G., & Goodpaster, B. H. (2018). Effects of Exercise and Aging on Skeletal Muscle. *Cold Spring Harbor Perspectives in Medicine*, *8*(3), a029785. https://doi.org/10.1101/cshperspect.a029785

Dludla, P. V., Jack, B., Viraragavan, A., Pheiffer, C., Johnson, R., Louw, J., & Muller, C. J. F. (2018). A dose-dependent effect of dimethyl sulfoxide on lipid content, cell viability and oxidative stress in 3T3-L1 adipocytes. *Toxicology Reports*, *5*, 1014–1020. https://doi.org/10.1016/j.toxrep.2018.10.002

Dludla, P. V., Joubert, E., Muller, C. J. F., Louw, J., & Johnson, R. (2017). Hyperglycemia-induced oxidative stress and heart disease-cardioprotective effects of rooibos flavonoids and phenylpyruvic acid-2-O-β-D-glucoside. *Nutrition and Metabolism*, *14*(1), 1–18. https://doi.org/10.1186/s12986-017-0200-8

Dresner, A., Laurent, D., Marcucci, M., Griffin, M. E., Dufour, S., Cline, G. W., Slezak, L. A., Andersen, D. K., Hundal, R. S., Rothman, D. L., Petersen, K. F., & Shulman, G. I. (1999). Effects of free fatty acids on glucose transport and IRS-1-associated phosphatidylinositol 3-kinase activity. *Journal of Clinical Investigation*, *103*(2), 253–259. https://doi.org/10.1172/JCI5001

Erridge, C., Bennett-Guerrero, E., & Poxton, I. R. (2002). Structure and function of lipopolysaccharides. *Microbes and Infection*, *4*(8), 837–851. https://doi.org/10.1016/S1286-4579(02)01604-0

Exeter, D., & Connell, D. (2010). Skeletal Muscle: Functional Anatomy and Pathophysiology. *Seminars in Musculoskeletal Radiology*, *14*(02), 097–105. https://doi.org/10.1055/s-0030-1253154

Fäldt, J., Wernstedt, I., Fitzgerald, S. M., Wallenius, K., Bergström, G., & Jansson, J.-O. (2004). Reduced Exercise Endurance in Interleukin-6-Deficient Mice. *Endocrinology*, *145*(6), 2680–2686. https://doi.org/10.1210/en.2003-1319

Feinstein, R., Kanety, H., Papa, M. Z., Lunenfeld, B., & Karasik, A. (1993). Tumor necrosis factor-alpha suppresses insulin-induced tyrosine phosphorylation of insulin receptor and its

substrates. *Journal of Biological Chemistry*, *268*(35), 26055–26058. https://doi.org/10.1016/S0021-9258(19)74276-8

Ferrante, A. W. (2007). Obesity-induced inflammation: a metabolic dialogue in the language of inflammation. *Journal of Internal Medicine*, *262*(4), 408–414. https://doi.org/10.1111/j.1365-2796.2007.01852.x

Foster, D. W. (2012). Malonyl-CoA: the regulator of fatty acid synthesis and oxidation. *Journal of Clinical Investigation*, *122*(6), 1958–1959. https://doi.org/10.1172/JCI63967

Franckhauser, S., Elias, I., Rotter Sopasakis, V., Ferré, T., Nagaev, I., Andersson, C. X., Agudo, J., Ruberte, J., Bosch, F., & Smith, U. (2008). Overexpression of Il6 leads to hyperinsulinaemia, liver inflammation and reduced body weight in mice. *Diabetologia*, *51*(7), 1306–1316. https://doi.org/10.1007/s00125-008-0998-8

Frenette, J., Cai, B., & Tidball, J. G. (2000). Complement Activation Promotes Muscle Inflammation during Modified Muscle Use. *The American Journal of Pathology*, *156*(6), 2103–2110. https://doi.org/10.1016/S0002-9440(10)65081-X

Frisard, M. I., Wu, Y., McMillan, R. P., Voelker, K. A., Wahlberg, K. A., Anderson, A. S., Boutagy, N., Resendes, K., Ravussin, E., & Hulver, M. W. (2015). Low Levels of Lipopolysaccharide Modulate Mitochondrial Oxygen Consumption in Skeletal Muscle. *Metabolism*, *64*(3), 416–427. https://doi.org/10.1016/j.metabol.2014.11.007

Frontera, W. R., & Ochala, J. (2015). Skeletal muscle: a brief review of structure and function. *Calcified Tissue International*, *96*(3), 183–195. https://doi.org/10.1007/s00223-014-9915-y

Frost, R. A., Nystrom, G. J., & Lang, C. H. (2002). Lipopolysaccharide regulates proinflammatory cytokine expression in mouse myoblasts and skeletal muscle. *American Journal of Physiology - Regulatory Integrative and Comparative Physiology*, *283*(3 52-3), R698–R709. https://doi.org/10.1152/ajpregu.00039.2002

Frost, R. A., Nystrom, G. J., & Lang, C. H. (2003). Lipopolysaccharide and proinflammatory cytokines stimulate interleukin-6 expression in C2C12 myoblasts: role of the Jun NH 2 -terminal kinase. *American Journal of Physiology-Regulatory, Integrative and Comparative Physiology*, *285*(5), R1153–R1164. https://doi.org/10.1152/ajpregu.00164.2003

Fu, X., Zhu, M., Zhang, S., Foretz, M., Viollet, B., & Du, M. (2016). Obesity impairs skeletal muscle regeneration through inhibition of AMPK. *Diabetes*, *65*(1), 188–200.

https://doi.org/10.2337/db15-0647

Fujimaki, S., Wakabayashi, T., Asashima, M., Takemasa, T., & Kuwabara, T. (2016). Treadmill running induces satellite cell activation in diabetic mice. *Biochemistry and Biophysics Reports*, *8*, 6–13. https://doi.org/10.1016/j.bbrep.2016.07.004

Gallagher, D., & Heymsfield, S. B. (1998). Muscle distribution: Variations with body weight, gender, and age. *Applied Radiation and Isotopes*, *49*(5–6), 733–734. https://doi.org/10.1016/S0969-8043(97)00096-1

Garcia-Elias, A., Alloza, L., Puigdecanet, E., Nonell, L., Tajes, M., Curado, J., Enjuanes, C., Díaz, O., Bruguera, J., Martí-Almor, J., Comín-Colet, J., & Benito, B. (2017). Defining quantification methods and optimizing protocols for microarray hybridization of circulating microRNAs. *Scientific Reports*, *7*(1), 1–14. https://doi.org/10.1038/s41598-017-08134-3

Gaster, M., Petersen, I., Højlund, K., Poulsen, P., & Beck-Nielsen, H. (2002). The diabetic phenotype is conserved in myotubes established from diabetic subjects: Evidence for primary defects in glucose transport and glycogen synthase activity. *Diabetes*, *51*(4), 921–927. https://doi.org/10.2337/diabetes.51.4.921

Gomes, J. M. G., Costa, J. de A., & Alfenas, R. de C. G. (2017). Metabolic endotoxemia and diabetes mellitus: A systematic review. *Metabolism*, *68*, 133–144. https://doi.org/10.1016/j.metabol.2016.12.009

Goodpaster, B. H., & Sparks, L. M. (2017). Metabolic Flexibility in Health and Disease. *Cell Metabolism*, *25*(5), 1027–1036. https://doi.org/10.1016/j.cmet.2017.04.015

Gordon, B. S., Kelleher, A. R., & Kimball, S. R. (2013). Regulation of muscle protein synthesis and the effects of catabolic states. *The International Journal of Biochemistry & Cell Biology*, *45*(10), 2147–2157. https://doi.org/10.1016/j.biocel.2013.05.039

Gransee, H. M., Mantilla, C. B., & Sieck, G. C. (2012). Respiratory muscle plasticity. *Comprehensive Physiology*, *2*(2), 1441–1462. https://doi.org/10.1002/cphy.c110050

Green, C. J., Pedersen, M., Pedersen, B. K., & Scheele, C. (2011). Elevated NF-κB activation is conserved in human myocytes cultured from obese type 2 diabetic patients and attenuated by AMP-activated protein kinase. *Diabetes*, *60*(11), 2810–2819. https://doi.org/10.2337/db11-0263

Green, H., & Kehinde, O. (1975). An established preadipose cell line and its differentiation in

culture II. Factors affecting the adipose conversion. *Cell*, *5*(1), 19–27. https://doi.org/10.1016/0092-8674(75)90087-2

Green, H., & Meuth, M. (1974). An established pre-adipose cell line and its differentiation in culture. *Cell*, *3*(2), 127–133. https://doi.org/10.1016/0092-8674(74)90116-0

Gros, J., Manceau, M., Thomé, V., & Marcelle, C. (2005). A common somitic origin for embryonic muscle progenitors and satellite cells. *Nature*, *435*(7044), 954–958. https://doi.org/10.1038/nature03572

Guerville, M., Leroy, A., Sinquin, A., Laugerette, F., Michalski, M.-C., & Boudry, G. (2017). Western-diet consumption induces alteration of barrier function mechanisms in the ileum that correlates with metabolic endotoxemia in rats. *American Journal of Physiology-Endocrinology and Metabolism*, *313*(2), E107–E120. https://doi.org/10.1152/ajpendo.00372.2016

Haddad, F., Zaldivar, F., Cooper, D. M., & Adams, G. R. (2005). IL-6-induced skeletal muscle atrophy. *Journal of Applied Physiology*, *98*(3), 911–917. https://doi.org/10.1152/japplphysiol.01026.2004

Haines, M. S., Dichtel, L. E., Santoso, K., Torriani, M., Miller, K. K., & Bredella, M. A. (2020). Association between muscle mass and insulin sensitivity independent of detrimental adipose depots in young adults with overweight/obesity. *International Journal of Obesity*, *44*(9), 1851–1858. https://doi.org/10.1038/s41366-020-0590-y

Han, H. Q., Zhou, X., Mitch, W. E., & Goldberg, A. L. (2013). Myostatin/activin pathway antagonism: Molecular basis and therapeutic potential. *The International Journal of Biochemistry & Cell Biology*, *45*(10), 2333–2347. https://doi.org/10.1016/j.biocel.2013.05.019

Han, S. J., Boyko, E. J., Kim, S. K., Fujimoto, W. Y., Kahn, S. E., & Leonetti, D. L. (2018). Association of thigh muscle mass with insulin resistance and incident type 2 diabetes mellitus in Japanese americans. *Diabetes and Metabolism Journal*, *42*(6), 488–495. https://doi.org/10.4093/dmj.2018.0022

Harkins, J. M., Moustaid-Moussa, N., Chung, Y.-J., Penner, K. M., Pestka, J. J., North, C. M., & Claycombe, K. J. (2004). Expression of Interleukin-6 Is Greater in Preadipocytes than in Adipocytes of 3T3-L1 Cells and C57BL/6J and ob/ob Mice. *The Journal of Nutrition*, *134*(10), 2673–2677. https://doi.org/10.1093/jn/134.10.2673

Hartwig, S., Raschke, S., Knebel, B., Scheler, M., Irmler, M., Passlack, W., Muller, S., Hanisch, F. G., Franz, T., Li, X., Dicken, H. D., Eckardt, K., Beckers, J., De Angelis, M. H., Weigert, C., Häring, H. U., Al-Hasani, H., Ouwens, D. M., Eckel, J., … Lehr, S. (2014). Secretome profiling of primary human skeletal muscle cells. *Biochimica et Biophysica Acta - Proteins and Proteomics*, *1844*(5), 1011–1017. https://doi.org/10.1016/j.bbapap.2013.08.004

Hasselgren, P.-O., Menconi, M. J., Fareed, M. U., Yang, H., Wei, W., & Evenson, A. (2005). Novel aspects on the regulation of muscle wasting in sepsis. *The International Journal of Biochemistry & Cell Biology*, *37*(10), 2156–2168. https://doi.org/10.1016/j.biocel.2005.01.017

Helge, J. W., Stallknecht, B., Pedersen, B. K., Galbo, H., Kiens, B., & Richter, E. A. (2003). The effect of graded exercise on IL-6 release and glucose uptake in human skeletal muscle. *The Journal of Physiology*, *546*(Pt 1), 299–305. https://doi.org/10.1113/jphysiol.2002.030437

Hill, B. G., Benavides, G. A., Lancaster, J. J. R., Ballinger, S., Dell'Italia, L., Zhang, J., & Darley-Usmar, V. M. (2012). Integration of cellular bioenergetics with mitochondrial quality control and autophagy. *Biological Chemistry*, *393*(12), 1485–1512. https://doi.org/10.1515/hsz-2012-0198

Holland, W. L., Bikman, B. T., Wang, L.-P., Yuguang, G., Sargent, K. M., Bulchand, S., Knotts, T. A., Shui, G., Clegg, D. J., Wenk, M. R., Pagliassotti, M. J., Scherer, P. E., & Summers, S. A. (2011). Lipid-induced insulin resistance mediated by the proinflammatory receptor TLR4 requires saturated fatty acid–induced ceramide biosynthesis in mice. *Journal of Clinical Investigation*, *121*(5), 1858–1870. https://doi.org/10.1172/JCI43378

Holland, W. L., Knotts, T. A., Chavez, J. A., Wang, L.-P., Hoehn, K. L., & Summers, S. A. (2008). Lipid Mediators of Insulin Resistance. *Nutrition Reviews*, *65*(SUPPL.1), S39–S46. https://doi.org/10.1111/j.1753-4887.2007.tb00327.x

Holten, M. K., Zacho, M., Gaster, M., Juel, C., Wojtaszewski, J. F. P., & Dela, F. (2004). Strength Training Increases Insulin-Mediated Glucose Uptake, GLUT4 Content, and Insulin Signaling in Skeletal Muscle in Patients With Type 2 Diabetes. *Diabetes*, *53*(2), 294–305. https://doi.org/10.2337/diabetes.53.2.294

Hong, Y., Lee, J. H., Jeong, K. W., Choi, C. S., & Jun, H. (2019). Amelioration of muscle wasting by glucagon-like peptide-1 receptor agonist in muscle atrophy. *Journal of*

Cachexia, Sarcopenia and Muscle, *10*(4), 903–918. https://doi.org/10.1002/jcsm.12434

Horsley, V., Jansen, K. M., Mills, S. T., & Pavlath, G. K. (2003). IL-4 acts as a myoblast recruitment factor during mammalian muscle growth. *Cell*, *113*(4), 483–494. https://doi.org/10.1016/S0092-8674(03)00319-2

Hotamisligil, G., Shargill, N., & Spiegelman, B. (1993). Adipose expression of tumor necrosis factor-alpha: direct role in obesity-linked insulin resistance. *Science*, *259*(5091), 87–91. https://doi.org/10.1126/science.7678183

Houštek, J., Klement, P., Floryk, D., Antonická, H., Hermanská, J., Kalous, M., Hansíková, H., Houšťková, H., Chowdhury, S. K. R., Rosipal, Š., Kmoch, S., Stratilová, L., & Zeman, J. (1999). A novel deficiency of mitochondrial ATPase of nuclear origin. *Human Molecular Genetics*, *8*(11), 1967–1974. https://doi.org/10.1093/hmg/8.11.1967

Howard, E. E., Pasiakos, S. M., Blesso, C. N., Fussell, M. A., & Rodriguez, N. R. (2020). Divergent Roles of Inflammation in Skeletal Muscle Recovery From Injury. *Frontiers in Physiology*, *11*, 87. https://doi.org/10.3389/fphys.2020.00087

Huh, J. Y., Dincer, F., Mesfum, E., & Mantzoros, C. S. (2014). Irisin stimulates muscle growth-related genes and regulates adipocyte differentiation and metabolism in humans. *International Journal of Obesity*, *38*(12), 1538–1544. https://doi.org/10.1038/ijo.2014.42

Hulmi, J. J., Silvennoinen, M., Lehti, M., Kivelä, R., & Kainulainen, H. (2012). Altered REDD1, myostatin, and Akt/mTOR/FoxO/MAPK signaling in streptozotocin-induced diabetic muscle atrophy. *American Journal of Physiology - Endocrinology and Metabolism*, *302*(3), 307–315. https://doi.org/10.1152/ajpendo.00398.2011

Hussey, S. E., Liang, H., Costford, S. R., Klip, A., DeFronzo, R. A., Sanchez-Avila, A., Ely, B., & Musi, N. (2013). TAK-242, a small-molecule inhibitor of Toll-like receptor 4 signalling, unveils similarities and differences in lipopolysaccharide- and lipidinduced inflammation and insulin resistance in muscle cells. *Bioscience Reports*, *33*(1), 37–47. https://doi.org/10.1042/BSR20120098

International Diabetes Federation. (2019). IDF Diabetes Atlas Ninth edition 2019. In *Dunia : IDF*.

Jack, B. U., Malherbe, C. J., Huisamen, B., Gabuza, K., Mazibuko-Mbeje, S., Schulze, A. E., Joubert, E., Muller, C. J. F., Louw, J., & Pheiffer, C. (2017). A polyphenol-enriched fraction of Cyclopia intermedia decreases lipid content in 3T3-L1 adipocytes and reduces body

weight gain of obese db/db mice. *South African Journal of Botany*, *110*, 216–229. https://doi.org/10.1016/j.sajb.2016.08.007

Jack, Babalwa U., Malherbe, C. J., Mamushi, M., Muller, C. J. F., Joubert, E., Louw, J., & Pheiffer, C. (2019). Adipose tissue as a possible therapeutic target for polyphenols: A case for Cyclopia extracts as anti-obesity nutraceuticals. *Biomedicine & Pharmacotherapy*, *120*, 109439. https://doi.org/10.1016/j.biopha.2019.109439

Jayashree, B., Bibin, Y. S., Prabhu, D., Shanthirani, C. S., Gokulakrishnan, K., Lakshmi, B. S., Mohan, V., & Balasubramanyam, M. (2014). Increased circulatory levels of lipopolysaccharide (LPS) and zonulin signify novel biomarkers of proinflammation in patients with type 2 diabetes. *Molecular and Cellular Biochemistry*, *388*(1–2), 203–210. https://doi.org/10.1007/s11010-013-1911-4

Jensen, J., Rustad, P. I., Kolnes, A. J., & Lai, Y.-C. (2011). The Role of Skeletal Muscle Glycogen Breakdown for Regulation of Insulin Sensitivity by Exercise. *Frontiers in Physiology*, *2*, 112. https://doi.org/10.3389/fphys.2011.00112

Jeon, Y. K., Kim, S. S., Kim, J. H., Kim, H. J., Kim, H. J., Park, J. J., Cho, Y. S., Joung, S. H., Kim, J. R., Kim, B. H., Song, S. H., Kim, I. J., Kim, Y. K., & Kim, Y.-B. (2020). Combined Aerobic and Resistance Exercise Training Reduces Circulating Apolipoprotein J Levels and Improves Insulin Resistance in Postmenopausal Diabetic Women. *Diabetes & Metabolism Journal*, *44*(1), 103. https://doi.org/10.4093/dmj.2018.0160

Joubert, E., Gelderblom, W. C. A. C. A., Louw, A., & de Beer, D. (2008). South African herbal teas: Aspalathus linearis, Cyclopia spp. and Athrixia phylicoides—A review. *Journal of Ethnopharmacology*, *119*(3), 376–412. https://doi.org/10.1016/j.jep.2008.06.014

Joubert, Elizabeth, & de Beer, D. (2012). Phenolic content and antioxidant activity of rooibos food ingredient extracts. *Journal of Food Composition and Analysis*, *27*(1), 45–51. https://doi.org/10.1016/j.jfca.2012.03.011

Jové, M., Planavila, A., Laguna, J. C., & Vázquez-Carrera, M. (2005). Palmitate-induced interleukin 6 production is mediated by protein kinase C and nuclear-factor B activation and leads to glucose transporter 4 down-regulation in skeletal muscle cells. *Endocrinology*, *146*(7), 3087–3095. https://doi.org/10.1210/en.2004-1560

Jové, M., Planavila, A., Sánchez, R. M., Merlos, M., Laguna, J. C., & Vázquez-Carrera, M. (2006). Palmitate Induces Tumor Necrosis Factor-α Expression in C2C12 Skeletal Muscle

Cells by a Mechanism Involving Protein Kinase C and Nuclear Factor-κB Activation. *Endocrinology*, *147*(1), 552–561. https://doi.org/10.1210/en.2005-0440

Kallman, D. A., Plato, C. C., & Tobin, J. D. (1990). The Role of Muscle Loss in the Age-Related Decline of Grip Strength: Cross-Sectional and Longitudinal Perspectives. *Journal of Gerontology*, *45*(3), M82–M88. https://doi.org/10.1093/geronj/45.3.M82

Kamakura, R., Son, M. J., de Beer, D., Joubert, E., Miura, Y., & Yagasaki, K. (2015). Antidiabetic effect of green rooibos (Aspalathus linearis) extract in cultured cells and type 2 diabetic model KK-Ay mice. *Cytotechnology*, *67*(4), 699–710. https://doi.org/10.1007/s10616-014-9816-y

Kataoka, Y., Matsumura, I., Ezoe, S., Nakata, S., Takigawa, E., Sato, Y., Kawasaki, A., Yokota, T., Nakajima, K., Felsani, A., & Kanakura, Y. (2003). Reciprocal Inhibition between MyoD and STAT3 in the Regulation of Growth and Differentiation of Myoblasts. *Journal of Biological Chemistry*, *278*(45), 44178–44187. https://doi.org/10.1074/jbc.M304884200

Kawano, A., Nakamura, H., Hata, S., Minakawa, M., Miura, Y., & Yagasaki, K. (2009). Hypoglycemic effect of aspalathin, a rooibos tea component from Aspalathus linearis, in type 2 diabetic model db/db mice. *Phytomedicine*, *16*(5), 437–443. https://doi.org/10.1016/j.phymed.2008.11.009

Kelley, D. E. (2005). Skeletal muscle fat oxidation: timing and flexibility are everything. *Journal of Clinical Investigation*, *115*(7), 1699–1702. https://doi.org/10.1172/JCI25758

Kern, P. A., Ranganathan, S., Li, C., Wood, L., & Ranganathan, G. (2001). Adipose tissue tumor necrosis factor and interleukin-6 expression in human obesity and insulin resistance. *American Journal of Physiology-Endocrinology and Metabolism*, *280*(5), E745–E751. https://doi.org/10.1152/ajpendo.2001.280.5.E745

Kershaw, E. E., & Flier, J. S. (2004). Adipose tissue as an endocrine organ. *Journal of Clinical Endocrinology and Metabolism*, *89*(6), 2548–2556. https://doi.org/10.1210/jc.2004-0395

Khan, M. A. B., Hashim, M. J., King, J. K., Govender, R. D., Mustafa, H., & Al Kaabi, J. (2019). Epidemiology of Type 2 Diabetes – Global Burden of Disease and Forecasted Trends. *Journal of Epidemiology and Global Health*, *10*(1), 107. https://doi.org/10.2991/jegh.k.191028.001

Kim, F., Pham, M., Luttrell, I., Bannerman, D. D., Tupper, J., Thaler, J., Hawn, T. R., Raines, E.

W., & Schwartz, M. W. (2007). Toll-Like Receptor-4 Mediates Vascular Inflammation and Insulin Resistance in Diet-Induced Obesity. *Circulation Research*, *100*(11), 1589–1596. https://doi.org/10.1161/CIRCRESAHA.106.142851

Kim, J., Bachmann, R. A., & Chen, J. (2009). Chapter 21 Interleukin-6 and Insulin Resistance. In *Vitamins and hormones* (Vol. 80, Issue C, pp. 613–633). Vitam Horm. https://doi.org/10.1016/S0083-6729(08)00621-3

Kim, Y.-B., Nikoulina, S. E., Ciaraldi, T. P., Henry, R. R., & Kahn, B. B. (1999). Normal insulin-dependent activation of Akt/protein kinase B, with diminished activation of phosphoinositide 3-kinase, in muscle in type 2 diabetes. *Journal of Clinical Investigation*, *104*(6), 733–741. https://doi.org/10.1172/JCI6928

Konopka, A. R., & Harber, M. P. (2014). Skeletal Muscle Hypertrophy After Aerobic Exercise Training. *Exercise and Sport Sciences Reviews*, *42*(2), 53–61. https://doi.org/10.1249/JES.0000000000000007

Körner, A., Wabitsch, M., Seidel, B., Fischer-Posovszky, P., Berthold, A., Stumvoll, M., Blüher, M., Kratzsch, J., & Kiess, W. (2005). Adiponectin expression in humans is dependent on differentiation of adipocytes and down-regulated by humoral serum components of high molecular weight. *Biochemical and Biophysical Research Communications*, *337*(2), 540–550. https://doi.org/10.1016/j.bbrc.2005.09.064

Krempler, A., & Brenig, B. (1999). Zinc finger proteins: watchdogs in muscle development. *Molecular and General Genetics MGG*, *261*(2), 209–215. https://doi.org/10.1007/s004380050959

Kruszynska, Y. T., Worrall, D. S., Ofrecio, J., Frias, J. P., Macaraeg, G., & Olefsky, J. M. (2002). Fatty acid-induced insulin resistance: Decreased muscle PI3K activation but unchanged Akt phosphorylation. *Journal of Clinical Endocrinology and Metabolism*, *87*(1), 226–234. https://doi.org/10.1210/jcem.87.1.8187

Kucharczyk, R., Zick, M., Bietenhader, M., Rak, M., Couplan, E., Blondel, M., Caubet, S.-D., & di Rago, J.-P. (2009). Mitochondrial ATP synthase disorders: molecular mechanisms and the quest for curative therapeutic approaches. *Biochimica et Biophysica Acta*, *1793*(1), 186–199. https://doi.org/10.1016/j.bbamcr.2008.06.012

Kudoh, A., Satoh, H., Hirai, H., Watanabe, T., & Shimabukuro, M. (2018). Preliminary evidence for adipocytokine signals in skeletal muscle glucose uptake. *Frontiers in Endocrinology*,

9(295). https://doi.org/10.3389/fendo.2018.00295

Kumar, N., & Dey, C. S. (2003). Development of insulin resistance and reversal by thiazolidinediones in C2C12 skeletal muscle cells. *Biochemical Pharmacology*, *65*(2), 249–257. https://doi.org/10.1016/S0006-2952(02)01509-5

Kurth-Kraczek, E. J., Hirshman, M. F., Goodyear, L. J., & Winder, W. W. (1999). 5' AMP-activated protein kinase activation causes GLUT4 translocation in skeletal muscle. *Diabetes*, *48*(8), 1667–1671. https://doi.org/10.2337/diabetes.48.8.1667

Lagirand-Cantaloube, J., Offner, N., Csibi, A., Leibovitch, M. P., Batonnet-Pichon, S., Tintignac, L. A., Segura, C. T., & Leibovitch, S. A. (2008). *The initiation factor eIF3-f is a major target for Atrogin1/MAFbx function in skeletal muscle atrophy*. *27*(8), 1266–1276. https://doi.org/10.1038/emboj.2008.52

Lang, C. H., Silvis, C., Nystrom, G., & Frost, R. A. (2001). Regulation of Myostatin by Glucocorticoids After Thermal Injury. *The FASEB Journal*, *15*(10), 1807–1809. https://doi.org/10.1096/fj.00-0849fje

Lange, P., Farina, P., Moreno, M., Ragni, M., Lombardi, A., Silvestri, E., Burrone, L., Lanni, A., Goglia, F., Lange, P., Farina, P., Moreno, M., Ragni, M., Lombardi, A., Silvestri, E., Burrone, L., Lanni, A., & Goglia, F. (2006). Sequential changes in the signal transduction responses of skeletal muscle following food deprivation. *The FASEB Journal*, *20*(14), 2579–2581. https://doi.org/10.1096/fj.06-6025fje

Langen, R. C. J., Schols, A. M. W. J., Kelders, M. C. J. M., Wouters, E. F. M., & Janssen-Heininger, Y. M. W. (2003). Enhanced myogenic differentiation by extracellular matrix is regulated at the early stages of myogenesis. *In Vitro Cellular & Developmental Biology. Animal*, *39*(3–4), 163–169. https://doi.org/10.1007/s11626-003-0011-2

Lassenius, M. I., Pietiläinen, K. H., Kaartinen, K., Pussinen, P. J., Syrjänen, J., Forsblom, C., Pörsti, I., Rissanen, A., Kaprio, J., Mustonen, J., Groop, P. H., & Lehto, M. (2011). Bacterial endotoxin activity in human serum is associated with dyslipidemia, insulin resistance, obesity, and chronic inflammation. *Diabetes Care*, *34*(8), 1809–1815. https://doi.org/10.2337/dc10-2197

Lautaoja, J. H., Pekkala, S., Pasternack, A., Laitinen, M., Ritvos, O., & Hulmi, J. J. (2020). Differentiation of murine C2C12 myoblasts strongly reduces the effects of myostatin on intracellular signaling. *Biomolecules*, *10*(5). https://doi.org/10.3390/biom10050695

Leahy, J. L. (2005). Pathogenesis of type 2 diabetes mellitus. *Archives of Medical Research*, *36*(3), 197–209. https://doi.org/10.1016/j.arcmed.2005.01.003

Lee, P., Linderman, J. D., Smith, S., Brychta, R. J., Wang, J., Idelson, C., Perron, R. M., Werner, C. D., Phan, G. Q., Kammula, U. S., Kebebew, E., Pacak, K., Chen, K. Y., & Celi, F. S. (2014). Irisin and FGF21 Are Cold-Induced Endocrine Activators of Brown Fat Function in Humans. *Cell Metabolism*, *19*(2), 302–309. https://doi.org/10.1016/j.cmet.2013.12.017

Lee, W., & Bae, J.-S. (2015). Anti-inflammatory Effects of Aspalathin and Nothofagin from Rooibos (Aspalathus linearis) In Vitro and In Vivo. *Inflammation*, *38*(4), 1502–1516. https://doi.org/10.1007/s10753-015-0125-1

Levels, J. H. M., Marquart, J. A., Abraham, P. R., van den Ende, A. E., Molhuizen, H. O. F., van Deventer, S. J. H., & Meijers, J. C. M. (2005). Lipopolysaccharide Is Transferred from High-Density to Low-Density Lipoproteins by Lipopolysaccharide-Binding Protein and Phospholipid Transfer Protein. *Infection and Immunity*, *73*(4), 2321–2326. https://doi.org/10.1128/IAI.73.4.2321-2326.2005

Li, F., Li, Y., Duan, Y., Hu, C.-A. A. A., Tang, Y., & Yin, Y. (2017). Myokines and adipokines: Involvement in the crosstalk between skeletal muscle and adipose tissue. *Cytokine & Growth Factor Reviews*, *33*, 73–82. https://doi.org/10.1016/j.cytogfr.2016.10.003

Liang, H., Hussey, S. E., Sanchez-Avila, A., Tantiwong, P., & Musi, N. (2013). Effect of Lipopolysaccharide on Inflammation and Insulin Action in Human Muscle. *PLoS ONE*, *8*(5), e63983. https://doi.org/10.1371/journal.pone.0063983

Liang, H., Lum, H., Alvarez, A., Garduno-Garcia, J. de J., Daniel, B. J., & Musi, N. (2018). A low dose lipid infusion is sufficient to induce insulin resistance and a pro-inflammatory response in human subjects. *PLOS ONE*, *13*(4), e0195810. https://doi.org/10.1371/journal.pone.0195810

Lipina, C., & Hundal, H. S. (2017). Lipid modulation of skeletal muscle mass and function. *Journal of Cachexia, Sarcopenia and Muscle*, *8*(2), 190–201. https://doi.org/10.1002/jcsm.12144

Lira, F. S., Rosa, J. C., Pimentel, G. D., Seelaender, M., Damaso, A. R., Oyama, L. M., & do Nascimento, C. O. (2012). Both adiponectin and interleukin-10 inhibit LPS-induced activation of the NF-κB pathway in 3T3-L1 adipocytes. *Cytokine*, *57*(1), 98–106.

https://doi.org/10.1016/j.cyto.2011.10.001

Lodish H, Berk A, Zipursky SL, et al. (2000). Oxidation of Glucose and Fatty Acids to CO2. In *Molecular Cell Biology* (4th editio). W. H. Freeman. https://www.ncbi.nlm.nih.gov/books/NBK21624/

Lowe, J. S., & Anderson, P. G. (2015). Contractile Cells. In J. S. Lowe & P. G. Anderson (Eds.), *Stevens Lowes Human Histology* (Fourth Edi, pp. 71–83). Elsevier. https://doi.org/10.1016/b978-0-7234-3502-0.00005-x

Lu, H., Huang, D., Saederup, N., Charo, I. F., Ransohoff, R. M., & Zhou, L. (2011). Macrophages recruited via CCR2 produce insulin-like growth factor-1 to repair acute skeletal muscle injury. *The FASEB Journal*, *25*(1), 358–369. https://doi.org/10.1096/fj.10-171579

Luo, W., Ai, L., Wang, B., & Zhou, Y. (2019). High glucose inhibits myogenesis and induces insulin resistance by down-regulating AKT signaling. *Biomedicine & Pharmacotherapy*, *120*, 109498. https://doi.org/10.1016/j.biopha.2019.109498

Makki, K., Froguel, P., & Wolowczuk, I. (2013). Adipose Tissue in Obesity-Related Inflammation and Insulin Resistance: Cells, Cytokines, and Chemokines. *ISRN Inflammation*, *2013*, 1–12. https://doi.org/10.1155/2013/139239

Mangnall, D., Bruce, C., & Fraser, R. B. (1993). Insulin-stimulated glucose uptake in C2C12 myoblasts. *Biochemical Society Transactions*, *21*(4), 438S-438S. https://doi.org/10.1042/bst021438s

Mao, Z., & Zhang, W. (2018). *Molecular Sciences Role of mTOR in Glucose and Lipid Metabolism*. https://doi.org/10.3390/ijms19072043

Marnewick, J. L., Rautenbach, F., Venter, I., Neethling, H., Blackhurst, D. M., Wolmarans, P., & MacHaria, M. (2011). Effects of rooibos (Aspalathus linearis) on oxidative stress and biochemical parameters in adults at risk for cardiovascular disease. *Journal of Ethnopharmacology*, *133*(1), 46–52. https://doi.org/10.1016/j.jep.2010.08.061

Martínez, J., Marmisolle, I., Tarallo, D., & Quijano, C. (2020). Mitochondrial Bioenergetics and Dynamics in Secretion Processes. *Frontiers in Endocrinology*, *11*, 319. https://doi.org/10.3389/fendo.2020.00319

Mazibuko-Mbeje, S. E., Dludla, P. V., Johnson, R., Joubert, E., Louw, J., Ziqubu, K., Tiano, L.,

Silvestri, S., Orlando, P., Opoku, A. R., & Muller, C. J. F. (2019). Aspalathin, a natural product with the potential to reverse hepatic insulin resistance by improving energy metabolism and mitochondrial respiration. *PLoS ONE*, *14*(5), e0216172. https://doi.org/10.1371/journal.pone.0216172

Mazibuko-Mbeje, S. E., Ziqubu, K., Dludla, P. V., Tiano, L., Silvestri, S., Orlando, P., Nyawo, T. A., Louw, J., Kappo, A. P., & Muller, C. J. F. (2020). Isoorientin ameliorates lipid accumulation by regulating fat browning in palmitate-exposed 3T3-L1 adipocytes. *Metabolism Open*, *6*, 100037. https://doi.org/10.1016/j.metop.2020.100037

Mazibuko, S. E., Muller, C. J. F., Joubert, E., De Beer, D., Johnson, R., Opoku, A. R., & Louw, J. (2013). Amelioration of palmitate-induced insulin resistance in C2C12 muscle cells by rooibos (Aspalathus linearis). *Phytomedicine*, *20*(10), 813–819. https://doi.org/10.1016/j.phymed.2013.03.018

Meex, R. C. R., Blaak, E. E., & Loon, L. J. C. (2019). Lipotoxicity plays a key role in the development of both insulin resistance and muscle atrophy in patients with type 2 diabetes. *Obesity Reviews*, *20*(9), 1205–1217. https://doi.org/10.1111/obr.12862

Metter, E. J., Conwit, R., Tobin, J., & Fozard, J. L. (1997). Age-associated loss of power and strength in the upper extremities in women and men. *Journals of Gerontology - Series A Biological Sciences and Medical Sciences*, *52*(5). https://doi.org/10.1093/gerona/52A.5.B267

Metter, E. J., Lynch, N., Conwit, R., Lindle, R., Tobin, J., & Hurley, B. (1999). Muscle Quality and Age: Cross-Sectional and Longitudinal Comparisons. *The Journals of Gerontology Series A: Biological Sciences and Medical Sciences*, *54*(5), B207–B218. https://doi.org/10.1093/gerona/54.5.B207

Millar, D. A., Bowles, S., Windvogel, S. L., Louw, J., & Muller, C. J. F. (2020). Effect of Rooibos (Aspalathus linearis) extract on atorvastatin-induced toxicity in C3A liver cells. *Journal of Cellular Physiology*, *235*(12), 9487–9496. https://doi.org/10.1002/jcp.29756

Mirzoev, T. M. (2020). Skeletal Muscle Recovery from Disuse Atrophy: Protein Turnover Signaling and Strategies for Accelerating Muscle Regrowth. *International Journal of Molecular Sciences*, *21*(21), 7940. https://doi.org/10.3390/ijms21217940

Mlinar, B., Marc, J., Janež, A., & Pfeifer, M. (2007). Molecular mechanisms of insulin resistance and associated diseases. *Clinica Chimica Acta*, *375*(1–2), 20–35.

https://doi.org/10.1016/j.cca.2006.07.005

Mohamed-Ali, V., Pinkney, J. H., & Coppack, S. W. (1998). Adipose tissue as an endocrine and paracrine organ. In *International Journal of Obesity* (Vol. 22, Issue 12, pp. 1145–1158). Elsevier. https://doi.org/10.1038/sj.ijo.0800770

Moran, J. L., Li, Y., Hill, A. A., Mounts, W. M., & Miller, C. P. (2002). Gene expression changes during mouse skeletal myoblast differentiation revealed by transcriptional profiling. *Physiological Genomics*, *2002*(10), 103–111. https://doi.org/10.1152/physiolgenomics.00011.2002

Morrison, S., & McGee, S. L. (2015). 3T3-L1 adipocytes display phenotypic characteristics of multiple adipocyte lineages. *Adipocyte*, *4*(4), 295–302. https://doi.org/10.1080/21623945.2015.1040612

Mosmann, T. (1983). Rapid colorimetric assay for cellular growth and survival: Application to proliferation and cytotoxicity assays. *Journal of Immunological Methods*, *65*(1–2), 55–63. https://doi.org/10.1016/0022-1759(83)90303-4

Mukund, K., & Subramaniam, S. (2019). Skeletal muscle: A review of molecular structure and function, in health and disease. *Wiley Interdisciplinary Reviews: Systems Biology and Medicine*, *12*(1), e1462. https://doi.org/10.1002/wsbm.1462

Muller, C. J. F., Joubert, E., de Beer, D., Sanderson, M., Malherbe, C. J., Fey, S. J., & Louw, J. (2012). Acute assessment of an aspalathin-enriched green rooibos (Aspalathus linearis) extract with hypoglycemic potential. *Phytomedicine*, *20*(1), 32–39. https://doi.org/10.1016/j.phymed.2012.09.010

Muñoz-Cánoves, P., Scheele, C., Pedersen, B. K., & Serrano, A. L. (2013). Interleukin-6 myokine signaling in skeletal muscle: A double-edged sword? In *FEBS Journal* (Vol. 280, Issue 17, pp. 4131–4148). Wiley-Blackwell. https://doi.org/10.1111/febs.12338

Muthuraman, P. (2014). Effect of coculturing on the myogenic and adipogenic marker gene expression. *Applied Biochemistry and Biotechnology*, *173*(2), 571–578. https://doi.org/10.1007/s12010-014-0866-6

Neupane, P., Bhuju, S., Thapa, N., & Bhattarai, H. K. (2019). ATP Synthase: Structure, Function and Inhibition. *Biomolecular Concepts*, *10*(1), 1–10. https://doi.org/10.1515/bmc-2019-0001

Nicholson, T., Church, C., Baker, D. J., & Jones, S. W. (2018). The role of adipokines in skeletal

muscle inflammation and insulin sensitivity. *Journal of Inflammation*, *15*(1), 9. https://doi.org/10.1186/s12950-018-0185-8

O'Neill, H. M., Lally, J. S., Galic, S., Thomas, M., Azizi, P. D., Fullerton, M. D., Smith, B. K., Pulinilkunnil, T., Chen, Z., Samaan, M. C., Jorgensen, S. B., Dyck, J. R. B., Holloway, G. P., Hawke, T. J., van Denderen, B. J., Kemp, B. E., & Steinberg, G. R. (2014). AMPK phosphorylation of ACC2 is required for skeletal muscle fatty acid oxidation and insulin sensitivity in mice. *Diabetologia*, *57*(8), 1693–1702. https://doi.org/10.1007/s00125-014-3273-1

Ojima, K., Oe, M., Nakajima, I., Shibata, M., Chikuni, K., Muroya, S., & Nishimura, T. (2014). Proteomic analysis of secreted proteins from skeletal muscle cells during differentiation. *EuPA Open Proteomics*, *5*, 1–9. https://doi.org/10.1016/j.euprot.2014.08.001

Ono, Y., Maejima, Y., Saito, M., Sakamoto, K., Horita, S., Shimomura, K., Inoue, S., & Kotani, J. (2020). TAK-242, a specific inhibitor of Toll-like receptor 4 signalling, prevents endotoxemia-induced skeletal muscle wasting in mice. *Scientific Reports*, *10*(1), 694. https://doi.org/10.1038/s41598-020-57714-3

Ono, Y., & Sakamoto, K. (2017). Lipopolysaccharide inhibits myogenic differentiation of C2C12 myoblasts through the Toll-like receptor 4-nuclear factor-κB signaling pathway and myoblast-derived tumor necrosis factor-α. *PLoS ONE*, *12*(7), e0182040. https://doi.org/10.1371/journal.pone.0182040

Orlando, P., Chellan, N., Louw, J., Tiano, L., Cirilli, I., Dludla, P., Joubert, E., & Muller, C. J. F. (2019). Aspalathin-rich green rooibos extract lowers LDL-cholesterol and oxidative status in high-fat diet-induced diabetic vervet monkeys. *Molecules*, *24*(9), 1713. https://doi.org/10.3390/molecules24091713

Pandurangan, M., & Hwang, I. (2014). Application of cell co-culture system to study fat and muscle cells. *Applied Microbiology and Biotechnology*, *98*(17), 7359–7364. https://doi.org/10.1007/s00253-014-5935-9

Pandurangan, M., Jeong, D., Amna, T., Van Ba, H., & Hwang, I. (2012). Co-culture of C2C12 and 3T3-L1 preadipocyte cells alters the gene expression of calpains, caspases and heat shock proteins. *In Vitro Cellular and Developmental Biology - Animal*, *48*(9), 577–582. https://doi.org/10.1007/s11626-012-9550-8

Patel, O., Muller, C., Joubert, E., Louw, J., Rosenkranz, B., & Awortwe, C. (2016). Inhibitory

interactions of Aspalathus linearis (rooibos) extracts and compounds, aspalathin and Z-2-(β-D-glucopyranosyloxy)-3-phenylpropenoic acid, on cytochromes metabolizing hypoglycemic and hypolipidemic drugs. *Molecules*, *21*(11), 1515. https://doi.org/10.3390/molecules21111515

Pedersen, B. K., Steensberg, A., Fischer, C., Keller, C., Keller, P., Plomgaard, P., Wolsk-Petersen, E., & Febbraio, M. (2004). The metabolic role of IL-6 produced during exercise: is IL-6 an exercise factor? *Proceedings of the Nutrition Society*, *63*(2), 263–267. https://doi.org/10.1079/PNS2004338

Pedersen, Bente K., & Fischer, C. P. (2007). Beneficial health effects of exercise--the role of IL-6 as a myokine. *Trends in Pharmacological Sciences*, *28*(4), 152–156. https://doi.org/10.1016/j.tips.2007.02.002

Pedersen, Bente Klarlund, Åkerström, T. C. A., Nielsen, A. R., & Fischer, C. P. (2007). Role of myokines in exercise and metabolism. *Journal of Applied Physiology*, *103*(3), 1093–1098. https://doi.org/10.1152/japplphysiol.00080.2007

Pedersen, Bente Klarlund, Steensberg, A., & Schjerling, P. (2001). Muscle-derived interleukin-6: possible biological effects. *The Journal of Physiology*, *536*(2), 329–337. https://doi.org/10.1111/j.1469-7793.2001.0329c.xd

Pellegrinelli, V., Rouault, C., Rodriguez-Cuenca, S., Albert, V., Edom-Vovard, F., Vidal-Puig, A., Clément, K., Butler-Browne, G. S., & Lacasa, D. (2015). Human adipocytes induce inflammation and atrophy in muscle cells during obesity. *Diabetes*, *64*(9), 3121–3134. https://doi.org/10.2337/db14-0796

Pereira, S. S., & Alvarez-Leite, J. I. (2014). Low-Grade Inflammation, Obesity, and Diabetes. *Current Obesity Reports*, *3*(4), 422–431. https://doi.org/10.1007/s13679-014-0124-9

Perry, B. D., Caldow, M. K., Brennan-Speranza, T. C., Sbaraglia, M., Jerums, G., Garnham, A., Wong, C., Levinger, P., Asrar Ul Haq, M., Hare, D. L., Price, S. R., & Levinger, I. (2016). Muscle atrophy in patients with Type 2 Diabetes Mellitus: Roles of inflammatory pathways, physical activity and exercise. *Exercise Immunology Review*, *22*, 94–108. http://eir-isei.de/2016/eir-2016-094-article.pdf

Perry, B. D., Rahnert, J. A., Xie, Y., Zheng, B., Woodworth-Hobbs, M. E., & Price, S. R. (2018). Palmitate-induced ER stress and inhibition of protein synthesis in cultured myotubes does not require Toll-like receptor 4. *PLOS ONE*, *13*(1), e0191313.

https://doi.org/10.1371/journal.pone.0191313

Petersen, K. F., Dufour, S., Savage, D. B., Bilz, S., Solomon, G., Yonemitsu, S., Cline, G. W., Befroy, D., Zemany, L., Kahn, B. B., Papademetris, X., Rothman, D. L., & Shulman, G. I. (2007). The role of skeletal muscle insulin resistance in the pathogenesis of the metabolic syndrome. *Proceedings of the National Academy of Sciences of the United States of America*, *104*(31), 12587–12594. https://doi.org/10.1073/pnas.0705408104

Petersen, M. C., & Shulman, G. I. (2018). Mechanisms of insulin action and insulin resistance. *Physiological Reviews*, *98*(4), 2133–2223. https://doi.org/10.1152/physrev.00063.2017

Podbregar, M., Lainscak, M., Prelovsek, O., & Mars, T. (2013). Cytokine response of cultured skeletal muscle cells stimulated with proinflammatory factors depends on differentiation stage. *The Scientific World Journal*, *2013*, 1–8. https://doi.org/10.1155/2013/617170

Poggi, M., Bastelica, D., Gual, P., Iglesias, M. A., Gremeaux, T., Knauf, C., Peiretti, F., Verdier, M., Juhan-Vague, I., Tanti, J. F., Burcelin, R., & Alessi, M. C. (2007). C3H/HeJ mice carrying a toll-like receptor 4 mutation are protected against the development of insulin resistance in white adipose tissue in response to a high-fat diet. *Diabetologia*, *50*(6), 1267–1276. https://doi.org/10.1007/s00125-007-0654-8

Poitout, V., & Robertson, R. P. (2008). Glucolipotoxicity: Fuel excess and β-cell dysfunction. In *Endocrine Reviews* (Vol. 29, Issue 3, pp. 351–366). Oxford Academic. https://doi.org/10.1210/er.2007-0023

Polge, C., Heng, A.-E., Jarzaguet, M., Ventadour, S., Claustre, A., Combaret, L., Béchet, D., Matondo, M., Uttenweiler-Joseph, S., Monsarrat, B., Attaix, D., & Taillandier, D. (2011). Muscle actin is polyubiquitinylated in vitro and in vivo and targeted for breakdown by the E3 ligase MuRF1. *The FASEB Journal*, *25*(11), 3790–3802. https://doi.org/10.1096/fj.11-180968

Polonsky, K. S., & Burant, C. F. (2016). Chapter 31 – Type 2 Diabetes Mellitus. In *Williams Textbook of Endocrinology*. Elsevier Inc. https://doi.org/10.1016/B978-0-323-29738-7.00031-9

Pradhan, A. D., Manson, J. E., Rifai, N., Buring, J. E., & Ridker, P. M. (2001). C-reactive protein, interleukin 6, and risk of developing type 2 diabetes mellitus. *Journal of the American Medical Association*, *286*(3), 327–334. https://doi.org/10.1001/jama.286.3.327

Radin, M. S., Sinha, S., Bhatt, B. A., Dedousis, N., & O'Doherty, R. M. (2008). Inhibition or deletion of the lipopolysaccharide receptor Toll-like receptor-4 confers partial protection against lipid-induced insulin resistance in rodent skeletal muscle. *Diabetologia*, *51*(2), 336–346. https://doi.org/10.1007/s00125-007-0861-3

Rasouli, N., & Kern, P. a. (2008). Adipocytokines and the Metabolic Complications of Obesity. *The Journal of Clinical Endocrinology & Metabolism*, *93*(11_supplement_1), s64–s73. https://doi.org/10.1210/jc.2008-1613

Reyna, S. M., Ghosh, S., Tantiwong, P., Meka, C. S. R. M., Eagan, P., Jenkinson, C. P., Cersosimo, E., Defronzo, R. A., Coletta, D. K., Sriwijitkamol, A., & Musi, N. (2008). Elevated toll-like receptor 4 expression and signaling in muscle from insulin-resistant subjects. *Diabetes*, *57*(10), 2595–2602. https://doi.org/10.2337/db08-0038

Richter, E. A., & Hargreaves, M. (2013). Exercise, GLUT4, and Skeletal Muscle Glucose Uptake. *Physiological Reviews*, *93*(3), 993–1017. https://doi.org/10.1152/physrev.00038.2012

Ríos, R., Carneiro, I., Arce, V. M., & Devesa, J. (2001). Myostatin Regulates Cell Survival during C2C12 Myogenesis. *Biochemical and Biophysical Research Communications*, *280*(2), 561–566. https://doi.org/10.1006/bbrc.2000.4159

Ríos, R., Carneiro, I., Arce, V. M., & Devesa, J. (2002). Myostatin is an inhibitor of myogenic differentiation. *American Journal of Physiology-Cell Physiology*, *282*(5), C993–C999. https://doi.org/10.1152/ajpcell.00372.2001

Roden, M., Price, T. B., Perseghin, G., Petersen, K. F., Rothman, D. L., Cline, G. W., & Shulman, G. I. (1996). Mechanism of free fatty acid-induced insulin resistance in humans. *Journal of Clinical Investigation*, *97*(12), 2859–2865. https://doi.org/10.1172/JCI118742

Rohr, M. W., Narasimhulu, C. A., Rudeski-Rohr, T. A., & Parthasarathy, S. (2019). Negative Effects of a High-Fat Diet on Intestinal Permeability: A Review. *Advances in Nutrition*, *11*(1), 77–91. https://doi.org/10.1093/advances/nmz061

Rommel, C., Bodine, S. C., Clarke, B. A., Rossman, R., Nunez, L., Stitt, T. N., Yancopoulos, G. D., & Glass, D. J. (2001). Mediation of IGF-1-induced skeletal myotube hypertrophy by PI(3)K/Akt/mTOR and PI(3)K/Akt/GSK3 pathways. *Nature Cell Biology*, *3*(11), 1009–1013. https://doi.org/10.1038/ncb1101-1009

Rosenberg, I. H. (1997). Sarcopenia: Origins and clinical relevance. *Journal of Nutrition*, *127*(5 SUPPL.). https://doi.org/10.1093/jn/127.5.990s

Rothman, D. L., Shulman, R. G., & Shulman, G. I. (1992). 31P nuclear magnetic resonance measurements of muscle glucose-6-phosphate: Evidence for reduced insulin-dependent muscle glucose transport or phosphorylation activity in non-insulin-dependent diabetes mellitus. *Journal of Clinical Investigation*, *89*(4), 1069–1075. https://doi.org/10.1172/JCI115686

Ruan, H., & Lodish, H. F. (2003). Insulin resistance in adipose tissue: Direct and indirect effects of tumor necrosis factor-α. *Cytokine and Growth Factor Reviews*, *14*(5), 447–455. https://doi.org/10.1016/S1359-6101(03)00052-2

Sam, S., & Mazzone, T. (2014). Adipose tissue changes in obesity and the impact on metabolic function. *Translational Research*, *164*(4), 284–292. https://doi.org/10.1016/j.trsl.2014.05.008

Sanderson, M., Mazibuko, S. E., Joubert, E., de Beer, D., Johnson, R., Pheiffer, C., Louw, J., & Muller, C. J. F. (2014). Effects of fermented rooibos (Aspalathus linearis) on adipocyte differentiation. *Phytomedicine : International Journal of Phytotherapy and Phytopharmacology*, *21*(2), 109–117. https://doi.org/10.1016/j.phymed.2013.08.011

Sandri, M. (2008). Signaling in muscle atrophy and hypertrophy. *Physiology*, *23*(3), 160–170. https://doi.org/10.1152/physiol.00041.2007

Sandri, M., Sandri, C., Gilbert, A., Skurk, C., Calabria, E., Picard, A., Walsh, K., Schiaffino, S., Lecker, S. H., & Goldberg, A. L. (2004). Foxo transcription factors induce the atrophy-related ubiquitin ligase atrogin-1 and cause skeletal muscle atrophy. *Cell*, *117*(3), 399–412. https://doi.org/10.1016/S0092-8674(04)00400-3

Sarr, O., Strohm, R., MacDonald, T., Gaudio, N., Reed, J., Foute-Nelong, J., Dyck, D., & Mutch, D. (2017). Subcutaneous and Visceral Adipose Tissue Secretions from Extremely Obese Men and Women both Acutely Suppress Muscle Insulin Signaling. *International Journal of Molecular Sciences*, *18*(5), 959. https://doi.org/10.3390/ijms18050959

Saxton, R. A., & Sabatini, D. M. (2017). mTOR Signaling in Growth, Metabolism, and Disease. *Cell*, *168*(6), 960–976. https://doi.org/10.1016/j.cell.2017.02.004

Schmitz-Peiffer, C. (2000). Signalling aspects of insulin resistance in skeletal muscle. *Cellular*

Signalling, *12*(9–10), 583–594. https://doi.org/10.1016/S0898-6568(00)00110-8

Scicchitano, B. M., Dobrowolny, G., Sica, G., & Musaro, A. (2018). Molecular Insights into Muscle Homeostasis, Atrophy and Wasting. *Current Genomics*, *19*(5), 356–369. https://doi.org/10.2174/1389202919666180101153911

Segawa, M., Fukada, S. ichiro, Yamamoto, Y., Yahagi, H., Kanematsu, M., Sato, M., Ito, T., Uezumi, A., Hayashi, S., Miyagoe-Suzuki, Y., Takeda, S., Tsujikawa, K., & Yamamoto, H. (2008). Suppression of macrophage functions impairs skeletal muscle regeneration with severe fibrosis. *Experimental Cell Research*, *314*(17), 3232–3244. https://doi.org/10.1016/j.yexcr.2008.08.008

Seldin, M. M., Peterson, J. M., Byerly, M. S., Wei, Z., & Wong, G. W. (2012). Myonectin (CTRP15), a Novel Myokine That Links Skeletal Muscle to Systemic Lipid Homeostasis*. *Journal of Biological Chemistry*, *287*(15), 11968–11980. https://doi.org/10.1074/jbc.M111.336834

Sell, H., Dietze-Schroeder, D., & Eckel, J. (2006). The adipocyte–myocyte axis in insulin resistance. *Trends in Endocrinology & Metabolism*, *17*(10), 416–422. https://doi.org/10.1016/j.tem.2006.10.010

Sell, H., Eckardt, K., Taube, A., Tews, D., Gurgui, M., Van Echten-Deckert, G., & Eckel, J. (2008). Skeletal muscle insulin resistance induced by adipocyte-conditioned medium: Underlying mechanisms and reversibility. *American Journal of Physiology - Endocrinology and Metabolism*, *294*(6), 1070–1077. https://doi.org/10.1152/ajpendo.00529.2007

Senn, J. J. (2006). Toll-like receptor-2 is essential for the development of palmitate-induced insulin resistance in myotubes. *Journal of Biological Chemistry*, *281*(37), 26865–26875. https://doi.org/10.1074/jbc.M513304200

Serrano, A., González-Sarrías, A., Tomás-Barberán, F. A., Avellaneda, A., Gironés-Vilaplana, A., Nieto, G., & Ros-Berruezo, G. (2020). Anti-Inflammatory and Antioxidant Effects of Regular Consumption of Cooked Ham Enriched with Dietary Phenolics in Diet-Induced Obese Mice. *Antioxidants*, *9*(7), 639. https://doi.org/10.3390/antiox9070639

Serrano, A. L., Baeza-Raja, B., Perdiguero, E., Jardí, M., & Muñoz-Cánoves, P. (2008). Interleukin-6 is an essential regulator of satellite cell-mediated skeletal muscle hypertrophy. *Cell Metabolism*, *7*(1), 33–44. https://doi.org/10.1016/j.cmet.2007.11.011

Seyoum, B., Fite, A., & Abou-Samra, A. B. (2011). Effects of 3T3 adipocytes on interleukin-6 expression and insulin signaling in L6 skeletal muscle cells. *Biochemical and Biophysical Research Communications*, *410*(1), 13–18. https://doi.org/10.1016/j.bbrc.2011.05.073

Shang, K., Zhang, J., Amna, T., Yang, J., Cheng, X., Zhang, C., & Hwang, I. (2015). Attenuation of cellular toxicity by calpain inhibitor induced by bacterial endotoxin: a mechanistic study using muscle precursor cells as a model system. *Molecular Biology Reports*, *42*(8), 1281–1288. https://doi.org/10.1007/s11033-015-3869-7

Shi, H., Kokoeva, M. V., Inouye, K., Tzameli, I., Yin, H., & Flier, J. S. (2006). TLR4 links innate immunity and fatty acid-induced insulin resistance. *Journal of Clinical Investigation*, *116*(11), 3015–3025. https://doi.org/10.1172/JCI28898

Shimabukuro, M., Zhou, Y. T., Levi, M., & Unger, R. H. (1998). Fatty acid-induced β cell apoptosis: A link between obesity and diabetes. *Proceedings of the National Academy of Sciences of the United States of America*, *95*(5), 2498–2502. https://doi.org/10.1073/pnas.95.5.2498

Shoelson, S. E. (2006). Inflammation and insulin resistance. *Journal of Clinical Investigation*, *116*(7), 1793–1801. https://doi.org/10.1172/JCI29069

Shou, J., Chen, P.-J., & Xiao, W.-H. (2020). Mechanism of increased risk of insulin resistance in aging skeletal muscle. *Diabetology & Metabolic Syndrome*, *12*(1), 14. https://doi.org/10.1186/s13098-020-0523-x

Sishi, B., Loos, B., Ellis, B., Smith, W., Du Toit, E. F., & Engelbrecht, A. M. (2011). Diet-induced obesity alters signalling pathways and induces atrophy and apoptosis in skeletal muscle in a prediabetic rat model. *Experimental Physiology*, *96*(2), 179–193. https://doi.org/10.1113/expphysiol.2010.054189

Sjøberg, K. A., Frøsig, C., Kjøbsted, R., Sylow, L., Kleinert, M., Betik, A. C., Shaw, C. S., Kiens, B., Wojtaszewski, J. F. P., Rattigan, S., Richter, E. A., & McConell, G. K. (2017). Exercise Increases Human Skeletal Muscle Insulin Sensitivity via Coordinated Increases in Microvascular Perfusion and Molecular Signaling. *Diabetes*, *66*(6), 1501–1510. https://doi.org/10.2337/db16-1327

Smith, C., & Swart, A. C. (2016). Rooibos (Aspalathus linearis) facilitates an anti-inflammatory state, modulating IL-6 and IL-10 while not inhibiting the acute glucocorticoid response to a mild novel stressor in vivo. *Journal of Functional Foods*, *27*, 42–54.

https://doi.org/10.1016/j.jff.2016.08.055

Smith, I. J., Aversa, Z., Alamdari, N., Petkova, V., & Hasselgren, P.-O. (2010). Sepsis downregulates myostatin mRNA levels without altering myostatin protein levels in skeletal muscle. *Journal of Cellular Biochemistry*, *111*(4), 1059–1073. https://doi.org/10.1002/jcb.22796

Soeters, M. R., Soeters, P. B., Schooneman, M. G., Houten, S. M., & Romijn, J. A. (2012). Adaptive reciprocity of lipid and glucose metabolism in human short-term starvation. *American Journal of Physiology-Endocrinology and Metabolism*, *303*(12), E1397–E1407. https://doi.org/10.1152/ajpendo.00397.2012

Sonnet, C., Lafuste, P., Arnold, L., Brigitte, M., Poron, F., Authier, F. J., Chrétien, F., Gherardi, R. K., & Chazaud, B. (2006). Human macrophages rescue myoblasts and myotubes from apoptosis through a set of adhesion molecular systems. *Journal of Cell Science*, *119*(12), 2497–2507. https://doi.org/10.1242/jcs.02988

Spranger, J., Kroke, A., Möhlig, M., Hoffmann, K., Bergmann, M. M., Ristow, M., Boeing, H., & Pfeiffer, A. F. H. (2003). Inflammatory Cytokines and the Risk to Develop Type 2 Diabetes. *Diabetes*, *52*(3), 812–817. https://doi.org/10.2337/DIABETES.52.3.812

Srikanthan, P., & Karlamangla, A. S. (2011). Relative Muscle Mass Is Inversely Associated with Insulin Resistance and Prediabetes. Findings from The Third National Health and Nutrition Examination Survey. *The Journal of Clinical Endocrinology & Metabolism*, *96*(9), 2898–2903. https://doi.org/10.1210/jc.2011-0435

Stitt, T. N., Drujan, D., Clarke, B. A., Panaro, F., Timofeyva, Y., Kline, W. O., Gonzalez, M., Yancopoulos, G. D., & Glass, D. J. (2004). The IGF-1/PI3K/Akt pathway prevents expression of muscle atrophy-induced ubiquitin ligases by inhibiting FOXO transcription factors. *Molecular Cell*, *14*(3), 395–403. https://doi.org/10.1016/S1097-2765(04)00211-4

Strober, W. (2015). Trypan Blue Exclusion Test of Cell Viability. *Current Protocols in Immunology*, *111*(1), A3.B.1-A3.B.3. https://doi.org/10.1002/0471142735.ima03bs111

Stumvoll, M., Goldstein, B. J., & van Haeften, T. W. (2005). Type 2 diabetes: principles of pathogenesis and therapy. *The Lancet*, *365*(9467), 1333–1346. https://doi.org/10.1016/S0140-6736(05)61032-X

Sukumaran, A., Choi, K., & Dasgupta, B. (2020). Insight on Transcriptional Regulation of the

Energy Sensing AMPK and Biosynthetic mTOR Pathway Genes. *Frontiers in Cell and Developmental Biology*, *8*, 671. https://doi.org/10.3389/fcell.2020.00671

Sumi, K., Ashida, K., & Koichi Nakazato, X. (2020). Resistance exercise with anti-inflammatory foods attenuates skeletal muscle atrophy induced by chronic inflammation. *J Appl Physiol*, *128*, 197–211. https://doi.org/10.1152/japplphysiol.00585.2019

Sun, K., Kusminski, C. M., & Scherer, P. E. (2011). Adipose tissue remodeling and obesity. In *Journal of Clinical Investigation* (Vol. 121, Issue 6, pp. 2094–2101). American Society for Clinical Investigation. https://doi.org/10.1172/JCI45887

Tajbakhsh, S., Rocancourt, D., Cossu, G., & Buckingham, M. (1997). Redefining the genetic hierarchies controlling skeletal myogenesis: Pax- 3 and Myf-5 act upstream of MyoD. *Cell*, *89*(1), 127–138. https://doi.org/10.1016/S0092-8674(00)80189-0

Taylor, W. E., Bhasin, S., Artaza, J., Byhower, F., Azam, M., Willard, D. H., Kull, F. C., & Gonzalez-Cadavid, N. (2001). Myostatin inhibits cell proliferation and protein synthesis in C2C12 muscle cells. *American Journal of Physiology. Endocrinology and Metabolism*, *280*(2), E221-8. https://doi.org/10.1152/ajpendo.2001.280.2.E221

Teng, S., & Huang, P. (2019). The effect of type 2 diabetes mellitus and obesity on muscle progenitor cell function. In *Stem Cell Research and Therapy* (Vol. 10, Issue 1, pp. 1–15). BioMed Central Ltd. https://doi.org/10.1186/s13287-019-1186-0

Thomas, M., Langley, B., Berry, C., Sharma, M., Kirk, S., Bass, J., & Kambadur, R. (2000). Myostatin, a negative regulator of muscle growth, functions by inhibiting myoblast proliferation. *Journal of Biological Chemistry*, *275*(51), 40235–40243. https://doi.org/10.1074/jbc.M004356200

Tisdale, M. J. (2008). Catabolic mediators of cancer cachexia. *Current Opinion in Supportive & Palliative Care*, *2*(4), 256–261. https://doi.org/10.1097/SPC.0b013e328319d7fa

Trierweiler, H., Kisielewicz, G., Jonasson, T. H., Petterle, R. R., Moreira, C. A., & Borba, V. Z. C. (2018). Sarcopenia: A chronic complication of type 2 diabetes mellitus. *Diabetology and Metabolic Syndrome*, *10*(1), 25. https://doi.org/10.1186/s13098-018-0326-5

Tripathy, D., & Chavez, A. O. (2010). Defects in Insulin Secretion and Action in the Pathogenesis of Type 2 Diabetes Mellitus. *Current Diabetes Reports*, *10*(3), 184–191. https://doi.org/10.1007/s11892-010-0115-5

Tsatsoulis, A., Mantzaris, M. D., Bellou, S., & Andrikoula, M. (2013). Insulin resistance: An adaptive mechanism becomes maladaptive in the current environment - An evolutionary perspective. *Metabolism: Clinical and Experimental*, *62*(5), 622–633. https://doi.org/10.1016/j.metabol.2012.11.004

Uličná, O., Vančová, O., Kucharská, J., Janega, P., & Waczulíková, I. (2019). Rooibos tea (Aspalathus linearis) ameliorates the CCl 4 -induced injury to mitochondrial respiratory function and energy production in rat liver. *General Physiology and Biophysics*, *38*(01), 15–25. https://doi.org/10.4149/gpb_2018037

Valley, M. P., Karassina, N., Aoyama, N., Carlson, C., Cali, J. J., & Vidugiriene, J. (2016). A bioluminescent assay for measuring glucose uptake. *Analytical Biochemistry*, *505*, 43–50. https://doi.org/10.1016/j.ab.2016.04.010

Vaughan, R. A., Gannon, N. P., Barberena, M. A., Garcia-Smith, R., Bisoffi, M., Mermier, C. M., Conn, C. A., & Trujillo, K. A. (2014). Characterization of the metabolic effects of irisin on skeletal muscle in vitro. *Diabetes, Obesity and Metabolism*, *16*(8), 711–718. https://doi.org/10.1111/dom.12268

Vendelbo, M. H., Clasen, B. F. F., Treebak, J. T., Møller, L., Krusenstjerna-Hafstrøm, T., Madsen, M., Nielsen, T. S., Stødkilde-Jørgensen, H., Pedersen, S. B., Jørgensen, J. O. L., Goodyear, L. J., Wojtaszewski, J. F. P., Møller, N., & Jessen, N. (2012). Insulin resistance after a 72-h fast is associated with impaired AS160 phosphorylation and accumulation of lipid and glycogen in human skeletal muscle. *American Journal of Physiology-Endocrinology and Metabolism*, *302*(2), E190–E200. https://doi.org/10.1152/ajpendo.00207.2011

Villaño, D., Pecorari, M., Testa, M. F., Raguzzini, A., Stalmach, A., Crozier, A., Tubili, C., & Serafini, M. (2010). Unfermented and fermented rooibos teas (Aspalathus linearis) increase plasma total antioxidant capacity in healthy humans. *Food Chemistry*, *123*(3), 679–683. https://doi.org/10.1016/j.foodchem.2010.05.032

von Maltzahn, J., Jones, A. E., Parks, R. J., & Rudnicki, M. A. (2013). Pax7 is critical for the normal function of satellite cells in adult skeletal muscle. *Proceedings of the National Academy of Sciences*, *110*(41), 16474–16479. https://doi.org/10.1073/pnas.1307680110

Vu, V., Kim, W., Fang, X., Liu, Y. T., Xu, A., & Sweeney, G. (2007). Coculture with primary visceral rat adipocytes from control but not streptozotocin-induced diabetic animals

increases glucose uptake in rat skeletal muscle cells: Role of adiponectin. *Endocrinology*, *148*(9), 4411–4419. https://doi.org/10.1210/en.2007-0020

Wang, X., Hu, Z., Hu, J., Du, J., Mitch, W. E., Laplante, M., Sabatini, D. M., Lagirand-Cantaloube, J., Offner, N., Csibi, A., Leibovitch, M. P., Batonnet-Pichon, S., Tintignac, L. A., Segura, C. T., Leibovitch, S. A., Wang, X., Hu, Z., Hu, J., Du, J., & Mitch, W. E. (2006). Insulin Resistance Accelerates Muscle Protein Degradation: Activation of the Ubiquitin-Proteasome Pathway by Defects in Muscle Cell Signaling. *Endocrinology*, *147*(9), 4160–4168. https://doi.org/10.1210/en.2006-0251

Weber, T. E., Small, B. C., & Bosworth, B. G. (2005). Lipopolysaccharide regulates myostatin and MyoD independently of an increase in plasma cortisol in channel catfish (Ictalurus punctatus). *Domestic Animal Endocrinology*, *28*(1), 64–73. https://doi.org/10.1016/j.domaniend.2004.05.005

Weisberg, S. P., McCann, D., Desai, M., Rosenbaum, M., Leibel, R. L., & Ferrante, A. W. (2003). Obesity is associated with macrophage accumulation in adipose tissue. *Journal of Clinical Investigation*, *112*(12), 1796–1808. https://doi.org/10.1172/JCI200319246

Wijngaarden, M. A., Bakker, L. E. H., van der Zon, G. C., 't Hoen, P. A. C., van Dijk, K. W., Jazet, I. M., Pijl, H., & Guigas, B. (2014). Regulation of skeletal muscle energy/nutrient-sensing pathways during metabolic adaptation to fasting in healthy humans. *American Journal of Physiology-Endocrinology and Metabolism*, *307*(10), E885–E895. https://doi.org/10.1152/ajpendo.00215.2014

Wilkes, J. J., Lloyd, D. J., & Gekakis, N. (2009). Loss-of-Function Mutation in Myostatin Reduces Tumor Necrosis Factor Production and Protects Liver Against Obesity-Induced Insulin Resistance. *Diabetes*, *58*(5), 1133–1143. https://doi.org/10.2337/db08-0245

Wong, C. Y., Al-Salami, H., & Dass, C. R. (2020). C2C12 cell model: its role in understanding of insulin resistance at the molecular level and pharmaceutical development at the preclinical stage. *Journal of Pharmacy and Pharmacology*, *72*(12), 1667–1693. https://doi.org/10.1111/jphp.13359

Woo, M., Isganaitis, E., Cerletti, M., Fitzpatrick, C., Wagers, A. J., Jimenez-Chillaron, J., & Patti, M. E. (2011). Early life nutrition modulates muscle stem cell number: Implications for muscle mass and repair. *Stem Cells and Development*, *20*(10), 1763–1769. https://doi.org/10.1089/scd.2010.0349

Wu, H., & Ballantyne, C. M. (2017). Skeletal muscle inflammation and insulin resistance in obesity. *The Journal of Clinical Investigation*, *127*(1), 43–54. https://doi.org/10.1172/JCI88880

Yablonka-Reuveni, Z. (2011). The Skeletal Muscle Satellite Cell: Still Young and Fascinating at 50. In *Journal of Histochemistry and Cytochemistry* (Vol. 59, Issue 12, pp. 1041–1059). https://doi.org/10.1369/0022155411426780

Yaffe, D., & Saxel, O. (1977). Serial passaging and differentiation of myogenic cells isolated from dystrophic mouse muscle. *Nature*, *270*(5639), 725–727. https://doi.org/10.1038/270725a0

Yang, Z.-Z., Tschopp, O., Baudry, A., Dümmler, B., Hynx, D., & Hemmings, B. A. (2004). Physiological functions of protein kinase B/Akt. *Biochemical Society Transactions*, *32*(2), 350–354. https://doi.org/10.1042/bst0320350

Ye, J. (2013). Mechanisms of insulin resistance in obesity. *Frontiers of Medicine*, *7*(1), 14–24. https://doi.org/10.1007/s11684-013-0262-6

Yin, H., Price, F., & Rudnicki, M. A. (2013). Satellite cells and the muscle stem cell niche. *Physiological Reviews*, *93*(1), 23–67. https://doi.org/10.1152/physrev.00043.2011

Yu, C., Chen, Y., Cline, G. W., Zhang, D., Zong, H., Wang, Y., Bergeron, R., Kim, J. K., Cushman, S. W., Cooney, G. J., Atcheson, B., White, M. F., Kraegen, E. W., & Shulman, G. I. (2002). Mechanism by which fatty acids inhibit insulin activation of insulin receptor substrate-1 (IRS-1)-associated phosphatidylinositol 3-kinase activity in muscle. *The Journal of Biological Chemistry*, *277*(52), 50230–50236. https://doi.org/10.1074/jbc.M200958200

Zhang, C., Li, Y., Wu, Y., Wang, L., Wang, X., & Du, J. (2013). Interleukin-6/Signal Transducer and Activator of Transcription 3 (STAT3) Pathway Is Essential for Macrophage Infiltration and Myoblast Proliferation during Muscle Regeneration. *Journal of Biological Chemistry*, *288*(3), 1489–1499. https://doi.org/10.1074/jbc.M112.419788

Zhang, Y., Li, R., Meng, Y., Li, S., Donelan, W., Zhao, Y., Qi, L., Zhang, M., Wang, X., Cui, T., Yang, L.-J., & Tang, D. (2014). Irisin Stimulates Browning of White Adipocytes Through Mitogen-Activated Protein Kinase p38 MAP Kinase and ERK MAP Kinase Signaling. *Diabetes*, *63*(2), 514–525. https://doi.org/10.2337/db13-1106

Zhao, R., Long, X., Yang, J., Du, L., Zhang, X., Li, J., & Hou, C. (2019). Pomegranate peel

polyphenols reduce chronic low-grade inflammatory responses by modulating gut microbiota and decreasing colonic tissue damage in rats fed a high-fat diet. *Food & Function*, *10*(12), 8273–8285. https://doi.org/10.1039/C9FO02077B

Zimmet, P. Z. (2017). Diabetes and its drivers: the largest epidemic in human history? *Clinical Diabetes and Endocrinology*, *3*(1), 1. https://doi.org/10.1186/s40842-016-0039-3

Zoico, E., Garbin, U., Olioso, D., Mazzali, G., Fratta Pasini, A. M., Di Francesco, V., Sepe, A., Cominacini, L., & Zamboni, M. (2009). The effects of adiponectin on interleukin-6 and MCP-1 secretion in lipopolysaccharide-treated 3T3-L1 adipocytes: role of the NF-kappaB pathway. *International Journal of Molecular Medicine*, *24*(6), 847–851. https://doi.org/10.3892/ijmm_00000302

8 Appendix I

8.1 Reagents and kits

Table 5: List of reagents and kits.

Reagents and Kits	Catalogue number	Supplier
β-mercaptoethanol		Fluka, Bucharest, Romania
β-actin (housekeeping)	Sc-47778	Santa Cruz Biotechnology
3-isobutyl -1-methyl-xanthine (IBMX)	I5879	Sigma-Aldrich, St Louis, MO, USA
3-(4, 5-dimethylthiazol-2-yl)-2, 5-diphenyl tetrazolium bromide	M5655	Sigma-Aldrich, Missouri, USA
3T3-L1 pre-adipocyte cell line	CL-173	American Type Culture Collection, Virginia, USA
Akt Antibody	9272S	Cell Signaling Technology, Inc., Massachusetts, USA
AMPKα Antibody	2532S	Cell Signaling Technology, Inc., Massachusetts, USA
Beta-2 Microglobulin (Mm00437762_m1) Assay	4331182	Applied Biosystems, Massachusetts, USA
Bovine Serum Albumin Standard	5000207	Bio-Rad, California, USA
C2C12 cell line	CRL-1772	American Type Culture Collection, Virginia, USA
Chloroform	136112-00-0	Sigma-Aldrich, Missouri, USA
Clarity™ Western enhanced chemiluminescence (ECL) Substrate	1705061	Bio-Rad, California, USA
Dexamethasone	D4902	Sigma-Aldrich, Missouri, USA
Dimethyl sulfoxide	276855	Sigma-Aldrich, Missouri, USA

Dulbecco's Modified Eagle's Medium	BE12-604F	Lonza, Basel, Switzerland
Dulbecco's Phosphate Buffered Saline	BE17-513F	Lonza, Basel, Switzerland
DuoSet Ancillary Reagent Kit	DY008	R&D Systems, Minnesota, USA
Ethanol (Absolute, Molecular Grade)	E7023-500	Sigma-Aldrich, Missouri, USA
GIBCO Fetal bovine serum (Heat Inactivated)	10493106	Thermo Fisher Scientific, Massachusetts, USA
Glucose	D5030	Sigma-Aldrich, Missouri, USA
Insulin (human)	I92785	Sigma-Aldrich, Missouri, USA
Isopropanol	I9516	Sigma-Aldrich, Missouri, USA
Laemmli protein sample buffer	1610747	Bio-Rad, California, USA
Lipopolysaccharides from Escherichia coli O127:B8	L4516-1MG	Sigma-Aldrich, Missouri, USA
Nuclease-free water (Ambion)	AM9920	Invitrogen, California, USA
Mouse Adiponectin/Acrp30 DuoSet ELISA kit	DY1119	R&D Systems, Minnesota, USA
Mouse IL-6 DuoSet ELISA Kit	DY406-05	R&D Systems, Minnesota, USA
Mouse IL-10 DuoSet ELISA kit	DY417-05	R&D Systems, Minnesota, USA
Mstn (myostatin) Assay (Mm01254559_m1)	4331182	Applied Biosystems, Massachusetts, USA
Myod1 Assay (Mm00440387_m1)	4331182	Applied Biosystems, Massachusetts, USA
Myog Assay (Mm00446194_m1)	4331182	Applied Biosystems, Massachusetts, USA

mTOR Antibody	2972S	Cell Signaling Technology, Inc., Massachusetts, USA
Phospho-AKT (Ser473)	ab81283	Abcam, Cambridge, UK
Phospho-AMPKα (Thr172)	2535S	Cell Signaling Technology, Inc., Massachusetts, USA
Phospho-mTOR (Ser2448)	2971S	Cell Signaling Technology, Inc., Massachusetts, USA
Phosphate Buffered Saline	BE17-516F	Lonza, Basel, Switzerland
Ponceau S solution	P7170	Sigma-Aldrich, Missouri, United States
Promega Glucose Uptake-GLO Assay Kit	PRJ1343	Promega, Wisconsin, USA
QIAzol Lysis Reagent	79306	Qiagen, Hilden, Germany
QuantiTect Rev. Transcription Kit	205311	Qiagen, Hilden, Germany
RC DC™ Protein Assay Kit II	5000122	Bio-Rad, California, USA
Seahorse XF9 Cell Mito Stress Test kit	103010-100	Agilent Technologies, California, USA
Sodium bicarbonate	S3817	Sigma-Aldrich, Missouri, USA
TaqMan Fast Advanced Master Mix	4444557	Applied Biosystems, Massachusetts, USA
TGX Stain-Free™ FastCast™ Acrylamide Kit, 12%	1610185	Bio-Rad, California, USA
Trans-Blot® Turbo™ Midi Nitrocellulose Transfer Pack	1704159	Bio-Rad, California, USA
Trans-Blot® Turbo™ RTA Mini Nitrocellulose Transfer Kit	1704270	Bio-Rad, California, USA

Tris/Glycine/SDS running buffer	1610732	Bio-Rad, California, USA
Trypan blue	15050-065	Invitrogen, California, USA
Trypsin Versene (0,5g/L trypsin 1:250 and 0,2g/L Versene	BE17-161E	Lonza, Basel, Switzerland
Water for Cell Culture	BE17-724Q	Lonza, Basel, Switzerland

8.2 Consumables

Table 6: List of consumables

Consumables	**Catalogue number**	**Supplier**
2ml Eppendorf Safe-Lock PCR Clean Tubes	EP0030123344	Eppendorf, Hamburg, Germany
10mL serological pipettes	607160	Greiner, Kremsmünster, Austria
15ml Centrifuge tubes	601001	Nest Scientific, Rahway, NJ, USA
25mL serological pipettes	760160	Greiner, Kremsmünster, Austria
50mL serological pipettes	768160	Greiner, Kremsmünster, Austria
50ml Self standing centrifuge tubes	602072	Nest Scientific, Rahway, NJ, USA
75cm² Cell culture flask	708001	Nest Scientific, Rahway, NJ, USA
96 Well CellBIND® Microplates	CLS3300	Corning, New York, USA
24 Well CellBIND® Multiple Well Plate	CLS3336	Corning, New York, USA
6 Well CellBIND® Multiple Well Plate	CLS3335	Corning, New York, USA
Cell Scrapers (Large), 280mm Handle, 20mm Blade	710011	Nest Scientific, Rahway, NJ, USA

Cell Scrapers (Small), 220mm Handle, 13mm Blade	710001	Nest Scientific, Rahway, NJ, USA
Contour Plus Glucometer Glucose Strips	84627470	Ascensia Diabetes Care Holdings AG, Basel, Switzerland
MicroAmp EnduraPlate Optical 384 Well Clear Reaction Plates	44-832-85	Applied Biosystems, Massachusetts, USA
Millex syringe filter unit (0.22 um)	SLGP033RS	Merk, Massachusetts, USA
SPL Insert Hanging, PET membrane, 24 well, 0.4um pore size	36024	SPL Life Sciences, Gyeonggi-do, Korea
Stainless steel beads (5 mm)	69989	Qiagen, Hilden, Germany
TPP vacuum filtration systems	99500	TPP Techno Plastic Products AG, Zollstrasse, Switzerland
XF96 Cell Culture Microplates	101085-004	Agilent Technologies, California, USA

8.3 Equipment and Software

Table 7: List of equipment and software

Equipment and Software	**Supplier**
cellSens Entry Imaging software	Olympus Corporation, Tokyo, Japan
Bio-Rad ChemiDoc™ MP System	Bio-Rad, California, United States
BioTek ELx800 microplate reader	BioTek Instruments, Inc., Winooski, VT, USA
Gen5 version 1.05	BioTek Instruments, Inc., Winooski, VT, USA

GraphPad Prism® 8.0.1	GraphPad Software, La Jolla, California, USA
Haemacytometer (Neubauer-improved)	Paul Marienfeld GmbH & Co., Lauda-Königshofen, Germany
ImageJ software (1.53g)	National Institutes of Health
Image Lab™ Software	Bio-Rad, California, United States
NIS-Elements Imaging Software	Nikon Instruments Inc., New York, USA
Nikon Inverted Microscope Eclipse Ti-S	Nikon Instruments Inc., New York, USA
Olympus CKX31 inverted light microscope	Olympus Corporation, Tokyo, Japan
PowerPac™ Basic	Bio-Rad, California, United States
QuantStudio™ 7 Flex Real-Time PCR System	Applied Biosystems, Massachusetts, USA
QuantStudio™ Real-Time PCR Software v1.7	Applied Biosystems, Massachusetts, USA
RS Biotech Galaxy R CO2 Incubator	Eppendorf Inc., Hamburg, Germany
Seahorse XFe96 Analyzer	Agilent Technologies, California, USA
Seahorse Wave Controller Software 2.4.2	Agilent Technologies, California, USA
SoftMax Pro 7 software, version 7.0.2	Molecular Devices, LLC, Sunnyvale, CA, USA
SpectraMax i3x multi-mode microplate reader	Molecular Devices, LLC, Sunnyvale, CA, USA
Thermo Scientific™ NanoDrop™ One Microvolume UV-Vis Spectrophotometer	Thermo Fisher Scientific, Massachusetts, USA
Trans-Blot® Turbo™ transfer cassette	Bio-Rad, California, United States

8.4 Complete growth media

Complete growth media was prepared aseptically in a biosafety cabinet by adding 50 mL of FBS to 450 mL of DMEM. This was carefully mixed by pipetting up and down. Media was stored at 4^0C.

8.5 Differentiation media

Differentiation media was prepared aseptically in a biosafety cabinet by adding 10 mL of HS to 490 mL of DMEM. The was mixed carefully and stored at 4^0C.

8.6 Sorenson's glycine buffer

To prepare the sorenson's buffer, 0.751 g of glycine and 0.584 g of NaCl was dissolved in 100 mL of cell culture tested dH_2O to yield a final concentration of 0.1 M buffer solution. The pH was adjusted to 10.5 using NaOH.

8.7 Krebs ringer bicarbonate HEPES buffer (KRBH)

Krebs buffer was prepared using the following formulation:

Table 8: Krebs ringer bicarbonate HEPES buffer

Reagent	Final concentration	Weight
NaCl	115 mM	3.36 g
$NaHCO_3$	24 mM	1.008 g
KCl	5 mM	0.186 g

$MgCl_2$	1 mM	0.048 g
$CaCl_2$	2.5 mM	0.139 g
BSA	0.1% (w/v)	0.5 g
HEPES (1 M)	10 mM	5 mL

Reagents were dissolved in 500 mL cell culture tested water and filter sterilized using a 0.22 µm filtration system. Buffer was stored at 4^0C.

9 Appendix II

SPRINGER NATURE LICENSE

TERMS AND CONDITIONS

Jul 04, 2021

This Agreement between Mrs. Nnini Obonye ("You") and Springer Nature ("Springer Nature") consists of your license details and the terms and conditions provided by Springer Nature and Copyright Clearance Center.

License Number	
License date	
Licensed Content Publisher	
Licensed Content Publication	
Licensed Content Title	
Licensed Content Author	Total
Licensed Content Date Type of Use	Terms and Conditions
Requestor type	
Format	
Portion	
Number of figures/tables/illustrations	
Will you be translating?	
Circulation/distribution	
Author of this SpringerNature content	
Title	
Institution name	
Expected presentation date	
Portions	
Requestor Location	

5013770546402

Feb 21, 2021

Springer Nature

Calcified Tissue International

e and FunctionWalter R. Frontera *et al*

Oct 8, 2014

Thesis/Dissertation

academic/university or research institute

print and electronic

figures/tables/illustrations

1

no

1 - 29

FIO

The effect of an aspalathin rich rooibos extract on inflammatory crosstalk between adipocytes andmuscle cells

Stellenbosch UniversityApr

2021

Figure 3, image structure of skeletal muscle on page 185

Mrs. Nnini Obonye

Francie van Zijil Drive

Cape Town, Western Cape 7501South

Africa

Attn: Private

0.00 USD

Springer Nature Customer Service Centre GmbH

Terms and Conditions

Skeletal Muscle: A Brief Review of Structur

This agreement sets out the terms and conditions of the licence (the **Licence)** between you and Springer **Nature Customer Service Centre GmbH** (the **Licensor).** By clicking 'accept' and completing the transaction for the material **(Licensed Material),** youalso confirm your acceptance of these terms and conditions.

1. Grant of License

1. 1. The Licensor grants you a personal, non-exclusive, non-transferable, world-wide licence to reproduce the Licensed Material for the purpose specified in your order only. Licences are granted for the specific use requested in the order and for no other use, subject to the conditions below.1. 2. The Licensor warrants that it has, to the best of its knowledge, the rights to license reuse of the Licensed Material. However, you should ensure that the material you are requesting is original to the Licensor and does not carry the copyrightof another entity (as credited in the published version).

1. 3. If the credit line on any part of the material you have requested indicates that it was reprinted or adapted with permission from another source, then you should also seek permission from that source to reuse the material.

2. Scope of Licence

2. 1. You may only use the Licensed Content in the manner and to the extent permitted by these Ts&Cs and any applicable laws.

2. 2. A separate licence may be required for any additional use of the Licensed Material, e.g. where a licence has been purchased for print only use, separate permission must be obtained for electronic re-use. Similarly, a licence is only valid in the language selected and does not apply for editions in other languages unless additional translation rights have been granted separately in the licence. Any content owned by third parties are expressly excluded from the licence.

2. 3. Similarly, rights for additional components such as custom editions and derivatives require additional permission and may be subject to an additional fee. Please apply to Journalpermissions@springernature.com/bookpermissions@springernature.com for these rights.

2. 4. Where permission has been granted **free of charge** for material in print, permission may also be granted for any electronic version of that work, provided that the material is incidental to your work as a whole and that the electronic versionis essentially equivalent to, or substitutes for, the print version.

2. 5. An alternative scope of licence may apply to signatories of the STM Permissions Guidelines, as amended from time to time.

3. Duration of Licence

3. 1. A licence for is valid from the date of purchase ('Licence Date') at the end of the relevant period in the below table:

Scope of Licence	Duration of Licence
Post on a website	12 months
Presentations	12 months

Books and journals	Lifetime of the edition in the language purchased

4. Acknowledgement

4. 1. The Licensor's permission must be acknowledged next to the Licenced Material in print. In electronic form, this acknowledgement must be visible at the same time as the figures/tables/illustrations or abstract, and must be hyperlinked to the journal/book's homepage. Our required acknowledgement format is in the Appendix below.

5. Restrictions on use

5. 1. Use of the Licensed Material may be permitted for incidental promotional use and minor editing privileges e.g. minor adaptations of single figures, changes of format, colour and/or style where the adaptation is credited as set out in Appendix 1 below. Any other changes including but not limited to, cropping, adapting, omitting material that affect the meaning, intention or moral rights of the author are strictly prohibited.

5. 2. You must not use any Licensed Material as part of any design or trademark.

5. 3. Licensed Material may be used in Open Access Publications (OAP) before publication by Springer Nature, but any Licensed Material must be removed from OAP sites prior to final publication.

6. Ownership of Rights

6. 1. Licensed Material remains the property of either Licensor or the relevant third party and any rights not explicitly granted herein are expressly reserved.

7. Warranty

IN NO EVENT SHALL LICENSOR BE LIABLE TO YOU OR ANY OTHER PARTY OR ANY OTHER PERSON OR FOR ANY SPECIAL, CONSEQUENTIAL, INCIDENTAL OR INDIRECT DAMAGES, HOWEVER CAUSED, ARISING OUT OF OR IN CONNECTION WITH THE DOWNLOADING, VIEWING OR USE OF THE MATERIALS REGARDLESS OF THE FORM OF ACTION, WHETHER FOR BREACH OF CONTRACT, BREACH OF WARRANTY, TORT, NEGLIGENCE, INFRINGEMENT OR OTHERWISE (INCLUDING, WITHOUT LIMITATION, DAMAGES BASED ON LOSS OF PROFITS, DATA, FILES, USE, BUSINESS OPPORTUNITY OR CLAIMS OF THIRD PARTIES), AND
WHETHER OR NOT THE PARTY HAS BEEN ADVISED OF THE POSSIBILITY OF SUCH DAMAGES. THIS LIMITATION SHALL APPLY NOTWITHSTANDING ANY FAILURE OF ESSENTIAL PURPOSE OF ANY LIMITED REMEDY PROVIDED HEREIN.

8. Limitations

8. 1. *BOOKS* Of\/LY':Where 'reuse in a **dissertation/thesis'** has been selected the following terms apply: Print rights of the final author's accepted manuscript (for clarity, NOT the published version) for up to 100 copies, electronic rights for use only on a personal website or institutional repository as defined by the Sherpa guideline (www.sherpa.ac.uk/romeo/).

8.2. For content reuse requests that qualify for permission under the STM Permissions Guidelines, which may be updated from time to time, the STM Permissions Guidelines supersede the terms and conditions contained in this licence.

9. Termination and Cancellation

9. 1. Licences will expire after the period shown in Clause 3 (above).

9.2. Licensee reserves the right to terminate the Licence in the event that payment is not received in full or if there has been a breach of this agreement by you.

Appendix 1 — Acknowledgements:For
Journal Content:
Reprinted by permission from [the Licensor]: [Journal Publisher (e.g. Nature/Springer/Palgrave)] [JOURNAL NAME] [REFERENCE CITATION (Article name, Author(s) Name), [COPYRIGHT] (year of publication)

For Advance Online **Publication papers:**
Reprinted by permission from [the Licensor]: [Journal Publisher (e.g. Nature/Springer/Palgrave)] [JOURNAL NAME] [REFERENCE CITATION (Article name, Author(s) Name), [COPYRIGHT] (year of publication), advance online publication, day month year (doi: 10.1038/sj.[JOURNAL ACRONYM].)

For Adaptations/Translations:
Adapted/Translated by permission from [the **Licensor]:** [Journal Publisher (e.g. Nature/Springer/Palgrave)] [JOURNAL NAME] [REFERENCE CITATION (Article name, Author(s) Name), [COPYRIGHT] (year of publication)
Note: For any republication **from the British** Journal of Cancer, **the following credit** line style applies:
Reprinted/adapted/translated by permission from [the **Licensor]:** on behalf of Cancer Research UK: : [Journal **Publisher** (e.g. Nature/Springer/Palgrave)] [JOURNAL NAME] [REFERENCE CITATION (Article name, Author(s) Name), [COPYRIGHT] (year of publication)

For Advance Online **Publication** papers:
Reprinted by permission from The [the Licensor]: on behalf of Cancer Research UK: [Journal Publisher (e.g. Nature/Springer/Palgrave)] [JOURNAL NAME] [REFERENCE CITATION (Article name, Author(s) Name), [COPYRIGHT](year of publication), advance online publication, day month year (doi: 10.1038/sj.[JOURNAL ACRONYM])

For Book content:

Turnitin report

Nnini Obonye_Thesis 2021

ORIGINALITY REPORT

24%	18%	17%	7%
SIMILARITY INDEX	INTERNET SOURCES	PUBLICATIONS	STUDENT PAPERS

PRIMARY SOURCES

1	scholar.sun.ac.za Internet Source	1%
2	afriplexgrt.com Internet Source	1%
3	hdl.handle.net Internet Source	1%
4	Submitted to University of Zululand Student Paper	1%
5	journals.plos.org Internet Source	1%
6	"Abstracts 2007", Diabetologia, 2007 Publication	1%
7	etheses.bham.ac.uk Internet Source	1%
8	qmro.qmul.ac.uk Internet Source	<1%
9	www.hindawi.com Internet Source	<1%

	mouse soleus muscle using radiation", Microscopy Research and Technique, 2021 Publication	
198	Sasaki, H.. "Acceleration of autoimmune diabetes in Rheb-congenic NOD mice with @b-cell-specific mTORC1 activation", Biochemical and Biophysical Research Communications, 20110506 Publication	<1 %
199	ueaeprints.uea.ac.uk Internet Source	<1 %
200	G. I. Shulman. "Unraveling the Cellular Mechanism of Insulin Resistance in Humans: New Insights from Magnetic Resonance Spectroscopy", Physiology, 08/01/2004 Publication	<1 %
201	Michiko Takahashi, Yutaka Takahashi, Kenichi Takahashi, Fyodor N. Zolotaryov et al. "Chemerin enhances insulin signaling and potentiates insulin-stimulated glucose uptake in 3T3-L1 adipocytes", FEBS Letters, 2008 Publication	<1 %
202	Rebecca Parish, Kitt Falk Petersen. "Mitochondrial dysfunction and type 2 diabetes", Current Diabetes Reports, 2005 Publication	<1 %